Decomposed relative interaction based multivariable process analysis and control system design

He, Maojun

2007

He, M. (2007). Decomposed relative interaction based multivariable process analysis and control system design. Doctoral thesis, Nanyang Technological University, Singapore.

https://hdl.handle.net/10356/39168

https://doi.org/10.32657/10356/39168

Decomposed Relative Interaction Based Multivariable Process Analysis and Control System Design

He Mao Jun

School of Electrical & Electronic Engineering

A thesis submitted to the Nanyang Technological University

in fulfillment of the requirements for the degree of

Doctor of Philosophy

2007

In Memory of My Dear Mum

Mum, I miss you everyday

Mum, I love you forever

Acknowledgments

First and foremost, I would like to express my sincere gratitude to my supervisor, associate professor Cai Wenjian, for his professional guidance, generous supports, encouragement and invaluable advices throughout the past three and half years. His insightful comment and thoughtful discussion has been an inspiration for my research. It has been a great pleasure to have professor Cai as my advisor.

I would also like to thank all my colleagues, friends and the technicians in the Process and Instrumentation Laboratory. Their support, encouragement and friendship will always be treasured. I would like to acknowledge the School of Electrical and Electronic Engineering, Nanyang Technological University for providing the financial support, research facilities and opportunity for this study.

Finally, my deep thanks go to all members of my family. My deepest gratitude, in love and affection, belongs to my parents, for their understanding, encouragement and strong supports. I am deeply regret to my mum and will cherish the memory of her for ever. I appreciate my parents-in-law for looking after my daughter during my difficult period. And I have to say sorry to my lovely daughter that I spent too little time with her. I save the last special thanks for my dear wife who stands by me through the most difficult time of this process, offering her unconditional love and tremendous support.

Summary

Most industrial processes are multivariable in nature and typically much more difficult to analyze, design and operate than single-input single-output processes, due to the interactions that occur between the input/output variables. Even though some existing methods or tools are available for measuring loop interactions and/or selecting control structures and/or determining controller parameters, they often either provide sufficient and necessary conditions only for lower dimensional processes or are too complex to be applied to higher dimensional processes. Hence, within process control community, the multivariable control related problems, i.e. control system configuration, integrity and design are still largely open. The main objectives of this thesis is to provide new theories, tools and algorithms to quantify loop interactions, select control structures, describe the interacted loops behaviors, and design the decentralized controller, so that the previous mentioned issues can be effectively solved. In this thesis, existing interaction measures are used and new theories as well as tools are introduced to:

- Analyze the interaction effects between a particular loop and the others under their possible open and close status, propose a novel interaction measure, and develop a new loop pairing criterion such that the selected decentralized control configuration has minimal loop interactions.

- Quantify the interaction effects to a particular control loop when the others closed in any probably sequence, derive the necessary and sufficient conditions for decentralized closed-loop integrity, and develop an effective al-

gorithm to evaluate the decentralized closed-loop integrity of decentralized control structure.

- Evaluate the dynamic loop interactions by taking the decentralized controller into account, propose an effective method to describe the interacted loops behaviors, and develop an effective decentralized proportional-integral-derivative controller design procedure.

- Develop empirical rules to establish the equivalent transfer functions of common used low order models of the multivariable process, and propose a simple and effective decentralized internal model control proportional-integral-derivative controller design algorithm.

- Investigate the interaction transmitting rules in the closed system, estimate the interaction effects to individual control loop from other individuals, and develop a systematic approach to treat the block control structure selection problem under a unified framework.

Table of Contents

List of Figures

List of Tables

Chapter 1

Introduction

1.1 Background and Motivation

Most of large and complex industrial processes are multivariable in nature [1]. Compared with single-input single-output (SISO) counterparts, multivariable control systems are much more difficult to analyze, design and operate due to the interactions that occur between the input/output variables [2]. Consequently, there are two issues which must be properly resolved in designing multivariable control systems: 1) determine control structure which has minimal loop interactions and tolerate loops failures; and 2) design controllers for satisfactory system performance. The research for second task has been historically divided into decentralized, block-diagonal and centralized controller designs, each from a different angle in tackling control loop interactions to satisfy the system performance requirements [3]. In the past several decades, both of these two issues have been intensively studied, and a significant amount of research results have been reported.

Despite the availability of sophisticated methods for designing centralized control systems, decentralized control remains popular in many industry applications for the following reasons [4, 5],

(1) Hardware simplicity: The cost of implementation of a decentralized control system is significantly lower than that of a centralized controller. A centralized control system for an $n \times n$ plant consists of $n!$ individual single-input single-output transfer functions, which significantly increases the complexity of the controller hardware. Furthermore, if the controlled and/or manipulated variables are physically far apart, a full controller could require numerous expensive communication links.

(2) Design and tuning simplicity: Decentralized controllers involve far fewer parameters, resulting in a significant reduction in the time and cost of tuning.

(3) Flexibility in operation: A decentralized structure allows operating personnel to restructure the control system by bringing subsystems in and out of service individually, which allows the system to handle changing control objectives during different operating conditions.

However, the potential disadvantage of using the limited control structure is the deteriorated closed-loop performance caused by interactions among loops as a result of the existence of nonzero off-diagonal elements in the transfer function matrix. Therefore, the primary task in the design of decentralized control systems is to determine loop pairings that have minimum cross interactions among individual loops. Consequently, the resulting multiple control loops mostly resemble their single-input single-output (SISO) counterparts such that controller tuning can be facilitated by SISO design techniques [2].

Since the pioneering work of Bristol [6], the relative gain array (RGA) based techniques for control-loop configuration have found widespread industry applications, including blending, energy conservation, and distillation columns, etc [7, 8, 9, 10]. The RGA-based techniques have many important advantages, such as very simple calculation because it is the only process steady-state gain matrix involved and independent scaling due to its ratio nature, etc [11]. To simultaneously consider the closed-loop properties, the RGA-based pairing rules are often used in

conjunction with the Niederlinski index (NI) [12] to guarantee the system stability [2, 7, 11, 13, 14, 15]. However, it has been pointed out that this RGA- and NI-based loop-pairing criterion is a necessary and sufficient condition only for a 2×2 system; it becomes a necessary condition for 3×3 and higher dimensional systems [11, 16]. Moreover, it is very difficult to determine which pairing has less interaction between loops when the RGA values of feasible pairings have similar deviations from unity.

To overcome the limitations of a RGA-based loop pairing criterion, several pairing methods have later been proposed. Witcher and McAvoy [17], as well as otherauthors [18, 19], defined the dynamic RGA (DRGA) to consider the effects of process dynamics and used a transfer function model instead of the steady-state gain matrix to calculate RGA, of which the denominator involved achieving perfect control at all frequencies, while the numerator was simply the open-loop transfer function. The $\mu-$interaction measure [20, 21, 22] is another measure for multivariable systems under diagonal or block-diagonal feedback controllers. By employment of structured singular value (SSV) techniques, it can be used not only to predict the stability of decentralized control systems but also to determine the performance loss caused by these control structures. In particular, its steady-state value provides a sufficient condition for achieving offset-free performance with the closed-loop system. Hovd and Skogestad [16, 23] introduced performance RGA (PRGA) to solve the problem that the RGA cannot indicate the significant one-way interactions in the case in which the process transfer function matrix is triangular.

The flexibility to bring subsystems in and out of service is very important also for the situations when actuators or sensors in some subsystems fail. The characteristic of failure tolerance is that without readjustment to the other parts of the control system, stability can be preserved in the case of any sensor failure and/or actuator failure [24]. The relative gain array (RGA) [6, 13], Niederlinski index (NI) [12] and block relative gain (BRG) [25] are widely used for eliminating pairing that produce

unstable closed-loop systems under failure conditions [11, 26, 27, 28]. Chiu and Arkun [29] introduced the concept of decentralized closed-loop integrity (DCLI) which requiring that the decentralized control structure should be stabilized by a controller having integral action and should maintain its nominal stability in the face of failures in its sensors and/or actuators. A number of necessary or sufficient conditions for DCLI were also developed [29, 30]. However, the necessary and sufficient conditions for DCLI are still not available. Morari and co-workers [27, 31] defined the decentralized integral controllability (DIC) to address the operational issues, which consider the failure tolerance as a sub-problem. Physically, a decentralized integral controllable system allows the operator to reduce the controller gains independently to zero without introducing instability (as a result of positive feedback). Some necessary and/or sufficient conditions for DIC were developed [27, 28, 32, 33]. Even using only the steady state gain information, however, the calculation [34] to verify the DIC is very complicated especially for high dimension system, which still is an open problem.

Even though the design and tuning of single loop PID controllers have been extensively researched [35, 36, 37, 38], they cannot be directly applied to the design of decentralized control systems because of the existence of interactions among control loops. Many methods had been proposed to extend single-input-single-output(SISO) PID tuning rules to decentralized control by compensating foe the effects of loop interactions. A common way is first to an design individual controller for each control loop by ignoring all interactions and then to detune each loop by a detuning factor. Luyben proposed the biggest log modulus tuning (BLT) method for multiloop PI controllers [39, 40]. In the BLT method, the well know Ziegler-Nichols rule is modified with the inclusion of a detuning factor, which determines the tradeoff between stability and performance of the system. Similar methods have also been addressed by Chien et al. [41]. There, the designed PID controllers for the diagonal elements are detunned according to the relative gain array values. Despite simple computations involved, the design regards interac-

tions as elements obstructing the system stability and attempts to dispose of them rather than control them to increase the speed of the individual control loops. It is hence too conservative to exploit process structures and characteristics for the best achievable performance.

Another strategy is to simultaneously consider loop interactions when designing individual control loop. In the sequential design method [42, 43], by taking interactions from the closed loops into account in a sequential fashion, multiple single-loop design strategies can be directly employed. The main drawback of this method is that the design must proceed in a very ad hoc manner. Design decisions are based on loops that have already closed which may have deleterious effects on the behavior of the remaining loops. The interactions are well taken care of only if the loops are of considerably different bandwidths and the closing sequence starts from the fastest loop. Lee et al. [44, 45] proposed an analytical method for multiloop PID controller design by using the frequency-dependent properties of the closed-loop interactions and the generalized internal model control(IMC)-PID tuning rule for SISO systems. The proportional and derivative terms are designed simply by neglecting the off-diagonal elements, whereas the integral term is designed by taking the off-diagonal elements into consideration. Bao et al. [46] formulated the multi-loop design as a nonlinear optimization problem with matrix inequality constraints. As has been illustrated, the formulation does not include the systems that have different input delays, which happens to be very common in multi-input-multi-output(MIMO) processes. Using a genetic algorithm to search the optimal settings was also proposed [47]. However, the results are very much dependent on the conditions defined in the objective function, and the controllers may result in an unstable control system, such as in the case of loop failure or where loops are closed in different orders.

In recent years, the new trend in a designing decentralized control system for multivariable processes is to handle the loop interactions first and then apply SISO PID tuning rules. The independent design methods have been used by several authors,

in which each controller is designed based on the paired transfer functions while satisfying some constraints due to the loop interactions [48, 49]. The constraints imposed on the individual loops are given by criteria such as the μ-interaction measure [20] and the Gershgorin bands [50]. Usually, stability and failure tolerance are automatically satisfied. Since the detailed information on controller dynamics in other loops is not used, the resulting performance may be poor [42]. In the trial-and-error method [51], Lee et al. extended the iterative continuous cycling method for SISO systems to decentralized PI controller tuning. It refined the Nyquist array method to provide less conservative stability conditions, and ultimate gains for decentralized tuning are then determined. The main disadvantages are due to not only the need for successive experiments but also the weak tie between the tuning procedure and the loop performance. To overcome the difficulty of controllers interacting with each other, Wang et al. [52] used a modified Ziegler-Nichols method to determine the controller parameters that will give specified gain margins. Although it presents an interesting approach, the design of a multi-loop controller by simultaneously solving a set of equations is numerically difficult. Huang et al. [53] formulated the effective transmission in each equivalent loop as the effective open-loop process (EOP), the design of controllers can then be carried out without referring to the controller dynamics of other loops. However, for high dimensional processes, the calculation of EOPs is complex, and the controllers have to be conservative for the inevitable modeling errors encountered in the formulation.

If better performance is preferred, a block decentralized structure would be required, where groups of inputs are paired with groups of outputs, producing a block diagonal controller structure. Because the number of such blocks and block decentralized alternatives increases rapidly with the system size, design for every alternative to compare their control system performances is impractical. Thus, effective tools are required to evaluate the interactions among control loops in order to find the best control structure among all the alternatives.

Manousiouthakis et al. [25] generalized the concept of the RGA to the block relative gain (BRG) for input-output controllability analysis and screening the alternative options for block decentralized control. The properties and pairing rules for BRG have been further considered in detail by Kariwala et al. [54]. Arkun has argued that rigorous closed-loop stability and performance analysis is not possible under the assumption of perfect control and has suggested the use of the dynamic BRG (dBRG) [55]. However, the applicability of the dBRG is limited because of its dependence upon controller tuning and extensive computational requirements. The μ-interaction [20] is another measure for multivariable systems under diagonal or block-diagonal feedback controllers. By employment of structured singular value (SSV) [56] techniques, it can be used not only to predict the stability of decentralized control systems but also to determine the performance loss caused by these control structures. In particular, its steady-state value provides a sufficient condition for achieving offset-free performance with the closed-loop system. Through extending the concept of decentralized integral controllability (DIC) [27] to block-decentralized integral controllability (BDIC) and deriving sufficient and necessary conditions for processes to be BDIC, Zhang et al. [57] presented a loop pairing rule for block diagonal pairing schemes. Chang et al. [58] generalized the concept of relative disturbance gain (RDG) to generalized relative disturbance gain (GRDG) to evaluate the disturbance rejection capabilities of all possible controller structures. Based upon a dynamic model of the process, Salgado et al. [59] proposed a Gramian-based index of interaction measure, which provides support for decentralized input-output pairing as well as for a richer controller architecture selection in both continuous and discrete-time frameworks.

Even though some existing methods are available for selecting control structures and/or determining controller parameters, they often either provide sufficient and necessary conditions only for lower dimensional processes or are too complex to be applied to higher dimensional processes. Hence, in these two research areas, several main problems are still open and require more research efforts. Our motivation

comes from these unsolved issues and discussed as follows:

- Decentralized control system configuration: The well known relative gain array (RGA) and Niederlinski index (NI) based loop-pairing criterion provide a necessary and sufficient condition only for a 2×2 system, and becomes a necessary condition for 3×3 and higher dimensional systems. Moreover, it is very difficult to determine which pairing has less interaction between loops when the RGA values of feasible pairings have similar deviations from unity. Since the RGA based tool can only estimate the overall interaction effect to individual control loop, it also can not answer: (i) what are the interaction effects to a particular loop when all other loops work together or individually? (ii) what are the reverse interaction effects from a particular loop open and closed to other open and closed loops? (iii) what is the feasible definition of the minimal interactions? These issues have motivated us to investigate the interactions among loops under different open and closed loop status, and propose a new method to measure loop interactions and select the control configuration which has minimal loop interactions.

- Decentralized closed-loop integrity evaluation: For most decentralized feedback control system, the decentralized closed-loop integrity (DCLI), which allows the decentralized control structure to tolerate failures of sensors and/or actuators, is often desired. A number of necessary or sufficient conditions for DCLI have been developed. However, the necessary and sufficient conditions for DCLI are still not available. Moreover, there is a lack of simple and effective method for DCLI evaluation. This has motivated us to examine the interactions to individual control loop under any status of all the other control loops with respect to their open and close status and develop the necessary and sufficient conditions as well as an effective algorithm to evaluate the DCLI of available control configurations.

- Decentralized proportional-integral-derivative controller design: Most of existing decentralized proportional-integral-derivative (PID) controller design

methods are naturally the extension of SISO PID tuning rules by simultaneously considering the loop interaction effects. Because the real interactions among control loops are controllers dependent, the performance of individual control loop cannot be evaluated without knowing the real controller parameters. Even though many researchers have tried to overcome this difficulty from different angles, the success has been largely limited to the low-dimensional (less than 3×3) processes. This has motivated us to examine the real loop interactions with implemented loop controllers to describe the interacted loops behaviors, and develop simple and effective decentralized PID controller design method especially for high dimensional processes.

- Block control structure selection: A block control structure would be preferred when the interactions among the control loops are so significant that desired performance can not be achieved by decentralized control. Even though some of existing techniques may lead to satisfactory block control structure selection, their applications are limited by either complex design procedure or without clear interpretations on physical meanings. This has motivated us to investigate the interactions transmitting rules in the closed system, quantify the interaction effect to individual control loop from another one, and develop a systematic approach to treat the control structure selection problem under a unified framework.

1.2 Objectives

The main objectives of this thesis is to provide new theories, tools and algorithms to measure loop interactions, evaluate DCLI of paired loops, describe the interacted loops behaviors, and design the decentralized PID controllers. Focusing on problems mentioned in Section 1.1, the objectives of the thesis are summarized as follows:

- Analyze the interaction effects between a particular loop and the others under their possible open and close status, propose a novel interaction measure, and develop a new loop pairing criterion to select the decentralized control configuration which has minimal loop interactions.

- Quantify the interaction effects to a particular control loop when the others closed in all probably sequences, derive the necessary and sufficient conditions for DCLI, and develop an effective algorithm to evaluate the DCLI of decentralized control structure.

- Evaluate the dynamic loop interactions by taking the decentralized controller into account, propose an effective method to describe the interacted loops behaviors, and develop an effective decentralized PID controller design procedure.

- Develop empirical rules to establish the equivalent transfer functions of common used low order models of the multivariable process, and propose a simple and effective decentralized internal model control (IMC) PID controller design algorithm.

- Investigate the interaction transmitting rules in the closed system, estimate the interaction effects to individual control loop from other individuals, and develop a systematic approach to treat the control structure selection problem under a unified framework.

1.3 Major Contribution of The Thesis

Major contributions of the thesis are summarized as follows:

(1) **Proposed a novel interaction measure as well as a new loop pairing criterion [60].** Control system configuration is a prerequisite for design of both decentralized control system and non-interacting/decoupling control

system. A novel interaction measure as well as a new loop pairing criterion is proposed in the thesis. By investigating four different cases of loop interactions, the decomposed relative interaction array (DRIA) is defined to evaluate the loop-by-loop interactions between a particularly loop and all other loops in their open and closed status. General Interaction (GI) based on the concept of interaction energy and DRIA is then introduced for loop interaction measure. Subsequently, a new loop-pairing criterion based on the GI is proposed for control system configuration.

(2) **Developed the necessary and sufficient conditions for DCLI and a simple and effective algorithm for evaluating the DCLI under decentralized control structure [61].** The flexibility to bring subsystems in and out of service while other loops are still under closed-loop control is very important for the situations when actuators or sensors in some subsystems fail. Through applying the left-right (LR) factorization to the DRIA, a decomposed relative interaction sequence (DRIS) is introduced to obtain important insights into the cause-effect results of loop interactions. By analyzing the relative interaction (RI) of an individual loop, the necessary and sufficient conditions for the DCLI of an individual loop under both single- and multiple-loop failure are derived. A simple and effective algorithm for evaluating the DCLI under decentralized control structure is developed.

(3) **Suggested an effective decentralized PID controller design procedure [62].** To extend the existing SISO controller design techniques to multivariable decentralized control systems, the interactions among control loops must be dealt with properly. Since the dynamic interactions in closed-loop control systems are controller dependent, there has no existing method for effectively measuring such interactions especially for high dimensional systems. By quantifying the dynamic loop interactions with the decentralized control characteristic being taken into account, an effective decentralized PID controller design procedure is developed.

(4) **Presented a simple yet effective algorithm to design decentralized IMC-PID controllers [63].** Even though more precise higher-order process models can be obtained by either physical model construction (following the mass and energy balance principles) or the classical parameter identification methods, from a practical point of view, the lower order process model is more convenient for controller design. Empirical rules for establishing equivalent transfer functions of six common used low order process models and determining parameters of their IMC based PID controllers are developed. 10 classical industrial processes are studied to verify the performance of the proposed decentralized IMC-PID controller design method.

(5) **Provided a systematic approach to treat the block control structure selection problem under a unified framework [64].** In case of existing significant interactions between control loops, a block-diagonal structure would be preferred for better performance and relative simple controller structure. By quantifying the interaction effects to individual control loop from other loops, a systematic approach to treat the control structure selection problem under a unified framework is developed. The synthesis of the control structure is performed in a straightforward manner using structure interaction acceptable index (SIAI). A Cai-He (C-H) diagram is proposed to facilitate control structure selection process.

1.4 Organization of The Thesis

The thesis is organized as follows:

Chapter 2 summarizes the main theoretical developments of this thesis. On the basis of the concept of DRIA, various new interaction measures are proposed to tackle control loop interactions from different angles: (i) The GI is introduced for determining the minimal loop interactions; (ii) The DRIS is

proposed to quantify the changes of interaction effect to a particular control loop when all other closed loops failed singly or multiply; (iii) The dynamic relative interaction (dRI) is proposed to estimate the dynamic interactions to individual control loop when the other control loops are under bandwidth-limited control; (iv) The DRGA is defined to evaluate the comprehensive transmitting interaction to an individual control loop from other individuals under full decentralized control. The four interaction measure forms the backbone of the whole thesis.

Chapter 3 proposes a novel interaction measure as well as a new loop pairing criterion. Loop pairings determined by this criterion have the minimum loop interactions in terms of interaction energy. The main contribution of this chapter is that it systematically analyzed the loop interaction from all aspects and derived a feasible solution for the problem. The effectiveness of the loop pairing criterion is demonstrated by several examples.

Chapter 4 presents a simple and effective algorithm for evaluating the DCLI of decentralized control structure. Through introducing the concept of decomposed relative interaction sequence, the maximum interactions from other loops under different combinations and sequences are derived, and consequently the necessary and sufficient conditions for the DCLI of an individual loop under both single- and multiple-loop failure. On the basis of the necessary and sufficient conditions, a simple and effective algorithm for verifying the DCLI for multivariable processes is developed. The usefulness of the proposed approach is illustrated by two classical examples.

Chapter 5 qualifies the dynamic loop interactions with the decentralized controller being taken into account, and develops an effective decentralized PID controller design procedure. On the basis of structure decomposition, the dynamic relative interaction is defined to derive the multiplicate model factors (MMFs) and construct the equivalent transfer functions. Consequently, controller parameters for each loop are determined by employing the single-

input-single-output controller tuning rules. The simulation results for two industrial systems show that the proposed design procedure is very effective and easy to be implemented.

Chapter 6 presents empirical rules for establishing equivalent transfer functions of all possible low order models, and develops a simple yet effective algorithm to design the decentralized IMC-PID controller. On the basis of the well know SISO IMC-PID controller design rules, the concept of design procedure proposed in Chapter 6 is extended to consider six commonly used low order process models. Empirical rules for establishing equivalent transfer functions of all these possible low order models are derived and a simple yet effective algorithm to design the decentralized IMC-PID controller is derived. A variety of 2×2, 3×3 and 4×4 industrial systems are studied in detail, and the simulation results conclude that the presented design algorithm is very simple and effective for both low and high dimensional processes.

Chapter 7 presents a new method to quantify the interaction effects to individual control loop from other individuals and a systematic approach to treat the block control structure selection problem under a unified frame work. By introducing DRGA, the overall interaction effects to individual control loop from another one are evaluated. A simple C-H diagram is proposed to facilitate control structure selection procedure. Two examples are presented to illustrate the advantages of the proposed approach.

Chapter 8 concludes the thesis and provides some possible future research directions.

Chapter 2

Main Theoretical Development

Most industrial processes are multivariable in nature and typically much more difficult to design and operate than single-input single-output (SISO) processes, due to the interactions that occur between the input and output variables [1, 2]. Therefore, interaction analysis must be performed as a prerequisite for both control structure selection and decentralized controller design. A number of methods [6, 12, 17, 65, 20] have been proposed to assess loop interaction from different angles. However, they fail to answer the following important problems:

- How to measure the loop-by-loop interactions between a particularly considered loop and all other loops in their open and closed status?
- What is the feasible definition of the minimal interactions?
- How to quantify the cause-effect results to individual control loop when some of others are taken out of service?
- What is the real interaction effect to individual control loop when the decentralized controller was taken into account?
- How to evaluate the comprehensive transmitting interaction to an individual control loop from another one in the closed system?

In this chapter, four different cases for testing the loop interaction are investigated, and the DRIA, which has a very clear physical interpretation is defined to evaluate the loop-by-loop interactions between a particularly considered loop and all other loops in their open and closed status. On the basis of the concept of DRIA, several new interaction measures are developed to describe interaction effects with respect to different design purposes: (i) The GI is introduced based on the concept of interaction energy and DRIA for determining control loop configuration with minimal loop interactions; (ii) The DRIS is developed to evaluate the cause-effect results of loop interaction for evaluating the DCLI of an individual control loop with respect to both single- and multiple-loop failures; (iii) The DRGA is proposed to quantify the comprehensive transmitting interaction to an individual control loop from other individuals for selecting control structures ranging from full decentralized control to full centralized control; (iv) The dRI is developed to estimate the dynamic interactions to individual control loop when others are under bandwidth-limited control and describe the interacted loop behaviors for designing decentralized controller. The proposed interaction measures are utilized to tackle the multivariable process analysis and control system design problems in the following chapters.

2.1 Preliminaries

We will deal with the general decentralized feedback configuration illustrated in Figure 2.1. It consists of the interconnected plant $\mathbf{G}(s) = [g_{ij}(s)]_{n\times n}$, the decentralized controller $\mathbf{C}(s) = \text{diag}\{c_i(s)\}$, and the pre-compensator $\mathbf{D} = [d_{ij}(s)]_{n\times n}$, which is an optional element used to compensate significant interactions between control loops to achieve satisfactory performance. $\mathbf{r}$, $\mathbf{u}$ and $\mathbf{y}$ are vectors of references, manipulated and controlled variables with their ith elements represented by $\mathbf{r}_i$, $\mathbf{u}_i$ and $\mathbf{y}_i$, respectively. Sometimes, we will omit the Laplace operator s for simplicity unless otherwise specified.

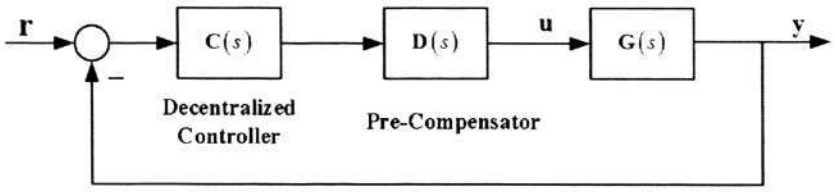

Figure 2.1: Block diagram of general multivariable control system

Definition 2.1.1 ([6]) *The relative gain for variable pairing* $\mathbf{y}_i - \mathbf{u}_j$ *is defined as the ratio of two gains representing, first, the process gain in an isolated loop and, second, the apparent process gain in the same loop when all other* $n-1$ *loops are closed*

$$\lambda_{ij} = \frac{(\partial \mathbf{y}_i / \partial \mathbf{u}_j)_{\mathbf{u}_{k\neq j}\text{constant}}}{(\partial \mathbf{y}_i / \partial \mathbf{u}_j)_{\mathbf{y}_{l\neq i}\text{constant}}} \tag{2.1}$$

and RGA, $\mathbf{\Lambda}(\mathbf{G})$*, in matrix form is defined as*

$$\mathbf{\Lambda}(\mathbf{G}) = [\lambda_{ij}] = \mathbf{G} \otimes \mathbf{G}^{-T} \tag{2.2}$$

where $\otimes$ *is the hadamard product and* $\mathbf{G}^{-T}$ *is the transpose of the inverse of* $\mathbf{G}$*.*

As a ratio, the relative gain indicates the degree to which the open-loop gain associated with a specific input-output pair is amplified or attenuated when the other control loops are closed. Very small relative gains imply significant amplification of the input-output gain, and very large relative gains indicate significant attenuation of the input-output gain. Negative relative gains indicate that the effective gain of the input-output pair will change direction when the other controllers are closed and is generally an undesirable pairing. Therefore, when the RGA pairing rule is followed, input and output variables paired with positive RGA elements that are closest to unity will result in minimum interaction from other control loops. The definition of the relative gain implies certain properties, including the fact that the sum of the elements in a given row or column is unity. The relative gain is also independent of the scaling of the process variables. Additional properties of the RGA are summarized in the textbook by McAvoy [13].

Definition 2.1.2 ([66]) *The relative interaction (RI) for loop pairing* $\mathbf{y}_i - \mathbf{u}_j$ *is defined as the ratio of two elements: the increment of the process gain after all other* $n-1$ *control loops are closed and the apparent gain in the same loop when all other control loops are open.*

$$\phi_{ij} = \frac{(\partial \mathbf{y}_i/\partial \mathbf{u}_j)_{\mathbf{y}_{l\neq i}\text{constant}} - (\partial \mathbf{y}_i/\partial \mathbf{u}_j)_{\mathbf{u}_{k\neq j}\text{constant}}}{(\partial \mathbf{y}_i/\partial \mathbf{u}_j)_{\mathbf{u}_{k\neq j}\text{constant}}}. \tag{2.3}$$

Unlike relative gain, the relative interaction focuses on both the magnitude and the direction of the increment portion of process gain after other control loops closed. Even though the interpretation of relative interaction is different from the relative gain, they are, nevertheless, equivalent through transformation of coordinates as

$$\phi_{ij} = \frac{1}{\lambda_{ij}} - 1.$$

Hence, the properties of relative interaction can be easily derived from the relative gain [66]. In the following development, we adopt relative interaction as a basic interaction measure because it is very simple to understand and can reflect the increment of process gain as well as the direction of interaction explicitly.

2.2 Decomposed Relative Interaction Analysis [60]

Since we are investigating the interactions between an arbitrary loop $\mathbf{y}_i - \mathbf{u}_j$ and all other loops of the multivariable system, the process from $\mathbf{u}$ to $\mathbf{y}$ can be explicitly expressed by

$$\mathbf{y}_i = g_{ij}\mathbf{u}_j + g_{i\bullet}^{ij}\mathbf{u}^j \tag{2.4}$$

$$\mathbf{y}^i = g_{\bullet j}^{ij}\mathbf{u}_j + \mathbf{G}^{ij}\mathbf{u}^j \tag{2.5}$$

where $\mathbf{G}^{ij}$ is the transfer function matrix $\mathbf{G}$ with its ith row and the jth column removed, and $g_{i\bullet}^{ij}$ and $g_{\bullet j}^{ij}$ indicate the ith row and the jth column of $\mathbf{G}$ with the

ijth element, g_{ij}, removed, respectively. For control loop $\mathbf{y}_i - \mathbf{u}_j$ and the remaining subsystem block, there are four interaction modes with respect to their open and closed states as shown in Figure 2.2.

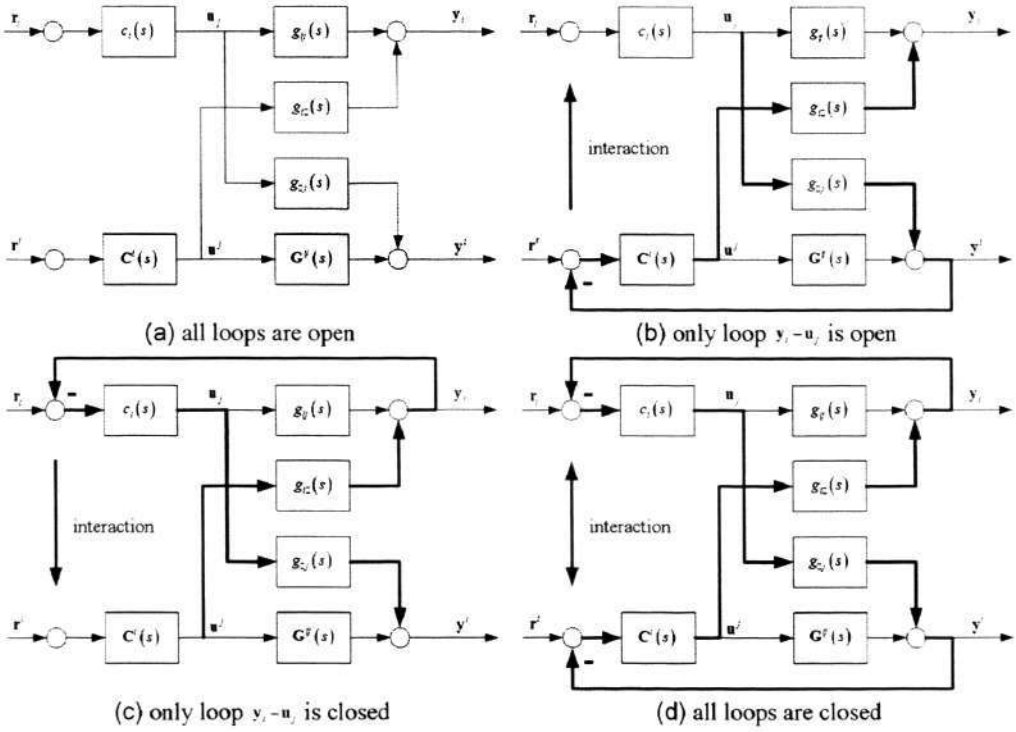

Figure 2.2: Four interaction modes for loop $\mathbf{y}_i - \mathbf{u}_j$

Mode 1. *All loops are open, as shown in Figure 2.2(a).* Obviously, no interaction exists among loops; thus, the process gain of an arbitrary pairing $\mathbf{y}_i - \mathbf{u}_j$ is the element g_{ij} in transfer function matrix $\mathbf{G}$.

Mode 2. *Loop $\mathbf{y}_i - \mathbf{u}_j$ is open and all other loops are closed, as shown in Figure 2.2(b).* This is the same condition for defining the RGA, and the direction of interactions is from the subsystem block of closed loops to loop $\mathbf{y}_i - \mathbf{u}_j$. The relative interaction can be obtained by matrix operation on equations 2.4 and 2.5 as

$$\phi_{ij} = -\frac{1}{g_{ij}} g^{ij}_{i\bullet} (\mathbf{G}^{ij})^{-1} g^{ij}_{\bullet j}. \tag{2.6}$$

Moreover, for an arbitrary loop $\mathbf{y}_k - \mathbf{u}_l$ in closed subsystem $\mathbf{G}^{ij}$, the process gain is affected by other control loops and according to definition 2.1.1, can be determined by

$$\hat{g}_{kl} = \frac{g_{kl}}{\lambda_{kl}^{ij}}, \tag{2.7}$$

where λ_{kl}^{ij} is the klth element of RGA $\mathbf{\Lambda}(\mathbf{G}^{ij})$.

Mode 3. *Loop $\mathbf{y}_i - \mathbf{u}_j$ is closed and all other loops are open, as shown in Figure 2.2(c).* In this case, the relative interaction is from closed loop $\mathbf{y}_i - \mathbf{u}_j$ to all other open loops, which can be derived from the 2×2 subsystem that includes loop $\mathbf{y}_i - \mathbf{u}_j$ and an arbitrary loop $\mathbf{y}_k - \mathbf{u}_l$ in subsystem $\mathbf{G}^{ij}$ ($k \neq i$ and $l \neq j$). The 2×2 subsystem is describes as

$$\begin{pmatrix} \mathbf{y}_i \\ \mathbf{y}_k \end{pmatrix} = \begin{pmatrix} g_{ij} & g_{il} \\ g_{kj} & g_{kl} \end{pmatrix} \begin{pmatrix} \mathbf{u}_j \\ \mathbf{u}_l \end{pmatrix}$$

Hence, according to definition 2.1.2, we obtain the relative interaction of loop $\mathbf{y}_k - \mathbf{u}_l$ from loop $\mathbf{y}_i - \mathbf{u}_j$ as

$$\phi_{ij,kl} = \frac{\triangle g_{ij,kl}}{g_{kl}} \tag{2.8}$$

where

$$\triangle g_{ij,kl} = -\frac{g_{il} g_{kj}}{g_{ij}} \tag{2.9}$$

is the incremental process gain of loop $\mathbf{y}_k - \mathbf{u}_l$ when loop $\mathbf{y}_i - \mathbf{u}_j$ is closed, and the subscript "ij, kl" indicates the relationship is to loop $\mathbf{y}_i - \mathbf{u}_j$ from loop $\mathbf{y}_k - \mathbf{u}_l$.

Mode 4. *All loops are closed, as shown in Figure 2.2(d).* In this case, the interaction between the closed loop $\mathbf{y}_i - \mathbf{u}_j$ and all other closed loops is bidirectional. Since the interaction from all other closed loops to control loop $\mathbf{y}_i - \mathbf{u}_j$ is covered by **Mode 2**. We now focus on investigating the interactions from

the closed loop $\mathbf{y}_i - \mathbf{u}_j$ to all other closed loops. Let $\mathbf{y}_k - \mathbf{u}_l$ indicate an arbitrary loop of the closed subsystem $\hat{\mathbf{G}}^{ij}$, then the subsystem that includes loops $\mathbf{y}_i - \mathbf{u}_j$ and $\mathbf{y}_k - \mathbf{u}_l$ is given as

$$\begin{pmatrix} \mathbf{y}_i \\ \mathbf{y}_k \end{pmatrix} = \begin{pmatrix} g_{ij} & g_{il} \\ g_{kj} & \hat{g}_{kl} \end{pmatrix} \begin{pmatrix} \mathbf{u}_j \\ \mathbf{u}_l \end{pmatrix}$$

Thus, the relative interaction from loop $\mathbf{y}_i - \mathbf{u}_j$ to the klth loop of closed subsystem $\hat{\mathbf{G}}^{ij}$ is obtained as

$$\psi_{ij,kl} = \frac{\triangle g_{ij,kl}}{\hat{g}_{kl}} \tag{2.10}$$

where $\triangle g_{ij,kl}$ is the increment of closed-loop process gain $\hat{g}_{kl}$ after loop $\mathbf{y}_i - \mathbf{u}_j$ is closed and it is the same as that shown in equation 2.9.

By extending eq 2.10 to all loops of the closed subsystem $\hat{\mathbf{G}}^{ij}$, we define the decomposed relative interaction array (DRIA) as following.

Definition 2.2.1 *The decomposed relative interaction array for loop pairing* $\mathbf{y}_i - \mathbf{u}_j$ *is defined as*

$$\mathbf{\Psi}_{ij} = [\psi_{ij,kl}]_{n-1 \times n-1} = \triangle \mathbf{G}^{ij} \odot \hat{\mathbf{G}}^{ij} \tag{2.11}$$

where $\odot$ *indicates element-by-element division, and*

$$\triangle \mathbf{G}^{ij} = -\frac{1}{g_{ij}} g^{ij}_{\bullet j} g^{ij}_{i \bullet} \tag{2.12}$$

is the incremental process gain matrix of subsystem $\hat{\mathbf{G}}^{ij}$ *after loop* $\mathbf{y}_i - \mathbf{u}_j$ *is closed.*

Theorem 2.2.1 *For an arbitrary loop pairing* $\mathbf{y}_i - \mathbf{u}_j$ *of multivariable process* $\mathbf{G}$*, its DRIA,* $\mathbf{\Psi}_{ij}$*, can be obtained by*

$$\mathbf{\Psi}_{ij} = \triangle \mathbf{G}^{ij} \otimes (\mathbf{G}^{ij})^{-T} \tag{2.13}$$

Proof. *From definition 2.1.1,*

$$\mathbf{\Lambda}(\mathbf{G}^{ij}) = \mathbf{G}^{ij} \odot \hat{\mathbf{G}}^{ij} = \mathbf{G}^{ij} \otimes (\mathbf{G}^{ij})^{-T}.$$

Then from equation 2.11, we have

$$\begin{aligned} \mathbf{\Psi}_{ij} &= \triangle\mathbf{G}^{ij} \otimes \mathbf{G}^{ij} \odot \mathbf{G}^{ij} \odot \hat{\mathbf{G}}^{ij} \\ &= \triangle\mathbf{G}^{ij} \otimes \mathbf{G}^{ij} \odot \mathbf{G}^{ij} \otimes (\mathbf{G}^{ij})^{-T} \\ &= \triangle\mathbf{G}^{ij} \otimes (\mathbf{G}^{ij})^{-T}. \end{aligned}$$

Furthermore, the relationship between RI and DRIA for an arbitrary loop pairing of system $\mathbf{G}$ is given by the following theorem.

Theorem 2.2.2 *For an arbitrary nonzero element g_{ij} of $\mathbf{G}$, the corresponding ϕ_{ij} is the sum of all elements in $\mathbf{\Psi}_{ij}$, i.e.,*

$$\phi_{ij} = \|\mathbf{\Psi}_{ij}\|_\Sigma = \sum_{k=1,\ k\neq i}^{n} \sum_{l=1,\ l\neq j}^{n} \psi_{ij,kl} \tag{2.14}$$

where $\|\bullet\|_\Sigma$ is the summation of all matrix elements.

Proof. *Using equations 2.6 and 2.12, we have*

$$\begin{aligned} \phi_{ij} &= -\frac{1}{g_{ij}} g_{i\bullet}^{ij} (\mathbf{G}^{ij})^{-1} g_{\bullet j}^{ij} \\ &= \|(-\frac{1}{g_{ij}} g_{\bullet j}^{ij} g_{i\bullet}^{ij}) \otimes (\mathbf{G}^{ij})^{-T}\|_\Sigma \\ &= \|(\triangle\mathbf{G}^{ij}) \otimes (\mathbf{G}^{ij})^{-T}\|_\Sigma \end{aligned}$$

Then from equation 2.13, we obtain the result of equation 2.14.

The significance of the DRIA are:

(i) From equations 2.7-2.8 and 2.10,

$$\psi_{ij,kl} = \frac{\triangle g_{ij,kl}}{\hat{g}_{kl}} = \frac{\triangle g_{ij,kl}}{g_{kl}} \frac{g_{kl}}{\hat{g}_{kl}} = \phi_{ij,kl} \lambda_{kl}^{ij}. \tag{2.15}$$

Thus, the relative interaction between control loops $\mathbf{y}_i - \mathbf{u}_j$ and $\mathbf{y}_k - \mathbf{u}_l$ is amplified or attenuated from $\phi_{ij,kl}$ to $\psi_{ij,kl}$ by a factor λ_{kl}^{ij} after the subsystem $\mathbf{G}^{ij}$ closed. Because the ideal situation is $\phi_{ij,kl} \to 0$ and $\lambda_{ij,kl} \to 1$, $\psi_{ij,kl}$ should be $\psi_{ij,kl} \to 0$ for minimal interactions.

(ii) Theorem 2.2.2 shows that the interaction effect to individual control loop $\mathbf{y}_i - \mathbf{u}_j$ is a cooperation results of all control loops in closed subsystem $\mathbf{G}^{ij}$. Since elements of $\mathbf{\Psi}_{ij}$ can be in different directions (signs), there inevitably have effects canceled by each other. Hence, small value of relative interaction ϕ_{ij} doesn't imply small loop-by-loop interactions. Conversely, a $\mathbf{\Psi}_{ij}$ with all elements small implies moderate interaction between control loop $\mathbf{y}_i - \mathbf{u}_j$ and subsystem $\mathbf{G}^{ij}$. Therefore, the DRIA obtains an important insight into the loop-by-loop interactions of closed system and provides an effective way to quantify them.

Remark 1. As an arbitrary element of $\mathbf{G}$, g_{ij} may be zero. In such a case, the values of $\phi_{ij,kl}$ and $\triangle g_{ij,kl}$ in equations 2.8 and 2.9 are indefinite. Fortunately, those variables are only used during the course of derivation (where $\epsilon \to 0$ may be used to replace the zero elements).

2.3 New Interaction Measures

As discussed in previous section, both relative gain and relative interaction can only reflect the overall interaction effect to individual control loop, thus they are necessary and sufficient for 2×2 system but becomes only necessary for higher dimensional system. Conversely, DRIA provides an effective way to quantify both magnitude and direction of the interaction effect between individual control loops.

However, it is of less convenience for DRIA to be applied directly due to its matrix form presentation. Also, different design issues are usually understood and solved from different angles. Therefore, based on the concept of DRIA, we here develop a series of simple and effective tools to analyze and measure loop interactions upon different design purposes.

2.3.1 General Interaction [60]

In order to extend the existing SISO controller tuning rules and have the closed-loop performance less deteriorated for decentralized control system design, the interactions between control loops are desired to be as small as possible. However, the conventional RGA based interaction measure can not accurately reflect the cause-effect interactions among control loops. Hence, based on the concept of interaction energy and DRIA, we define the general interaction (GI) for selection of loop pairings with minimal interactions.

Definition 2.3.1 *For an arbitrary loop pairing* $\mathbf{y}_i - \mathbf{u}_j$ *of multivariable process* $\mathbf{G}$, *its general interaction (GI)* ω_{ij} *is the interaction energy (2−norm) of matrix* $\mathbf{\Psi}_{ij}$, *and correspondingly* ω_{ij} *is the* ij*th element of the GI array (GIA)* $\mathbf{\Omega}$,

$$\mathbf{\Omega} \triangleq \{\omega_{ij} | \omega_{ij} = \|\mathbf{\Psi}_{ij}\|_2, \qquad i, j = 1,\ 2,\ \cdots,\ n\}, \tag{2.16}$$

where $\| \bullet \|_2$ *denotes the* $2-$*norm of the matrix defined as*

$$\|\mathbf{\Psi}_{ij}\|_2 \triangleq \sigma_{\max}(\mathbf{\Psi}_{ij})$$

Definition 2.3.1 takes $\mathbf{\Psi}_{ij}$ as a $n-1 \times n-1$ dimension vector and defines its "length" or "energy" as general interaction. Smaller GI indicates the overall interaction effects in all directions are small. Hence, GI provides a much better quantification of loop interactions than both relative gain and relative interaction, especially for higher dimensional processes.

On the basis of GI, we have developed a new loop pairing criterion as shown in Chapter 3.

2.3.2 Decomposed Relative Interaction Sequence [61]

Beside minimal interactions among control loops, the control system designer usually prefers that the selected decentralized control structure is structurally stable in face of single- or multiple-loop failure, i.e. decentralized closed-loop integrity. However, the RGA and NI based tools can not provide the necessary and sufficient conditions for DCLI evaluation. In order to evaluate the DCLI of the selected decentralized control structure, the changes of interaction effects to control loops should be investigated.

To facilitate our development, the transfer function matrix $\mathbf{G}$ will be re-arranged so that the selected loop pairings correspond to the diagonal elements of $\mathbf{G}$. Regarding the interaction effect to an arbitrary control loop $\mathbf{y}_i - \mathbf{u}_i$, it changes with respect to the single- or multiple-loop failure of the closed subsystem $\mathbf{G}^{ii}$. Since a series of single-loop failure results in multiple-loop failure, without loss of generality, we assume the remaining $n-1$ control loops of closed subsystem $\mathbf{G}^{ii}$ fail one-by-one i.e. in some sequence. It is easy to verify that there has as many as such $(n-1)!$ failure sequences. In order to clearly describe all possible failure sequences, we here define a failure index set M: $M = \{M_1, \cdots, M_k, \cdots, M_{(n-1)!}\}$, of which an individual failure index M_k contains $n-1$ different integers ranging from 1 to $n-1$: $M_k = (i_1^{M_k}, \cdots, i_p^{M_k}, \cdots, i_{n-1}^{M_k})$, where $i_p^{M_k}$ denotes the $(n-p)$th failed control loop under loop failure sequence M_k.

Let $\mathbf{\Psi}_{ii}^{M_k}$ indicates the DRIA with respect to failure index M_k, then, following the basic LR matrix factorization [67], the DRIA can be written as

$$\mathbf{\Psi}_{ii}^{M_k} = \mathbf{L}_{ii}^{M_k} \times \mathbf{R}_{ii}^{M_k}, \tag{2.17}$$

where $\mathbf{L}_{ii}^{M_k}$ is a $n-1 \times n-1$ lower triangular matrix with its diagonal elements

equal to unity and $\mathbf{R}_{ii}^{M_k}$ is a $n-1 \times n-1$ upper triangular matrix. We now can have the following theorem in terms of the decomposed relative interaction sequence (DRIS) to quantify the changes of interaction effect to individual control loop from the others in case of single or multiple of them fail.

Theorem 2.3.1 *For control loop $\mathbf{y}_i - \mathbf{u}_i$ in system $\mathbf{G}$, the DRIS with respect to an arbitrary failure index M_k consists of $n-1$ elements as*

$$\mathbf{S}_{ii}^{M_k} = \{s_{ii,1}^{M_k}, \cdots s_{ii,p}^{M_k}, \cdots, s_{ii,n-1}^{M_k}\}, \tag{2.18}$$

which satisfies

$$\phi_{ii,m}^{M_k} = \sum_{p=1}^{m} s_{ii,p}^{M_k}, \qquad m = 1, \cdots, n-1, \tag{2.19}$$

and the decomposed relative interaction factor (DRIF), $s_{ii,p}^{M_k}$, in DRIS, $\mathbf{S}_{ii}^{M_k}$, can be determined by

$$s_{ii,p}^{M_k} = \sum [\mathbf{L}_{ii}^{M_k}]_{\bullet p} \times \sum [\mathbf{R}_{ii}^{M_k}]_{p\bullet}, \tag{2.20}$$

where $\phi_{ii,m}^{M_k}$ is the relative interaction to control loop $\mathbf{y}_i - \mathbf{u}_i$ when other control loops fail in sequence M_k, $\sum$ indicates summation of all elements in vector, $\bullet p$ and $p\bullet$ indicate the pth column and row of corresponding matrix respectively.

Theorem 2.3.1 provides an effective method for quantifying the changes of interaction effects to a considered control loop in case of other loops fail. The physical meaning of DRIS is that, with respect to an arbitrary failure sequence M_k, if the first $n-p-1$ loops has failed, then the relative interaction to control loop $\mathbf{y}_i - \mathbf{u}_i$ will has a change of $s_{ii,p}^{M_k}$ after the $n-p$th loop failed.

The proof of theorem 2.3.1 and the necessary and sufficient conditions for DCLI as well as an algorithm for evaluating the DCLI of decentralized control structure, which are based on the concept of DRIS, have been developed as elaborated in Chapter 4.

2.3.3 Dynamic Relative Interaction [62]

It is well known that the real interaction effects between control loops are controller dependent and different from those derived under perfect control. In order to evaluate the interaction effects between control loops under limited bandwidth control, the dynamic relative interaction (dRI) is defined as following.

Theorem 2.3.2 *Suppose the multivariable process* $\mathbf{G}$ *was controlled by a decentralized controller has* $\mathbf{C}$*, then the dynamic DRIA of individual control loop* $\mathbf{y}_i - \mathbf{u}_i$ *is*

$$\mathbf{\Psi}_{ii} = \triangle\mathbf{G}_{ii} \otimes (\bar{\mathbf{G}}^{ii})^{-T}, \tag{2.21}$$

and the dRI, ϕ_{ii}*, is the summation of all elements of* $\mathbf{\Psi}_{ii}$*, i.e.*

$$\phi_{ii} = \|\mathbf{\Psi}_{ii}\|_\Sigma = \|\triangle\mathbf{G}_{ii} \otimes (\bar{\mathbf{G}}^{ii})^{-T}\|_\Sigma. \tag{2.22}$$

where $\bar{\mathbf{G}} = \mathbf{G} + \mathbf{C}^{-1}$

For decentralized PI or PID control, we have $\mathbf{C}^{-1}(j0) = \mathbf{0}$, and $\bar{\mathbf{G}}(j0) = \mathbf{G}(j0)$, which implies that the RI and the dRI are equivalent at steady state. However, because the dRI measure interactions under practical imperfect control conditions in frequency domain, it is more accurate in estimating the dynamic loop interactions and more effective in designing decentralized controllers.

Based on the concept of dRI, a general decentralized controller design procedure is developed in Chapter 5, which is further been applied to six common used low order process models to obtain the empirical rules of designing decentralized IMC-PID controller as shown in Chapter 6.

2.3.4 Decomposed Relative Gain Array [64]

To evaluate the interaction effects between the n individual control loops of closed system $\mathbf{G}$, the decomposed relative gain array (DRGA) is developed base on DRIA as following.

Theorem 2.3.3 *The DRGA, $\mathbf{\Gamma}$, is an $n \times n$ matrix with its element, γ_{ik}, determined by*

$$\mathbf{\Gamma} \triangleq \{\gamma_{ik} | \gamma_{ik} = \begin{cases} \frac{1}{2}(\alpha_{ik} + \beta_{ki}) & k \neq i \\ 1 & k = i \end{cases}, \quad i = 1, 2, \cdots, n\}, \tag{2.23}$$

where

$$\alpha_{ik} = \sum_{m=1, m \neq i}^{n} [\mathbf{\Psi}_{ii}]_{mk}, \tag{2.24}$$

and

$$\beta_{ki} = \sum_{m=1, m \neq i}^{n} [\mathbf{\Psi}_{ii}]_{km}, \tag{2.25}$$

are the relative interaction transmitted by individual element g_{ki} and g_{ik}, respectively.

Obviously, α_{ik} can be regarded as an output disturbance to the output of the kth control loop from the ith control loop, while β_{ki} can be regarded as an output disturbance to the output of the ith control loop from the kth control loop. Hence, as an average, the decomposed relative gain, γ_{ik}, comprehensively reflects the interaction to the control loop $\mathbf{y}_i - \mathbf{u}_i$ from control loop $\mathbf{y}_k - \mathbf{u}_k$ in the closed subsystem $\mathbf{G}$.

On the basis of the concept of DRGA, an algorithm for selecting control structures which range from full decentralized control to centralized control has been developed as elaborated in Chapter 7.

In this chapter, four different cases for testing the loop interaction have been investigated, and the decomposed relative interaction array (DRIA), which has a very clear physical interpretation was defined to evaluate the loop-by-loop interactions between a particularly considered loop and all other loops in their open and closed status. On the basis of DRIA, various new interaction measures were proposed to tackle control loop interactions from different angles: (i) The generalized interaction (GI) based on the concept of interaction energy and DRIA was introduced for determining the minimal loop interactions; (ii) The decomposed relative interaction sequence (DRIS) based on the LR factorization of DRIA was proposed to quantify the changes of interaction effect to a particular control loop when all other closed loops failed singly or multiply; (iii) The dynamic relative interaction (dRI) based the dynamic DRIA was proposed to estimate the dynamic interactions to individual control loop when the other control loops are under bandwidth-limited control; (iv) The decomposed relative gain array (DRGA) based on combination of interaction transmitting channels was defined to evaluate the comprehensive transmitting interaction to an individual control loop from other individuals under full decentralized control. The proposed interaction measures are utilized to tackle the multivariable process analysis and control system design problems in the following chapters.

Chapter 3

New Techniques for Assessing Loop Interactions in Multivariable Processes

In this chapter, we propose a new loop pairing criterion based on a new method for interaction measure. Four different cases for testing the loop interaction are investigated, and the decomposed relative interaction array (DRIA) is defined to evaluate the loop-by-loop interactions between a particularly considered loop and all other loops in their open and closed status. The generalized interaction (GI) that is based on the concept of interaction energy and DRIA is then introduced for loop interaction measures. Consequently, a new loop-pairing criterion based on the GI is proposed for control structure configuration. Several examples are given to demonstrate the effectiveness of the proposed variable-pairing criterion.

The organization of this chapter is as follows: Section 3.1 presents a brief review of the conventional RGA- and NI-based loop-pairing criterion and their limitations. It is then followed by the mathematical derivation of DRIA based on the decomposed interaction analysis in section 3.2. Subsequently, a new loop-pairing criterion based on the new interaction measure is proposed in section 3.3. Finally, two examples

are employed to illustrate the effectiveness of the proposed loop-pairing criterion in section 3.4.

3.1 Preliminaries

Throughout this chapter, it is assumed that the system we are dealing with is square $(n \times n)$, open-loop stable, and nonsingular at steady state with a decentralized control structure as shown in Figure 3.1. The transfer function matrix relating outputs and inputs of the process, its steady-state gain matrix, and individual elements are represented by $\mathbf{G}(s)$, $\mathbf{G}(0)$ (or simply $\mathbf{G} \in \mathbb{R}^{n\times n}$), and g_{ij}, respectively. $\mathbf{G}^{ij}$ denotes the matrix $\mathbf{G}$ with its ith row and jth column removed. $\mathbf{r}$, $\mathbf{u}$, and $\mathbf{y}$ are vectors of references and manipulated and controlled variables, while $\mathbf{r}_i$, $\mathbf{u}_i$, and $\mathbf{y}_i$ are the ith references and manipulated and controlled variables, and $\mathbf{r}^i$, $\mathbf{u}^i$, and $\mathbf{y}^i$ denote the reference, input, and output vectors with variables $\mathbf{r}_i$, $\mathbf{u}_i$, and $\mathbf{y}_i$ removed.

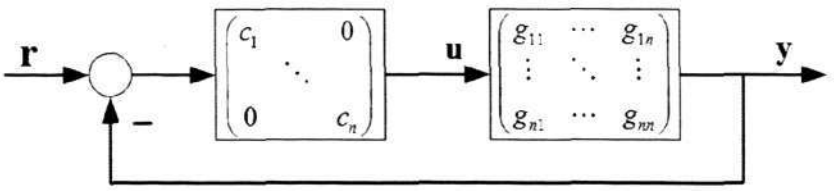

Figure 3.1: Decentralized control of multivariable systems.

Because we are investigating the interactions between an arbitrary loop $\mathbf{y}_i - \mathbf{u}_j$ and all other loops of the multivariable system, the process from $\mathbf{u}$ to $\mathbf{y}$ can be explicitly expressed by

$$\begin{aligned} \mathbf{y}_i &= g_{ij}\mathbf{u}_j + g_{i\bullet}^{ij}\mathbf{u}^j \\ \mathbf{y}^i &= g_{\bullet j}^{ij}\mathbf{u}_j + \mathbf{G}^{ij}\mathbf{u}^j \end{aligned} \tag{3.1}$$

where $g_{i\bullet}^{ij}$ and $g_{\bullet j}^{ij}$ denote the ith row vector and the jth column vector of matrix

$\mathbf{G}$ with element g_{ij} removed.

3.1.1 Niederlinski Index

When the RGA pairing rule is followed [6], input and output variables paired with positive RGA elements that are closest to unity will result in minimum interaction from other control loops. Even though this pairing rule gives a clear indication for minimum interaction, it is often necessary (especially with 3×3 and higher dimensional systems) to use this rule in conjunction with stability considerations provided by the following theorem originally given by Niederlinski [12] and later modified by Grosdidier and Morari [11].

Theorem 3.1.1 *Consider an $n \times n$ multivariable system whose manipulated and controlled variables have been paired as follows: $\mathbf{y}_1 - \mathbf{u}_1$, $\mathbf{y}_2 - \mathbf{u}_2$, $\cdots, \mathbf{y}_n - \mathbf{u}_n$, resulting in a transfer function model of the form*

$$\mathbf{y} = \mathbf{G}\mathbf{u}$$

Further, let each element of $\mathbf{G}$, g_{ij}, be rational and open-loop stable and n individual feedback controllers (which have integral action) be designed for each loop so that each one of the resulting n feedback control loops is stable when all other $n-1$ loops are open. Then, under closed-loop conditions in all n loops, the multiloop system will be unstable for all possible values of controller parameters (i.e., it will be "structurally monotonically unstable") if the NI defined below is negative, i.e.,

$$\mathrm{NI} = \frac{\det[\mathbf{G}(0)]}{\Pi_{i=1}^{n} g_{ii}(0)} < 0 \tag{3.2}$$

One point that must be emphasized is that eq 3.2 is both necessary and sufficient only for 2×2 systems, but for higher dimensional systems, it provides only sufficient conditions: i.e., if eq 3.2 holds, then the system is definitely unstable; otherwise, the system may, or may not, be unstable because the stability will, in this case, depend on the values taken of the controller parameters.

3.1.2 RGA-based Loop-Pairing Criterion [68]

Manipulated and controlled variables in a decentralized control system should be paired in the following way:

(i) The paired RGA elements are closest to 1.0.

(ii) NI is positive.

(iii) All paired RGA elements are positive.

(iv) Large RGA elements should be avoided.

In this criterion, both RGA and NI offer important insights into the issue of control structure selection. RGA is used to measure interactions, while NI is used as a sufficient condition to screen out the closed-loop unstable pairings. However, for higher dimensional systems, the RGA element λ_{ij} only takes the overall interaction from all other closed loops to the loop $\mathbf{y}_i - \mathbf{u}_j$ into consideration; it failed to yield information on the interactions from other individual loops to the loop $\mathbf{y}_i - \mathbf{u}_j$. Consequently, the control structure configuration selected according to the RGA- and NI-based loop pairing criterion may result in an undesirable control system performance. Example 1 illustrates this point.

Example 1.

Consider the process [16]

$$\mathbf{G}(s) = \frac{1-s}{(1+5s)^2}\begin{pmatrix} 1 & -4.19 & -25.96 \\ 6.19 & 1 & -25.96 \\ 1 & 1 & 1 \end{pmatrix}$$

The steady-state RGA is

$$\mathbf{\Lambda}[\mathbf{G}(0)] = \begin{pmatrix} 1 & 5 & -5 \\ -5 & 1 & 5 \\ 5 & -5 & 1 \end{pmatrix}$$

which results in two pairing structures with positive RGA and NI values as shown in Table 3.1.

Table 3.1: Feasible pairing structure for Example 1

	feasible pairing structure	
	$1-1/2-2/3-3$	$1-2/2-3/3-1$
RGA	$1-1-1$	$5-5-5$
NI	26.9361	0.2476

Hence, according to the RGA-based loop-pairing criterion, the pairing of $1-1/2-2/3-3$ should be preferred for the zero interaction to any one loop from all other closed loops. However, the resulting closed-loop performance for the pairing $1-2/2-3/3-1$ is significantly better than that of $1-1/2-2/3-3$ based on the same controller tuning rule [16]. Through analysis, the main reasons can be explained as follows:

(i) For the pairing of $1-1/2-2/3-3$, if loops $\mathbf{y}_2-\mathbf{u}_2$ and $\mathbf{y}_3-\mathbf{u}_3$ are closed one by one, the gain of loop $\mathbf{y}_1-\mathbf{u}_1$ will first increase by a factor of about 27 and then decrease by another factor of about 27; consequently, as reflected by the RGA, the gain of loop $\mathbf{y}_1-\mathbf{u}_1$ is not changed after all other loops are closed.

(ii) For the pairing of $1-2/2-3/3-1$, if loops $\mathbf{y}_2-\mathbf{u}_3$ and $\mathbf{y}_3-\mathbf{u}_1$ are closed one by one, the gain of loop $\mathbf{y}_1-\mathbf{u}_2$ will first increase by a factor of about 1.24 and then decrease by another factor of about 6.2; consequently, as reflected by the RGA, the gain of loop $\mathbf{y}_1-\mathbf{u}_2$ is decreased by a factor of about 5 after all other loops are closed.

Hence, even the RGA demonstrates that the closed loop gain of loop $\mathbf{y}_1-\mathbf{u}_1$ in the pairing of $1-1/2-2/3-3$ is unchanged; the interactions among loops are significant. On the contrary, even the gain of loop $\mathbf{y}_1-\mathbf{u}_2$ is decreased by a factor of about 5 after all other loops are closed; the interactions among loops in

the pairing of $1-2/2-3/3-1$ are smaller. This example reveals that both the overall interaction to the considered loop from all other closed loops and individual interactions among loops will affect the overall closed-loop performance. Therefore, a loop-by-loop analysis to establish individual interaction cause-effect relations is necessary for developing a new and effective interaction measure.

3.2 Decomposed Interaction Analysis

To investigate the interactions between an arbitrary loop $\mathbf{y}_i - \mathbf{u}_j$ and all other loops of the multivariable processes in their open and closed states, we use the relative interaction (RI) [66, 69, 70, 71] to measure the interactions among loops because it can directly reflect the increment of process gain and the direction of interaction with its sign.

Definition 3.2.1 ([66, 69, 70, 71]) *The RI for loop pairing $\mathbf{y}_i - \mathbf{u}_j$ is defined as the ratio of two elements: the increment of the process gain after all other control loops are closed and the apparent gain in the same loop when all other control loops are open.*

$$\phi_{ij} = \frac{(\partial \mathbf{y}_i/\partial \mathbf{u}_j)_{\mathbf{y}_{l\neq i}\text{constant}} - (\partial \mathbf{y}_i/\partial \mathbf{u}_j)_{\mathbf{u}_{k\neq j}\text{constant}}}{(\partial \mathbf{y}_i/\partial \mathbf{u}_j)_{\mathbf{u}_{k\neq j}\text{constant}}} = \frac{1}{\lambda_{ij}} - 1 \tag{3.3}$$

Equation 3.3 shows that, even though the interpretation of RI is different from the RGA, they are, nevertheless, equivalent through transformation of coordinates. Hence, the properties of RI can be easily derived from the RGA [66, 69, 70, 71].

For an arbitrary loop $\mathbf{y}_i - \mathbf{u}_j$ and the remaining subsystem block, there are four interaction scenarios corresponding to the combination of their open and closed states, which are listed in Table 3.2 and indicated in Figure 3.2.

Case 1. All loops are open, as shown in Figure 3.2(a). Obviously, no interaction exists among loops; thus, the process gain of an arbitrary pairing $\mathbf{y}_i - \mathbf{u}_j$ is

Table 3.2: Four interaction scenarios for loop $\mathbf{y}_i - \mathbf{u}_j$ [a]

case	loop $\mathbf{y}_i - \mathbf{u}_j$	all other loops	Figure 2
1	OL	OL	a
2	OL	CL	b
3	CL	OL	c
4	CL	CL	d

[a] OL and CL mean open loop and closed loop, respectively.

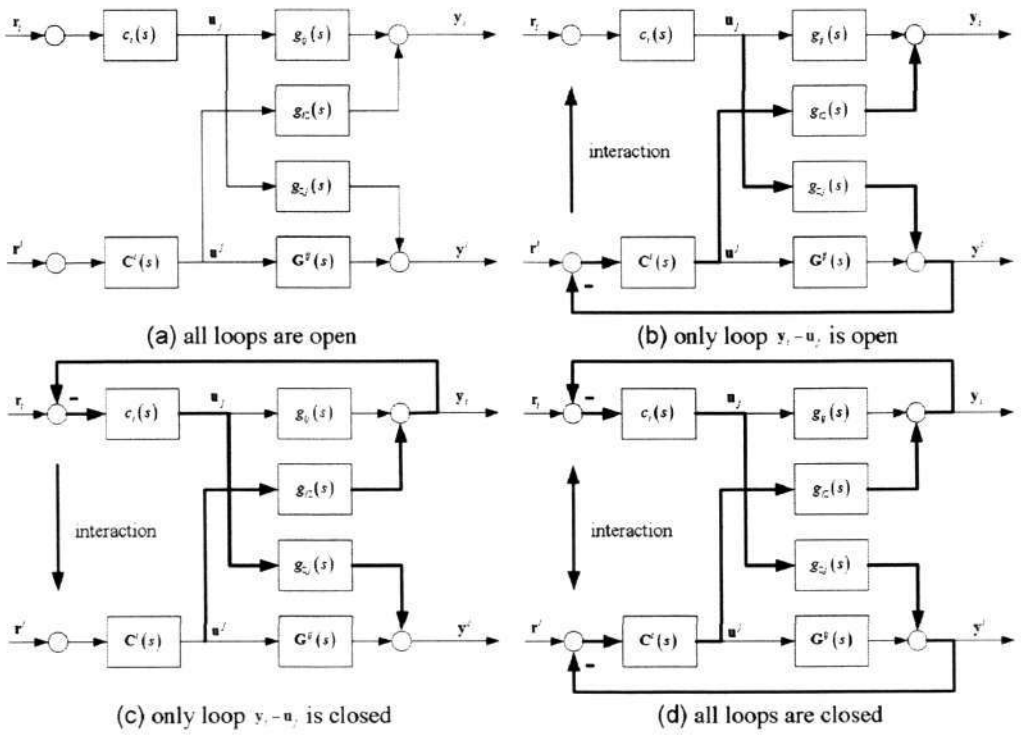

Figure 3.2: Four interaction scenarios for loop $\mathbf{y}_i - \mathbf{u}_j$

the element g_{ij} in transfer function matrix $\mathbf{G}$.

Case 2. Loop $\mathbf{y}_i - \mathbf{u}_j$ is open and all other loops are closed, as shown in Figure 3.2(b). This is the very condition for deriving the RGA, and the direction of interactions is from the subsystem block of closed loops to loop $\mathbf{y}_i - \mathbf{u}_j$. RI can be obtained by matrix operation as

$$\phi_{ij} = -\frac{1}{g_{ij}} g^{ij}_{i\bullet} (\mathbf{G}^{ij})^{-1} g^{ij}_{\bullet j} \tag{3.4}$$

Case 3. Loop $\mathbf{y}_i - \mathbf{u}_j$ is closed and all other loops are open, as shown in Figure 3.2(c). In this case, the interaction is from closed loop $\mathbf{y}_i - \mathbf{u}_j$ to all other open loops, and the RI can be derived from the 2×2 subsystem that includes loop $\mathbf{y}_i - \mathbf{u}_j$ and an arbitrary loop $\mathbf{y}_k - \mathbf{u}_l$ of subsystem $\mathbf{G}^{ij}$ ($k \neq i$ and $l \neq j$). This describes the 2×2 subsystem as

$$\begin{pmatrix} \mathbf{y}_i \\ \mathbf{y}_k \end{pmatrix} = \begin{pmatrix} g_{ij} & g_{il} \\ g_{kj} & g_{kl} \end{pmatrix} \begin{pmatrix} \mathbf{u}_j \\ \mathbf{u}_l \end{pmatrix}$$

Hence, according to definition 2, we obtain the RI of loop $\mathbf{y}_k - \mathbf{u}_l$ from loop $\mathbf{y}_i - \mathbf{u}_j$ as

$$\phi_{kl}^{ij} = \frac{g_{kl}|_{\mathbf{y}_i - \mathbf{u}_j,\ \mathrm{CL}} - g_{kl}}{g_{kl}} = \frac{\triangle g_{kl}^{ij}}{g_{kl}} \tag{3.5}$$

where

$$\triangle g_{kl}^{ij} = -g_{il} g_{kj} / g_{ij} \tag{3.6}$$

is the incremental process gain of loop $\mathbf{y}_k - \mathbf{u}_l$ when loop $\mathbf{y}_i - \mathbf{u}_j$ is closed. By extending eq 3.5, 3.6 to all loops of the subsystem $\mathbf{G}^{ij}$, we have

$$\mathbf{\Phi}^{ij} = (\mathbf{G}^{ij}|_{\mathbf{y}_i - \mathbf{u}_j,\ \mathrm{CL}} - \mathbf{G}^{ij}) \odot \mathbf{G}^{ij} = \triangle \mathbf{G}^{ij} \odot \mathbf{G}^{ij} \tag{3.7}$$

where $\odot$ indicates element-by-element division, and

$$\triangle \mathbf{G}^{ij} = -\frac{1}{g_{ij}} g_{\bullet j}^{ij} g_{i\bullet}^{ij} \tag{3.8}$$

is the incremental process gain matrix of subsystem $\mathbf{G}^{ij}$ when loop $\mathbf{y}_i - \mathbf{u}_j$ is closed. Thus, $\mathbf{\Phi}^{ij}$ is called the RIA to the open subsystem $\mathbf{G}^{ij}$ when loop $\mathbf{y}_i - \mathbf{u}_j$ is closed.

Case 4. All loops are closed, as shown in Figure 3.2(d). In this case, the interaction between the closed loop $\mathbf{y}_i - \mathbf{u}_j$ and all other closed loops is bidirectional. Because the interaction to loop $\mathbf{y}_i - \mathbf{u}_j$ from all other closed loops is the same as what has been studied in case 2, the interactions in this direction are not considered here. We now focus on the interaction from the isolated loop $\mathbf{y}_i - \mathbf{u}_j$ to all other closed loops.

Suppose all loops of subsystem $\mathbf{G}^{ij}$ are closed and the following:

(i) If loop $\mathbf{y}_i - \mathbf{u}_j$ is open, then the gain of an arbitrary loop $\mathbf{y}_k - \mathbf{u}_l$ is affected by the RGA value of $\mathbf{G}^{ij}$; therefore, according to the definition of RGA, it is

$$\hat{g}_{kl} = g_{kl}/\lambda_{kl}^{ij} \tag{3.9}$$

where "arc" indicates the changed process gain in the closed subsystem $\mathbf{G}^{ij}$. When eq 3.9 is extended to all loops of subsystem $\mathbf{G}^{ij}$, the closed-loop transfer function matrix is obtained as

$$\hat{\mathbf{G}}^{ij} = \mathbf{G}^{ij} \odot \mathbf{\Lambda}^{ij} \tag{3.10}$$

(ii) If loop $\mathbf{y}_i - \mathbf{u}_j$ is closed, then the subsystem that includes loops $\mathbf{y}_i - \mathbf{u}_j$ and $\mathbf{y}_k - \mathbf{u}_l$ in the closed subsystem $\hat{\mathbf{G}}^{ij}$ is given as

$$\begin{pmatrix} \mathbf{y}_i \\ \mathbf{y}_k \end{pmatrix} = \begin{pmatrix} g_{ij} & g_{il} \\ g_{kj} & \hat{g}_{kl} \end{pmatrix} \begin{pmatrix} \mathbf{u}_j \\ \mathbf{u}_l \end{pmatrix}$$

Thus, the RI from loop $\mathbf{y}_i - \mathbf{u}_j$ to loop $\mathbf{y}_k - \mathbf{u}_l$ is obtained as

$$\psi_{kl}^{ij} = \frac{\hat{g}_{kl}|_{\mathbf{y}_i - \mathbf{u}_j,\ \mathrm{CL}} - \hat{g}_{kl}}{\hat{g}_{kl}} = \frac{\triangle g_{kl}^{ij}}{\hat{g}_{kl}} \tag{3.11}$$

where $\triangle g_{kl}^{ij}$ is the increment of closed-loop process gain $\hat{g}_{kl}$ after loop $\mathbf{y}_i - \mathbf{u}_j$ is closed and it is the same as that shown in eq 3.6. Extending eq 3.11 to all loops of the subsystem $\hat{\mathbf{G}}^{ij}$, we obtain

$$\mathbf{\Psi}_{ij} = (\hat{\mathbf{G}}^{ij}|_{\mathbf{y}_i - \mathbf{u}_j,\ \mathrm{CL}} - \hat{\mathbf{G}}^{ij}) \odot \hat{\mathbf{G}}^{ij} = \triangle \mathbf{G}^{ij} \odot \hat{\mathbf{G}}^{ij} \tag{3.12}$$

where $\triangle \mathbf{G}^{ij}$ is the incremental matrix of subsystem $\hat{\mathbf{G}}^{ij}$ after loop $\mathbf{y}_i - \mathbf{u}_j$ is closed and it is the same as that shown in eq 3.8. Thus, $\mathbf{\Psi}_{ij}$ is called the RIA to the closed subsystem $\hat{\mathbf{G}}^{ij}$, which reflects the interactions to $\hat{\mathbf{G}}^{ij}$ when loop $\mathbf{y}_i - \mathbf{u}_j$ is closed.

Remark 1. As an arbitrary element of $\mathbf{G}$, g_{ij} may be zero. In such a case, the values of $\triangle g_{kl}^{ij}$ and ϕ_{kl}^{ij} in eq 3.5, 3.6 are indefinite. Fortunately, those variables are only used during the course of derivation (where $\epsilon \to 0$ may be used to replace the zero elements).

For practical calculation, $\mathbf{\Psi}_{ij}$ of the ijth element g_{ij} can be directly obtained by substituting eq 2.2 with eq 3.10 into eq 3.12 to result in

$$\mathbf{\Psi}_{ij} = \triangle \mathbf{G}^{ij} \otimes (\mathbf{G}^{ij})^{-T} \tag{3.13}$$

To explore the inherent relationship between RGA and RI and on the basis of the definition of the RGA, rewrite eq 3.11 as

$$\psi_{kl}^{ij} = \frac{\triangle g_{kl}^{ij}}{\hat{g}_{kl}^{ij}} = \frac{\triangle g_{kl}^{ij}}{g_{kl}} \frac{g_{kl}}{\hat{g}_{kl}} = \phi_{kl}^{ij} \lambda_{kl}^{ij} \tag{3.14}$$

Extending eq 3.14 to all loops of subsystem $\hat{\mathbf{G}}^{ij}$, we obtain another important matrix form for $\mathbf{\Psi}_{ij}$

$$\mathbf{\Psi}_{ij} = \mathbf{\Phi}^{ij} \otimes \mathbf{\Lambda}^{ij} \tag{3.15}$$

Furthermore, the relationship between ϕ_{ij} and $\mathbf{\Psi}_{ij}$ for an arbitrary nonzero element of system $\mathbf{G}$ is given by the following theorem.

Theorem 3.2.1 *For an arbitrary nonzero element g_{ij} of $\mathbf{G}$, the corresponding ϕ_{ij} is the sum of all elements in $\mathbf{\Psi}_{ij}$, i.e.,*

$$\phi_{ij} = \|\mathbf{\Psi}_{ij}\|_{\Sigma} = \sum_{k=1,\ k\neq i}^{n} \sum_{l=1,\ l\neq j}^{n} \psi_{kl}^{ij} \tag{3.16}$$

where $\| \bullet \|_{\Sigma}$ is the summation of all matrix elements.

Proof.

Using eqs 3.4 and 3.7-3.8, we have

$$\begin{aligned}\phi_{ij} &= -\frac{1}{g_{ij}} g_{i\bullet}^{ij} (\mathbf{G}^{ij})^{-1} g_{\bullet j}^{ij} \\ &= \|(-\frac{1}{g_{ij}} g_{\bullet j}^{ij} g_{i\bullet}^{ij}) \otimes (\mathbf{G}^{ij})^{-T}\|_{\Sigma} \\ &= \|(\triangle \mathbf{G}^{ij}) \otimes (\mathbf{G}^{ij})^{-T}\|_{\Sigma}\end{aligned}$$

Then from eq 3.13, we obtain the result of eq 3.16.

Because $\mathbf{\Psi}_{ij}$ reveals the information on loop-by-loop interaction, we define it as DRIA.

The significances of the development in this section are as follows:

(i) Equation 3.5-3.6 indicates that the pairing structure with a small value of ϕ_{kl}^{ij}, i.e., $\phi_{kl}^{ij} \to 0$, should be preferred.

(ii) Equation 3.11 indicates that a large value of ψ_{kl}^{ij} implies that the interaction from the closed loop $\mathbf{y}_i - \mathbf{u}_j$ to an arbitrary loop $\mathbf{y}_k - \mathbf{u}_l$ in the closed subsystem $\hat{\mathbf{G}}^{ij}$ is large. Therefore, the corresponding pairing structure should be avoided.

(iii) Equation 3.14 indicates that ψ_{kl}^{ij}, because the RI from loop $\mathbf{y}_i - \mathbf{u}_j$ to loop $\mathbf{y}_k - \mathbf{u}_l$ in the closed subsystem $\hat{\mathbf{G}}^{ij}$ is the product of λ_{kl}^{ij} and ϕ_{kl}^{ij} and because the ideal situation is $\lambda_{kl}^{ij} \to 1$ and $\phi_{kl}^{ij} \to 0$, ψ_{kl}^{ij} should be $\psi_{kl}^{ij} \to 0$ for minimal interactions.

(iv) Equation 3.15 indicates that, compared with case 3, the RI from loop $\mathbf{y}_i - \mathbf{u}_j$ to an arbitrary loop $\mathbf{y}_k - \mathbf{u}_l$ of the subsystem $\mathbf{G}^{ij}$ in case 4 is changed by a factor of λ_{kl}^{ij}, whereas this RGA is determined by the other loops of subsystem $\mathbf{G}^{ij}$; thus, the element ψ_{kl}^{ij} of DRIA reflects more information on the interaction effect to $\mathbf{y}_i - \mathbf{u}_j$ from all of the other loops working together. Apparently,

the best pairing structure should be $\lambda_{kl}^{ij} \to 1$, which is consistent with the conventional pairing rule.

(v) Equation 3.16 indicates that $\mathbf{\Psi}_{ij}$ given in a matrix form provides loop-by-loop information of the RIs between $\mathbf{y}_i - \mathbf{u}_j$ and all other loops as well as their distributions; therefore, it is more precise than ϕ_{ij} in measuring the loop interactions.

To illustrate the implication of DRIA in analyzing loop interactions, we continue with example 1.

Example 1 continued

For the two variable pairings derived from example 1, the values of RGA, RI, and DRIA are listed in Table 3.3. Table 3.3 clearly shows the following:

(i) $\lambda_{11} = 1$ and $\phi_{11} = 0$ indicate that there are no interactions to loop $\mathbf{y}_1 - \mathbf{u}_1$ when all other loops are closed.

(ii) ϕ_{11} is the summation of all elements in corresponding $\mathbf{\Psi}_{11}$, as given in eq 3.16, but $\phi_{11} = 0$ does not necessarily mean that all elements of $\mathbf{\Psi}_{11}$ are zeros; some of them can even be large values.

(iii) From eq 3.14, ψ_{32}^{11} in $\mathbf{\Psi}_{11}$ is the product of ϕ_{32}^{11} and λ_{32}^{11}. The large value of $\psi_{32}^{11} = 4.0346$ indicates that either ϕ_{32}^{11} or λ_{32}^{11} is large, which points out that the interaction between loops $\mathbf{y}_1 - \mathbf{u}_1$ and $\mathbf{y}_3 - \mathbf{u}_2$ is large (a large ϕ_{32}^{11} value implies severe interaction between loops $\mathbf{y}_1 - \mathbf{u}_1$ and $\mathbf{y}_3 - \mathbf{u}_2$ when the subsystem $\mathbf{G}^{11}$ is open, while a large λ_{32}^{11} value implies that the gain of loop $\mathbf{y}_3 - \mathbf{u}_2$ will undergo a big change after all other loops in subsystem $\mathbf{G}^{11}$ are closed).

(iv) For the $1-2/2-3/3-1$ pairing, even though $\lambda_{ii} = 5$, $\phi_{ii} = -0.8$ is not as good as those of the $1-1/2-2/3-3$ pairing based on the RGA loop-pairing

criterion; the smaller elements in DRIA imply smaller interaction between the considered loop and the other loops.

Table 3.3: Values of RGA, RI and DRIA corresponding to different pairing structures

	feasible pairing structure	
	$1-1/2-2/3-3$	$1-2/2-3/3-1$
RGA	$1/1/1$	$5/5/5$
RI	$0/0/0$	$-0.8/-0.8/-0.8$
DRIA	$\mathbf{\Psi}_{11}=\begin{pmatrix}0.9620 & -5.9604\\ 4.0346 & 0.9629\end{pmatrix}$ $\mathbf{\Psi}_{22}=\begin{pmatrix}0.9620 & 4.0346\\ -5.9604 & 0.9629\end{pmatrix}$ $\mathbf{\Psi}_{33}=\begin{pmatrix}0.9638 & -5.9657\\ 4.0382 & 0.9638\end{pmatrix}$	$\mathbf{\Psi}_{12}=\begin{pmatrix}0.0074 & 0.1927\\ 0.1927 & -1.1929\end{pmatrix}$ $\mathbf{\Psi}_{23}=\begin{pmatrix}-1.1927 & 0.1927\\ 0.1925 & 0.0074\end{pmatrix}$ $\mathbf{\Psi}_{31}=\begin{pmatrix}0.1927 & 0.0074\\ -1.1927 & 0.1925\end{pmatrix}$

The analysis above suggests that the RGA and RI may not be able to reflect the interactions among loops accurately, while through DRIA analysis, loop interactions in the matrix form can be revealed categorically.

3.3 New Loop-Pairing Criterion

Based on the DRIA, we can now define loop-by-loop interaction energy as below.

Definition 3.3.1 *The GI ω_{ij} is the interaction "energy"(2−norm) of matrix $\mathbf{\Psi}_{ij}$, and correspondingly ω_{ij} is the ijth element of the GI array (GIA) $\mathbf{\Omega}$*

$$\mathbf{\Omega} \triangleq \{\omega_{ij} | \omega_{ij} = \|\mathbf{\Psi}_{ij}\|_2, \qquad i,j = 1,\ 2,\ \cdots,\ n\} \tag{3.17}$$

where $\| \bullet \|_2$ denotes the 2−norm of the matrix defined as

$$\|\mathbf{\Psi}_{ij}\|_2 \triangleq \sigma_{\max}(\mathbf{\Psi}_{ij})$$

Equation 3.17 represents the interaction "energy" to all closed loops of the subsystem $\mathbf{G}^{ij}$ from loop $\mathbf{y}_i - \mathbf{u}_j$. Moreover, it also reflects the interaction energy to loop $\mathbf{y}_i - \mathbf{u}_j$ from all remaining $n-1$ closed loops in $\mathbf{G}$. Therefore, GI reflects the intensity of the interactions among all loops.

In analogy to RGA and NI, we here provide some important properties of the GI:

(i) The GI only depends on the steady-state gain of the multivariable system.

(ii) The GI is not affected by any permutation of $\mathbf{G}$.

(iii) The GI is scaling-independent (e.g., independent of units chosen for $\mathbf{u}$ and $\mathbf{y}$); this property is easily proven from the property of RGA, eqs 3.5, 3.6, 3.7, 3.8, 3.15, and 3.17.

(iv) If the transfer function matrix $\mathbf{G}$ is diagonal or triangular, the corresponding GI is equal to zero.

The new loop-pairing criterion based on definition 3 is given as follows:

New Loop-Pairing Criterion

Manipulated and controlled variables in a decentralized control system should be paired in such a way that (i) all paired RGA elements are positive, (ii) NI is positive, and (iii) the pairings have the smallest ω_{ij} value.

Example 1. Continued

For the two possible pairings, the corresponding RGA, RI, and ω_{ij} values are shown in Table 3.4.

Thus, on the basis of the new loop-pairing criterion, the second pairing is preferred, which draws the same conclusion as that in ref [16].

Remark 2.

For two or more pairing structures that have passed all three variable-pairing steps but with similar GI values, the pairing structure that has the smallest product of

Table 3.4: Corresponding ω_{ij} for different pairing structures

	feasible pairing structure	
	$1-1/2-2/3-3$	$1-2/2-3/3-1$
RGA	1/1/1	5/5/5
RI	0/0/0	$-0.8/-0.8/-0.8$
GI	6.0/6.0/6.0	1.2/1.2/1.2

all GIs are preferred because the interactions are transferable through interactive loops, i.e., selecting

$$\min\{\prod_{i=1}^{n}\omega_i\} \tag{3.18}$$

where ω_i is the GI corresponding to the ith output.

On the basis of the proposed loop-pairing criterion, an algorithm to select the best control structure can be summarized as follows:

Algorithm 1.

Step 1. For a given transfer function $\mathbf{G}(s)$, obtain steady-state gain matrix $\mathbf{G}(0)$.

Step 2. Calculate RGA and NI by eqs 2.2 and 3.2, respectively.

Step 3. Eliminate pairs having negative RGA and NI values.

Step 4. Calculate $\triangle\mathbf{G}^{ij}$ and $\mathbf{\Psi}_{ij}$ by eqs 3.8 and 3.13, respectively.

Step 5. Calculate ω_{ij} and form $\mathbf{\Omega}$ by eq 3.17.

Step 6. Select the pairing that has the smallest value of ω_{ij} in $\mathbf{\Omega}$.

Step 7. Use eq 3.18 to select the best one if two or more pairings have similar GI values.

Step 8. End

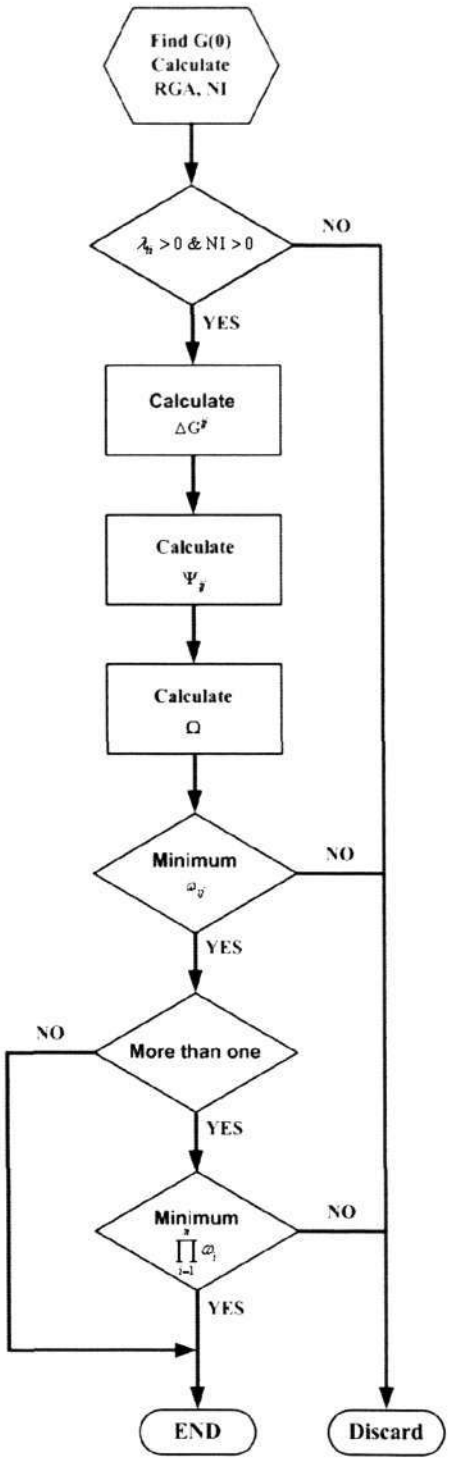

Figure 3.3: Flow chart of variable pairing selection procedure

The procedure for the variable-pairing selection is demonstrated by the flowchart as shown in Figure 3.3.

Remark 3. For the system that has the pure integral element, GIA and DRIA can be calculated by using a method similar to that proposed by Arkun and Downs [72].

Remark 4. For 2×2 system, from eqs 3.4, 3.5, 3.6, 3.11, 3.14, and 3.17, we obtain the GI value of element g_{11} as

$$\omega_{11} = |\phi_{11}| = |\phi_{22}| = |\psi_{22}^{11}| = |\psi_{11}^{22}|$$

Furthermore, from properties of RGA and RI, we can obtain an equation as

$$\lambda_{11} + \lambda_{12} = 1 \Rightarrow \phi_{11}\phi_{12} = 1$$

which indicates ϕ_{11} and ϕ_{12} must have the same sign, and a smaller $|\phi_{11}|$ means less interaction. Therefore, selecting the pairings that have the smallest GIA elements is equivalent to the RGA-based loop-pairing criterion to select the RGA value closest to unity.

Remark 5. Even though the procedure to derive the new loop-pairing criterion is tedious, the calculation for the control structure configuration can be achieved automatically and can easily be programmed into a computer.

3.4 Case Study

In this section, we give two more examples to demonstrate the effectiveness of the proposed control-loop configuration criterion.

3.4.1 Example 2.

Consider the process with its steady state gain matrix [15]

$$\mathbf{G}(0) = \begin{pmatrix} 1.0 & 1.0 & -0.1 \\ 1.0 & -3.0 & 1.0 \\ 0.1 & 2.0 & -1.0 \end{pmatrix}$$

and the RGA is obtained as

$$\mathbf{\Lambda}[\mathbf{G}(0)] = \begin{pmatrix} 0.5348 & 0.5882 & -0.1230 \\ 0.4278 & 1.5882 & -1.0160 \\ 0.0374 & -1.1765 & 2.1390 \end{pmatrix}$$

Obviously, pairings of $1-1/2-2/3-3$ and $1-2/2-1/3-3$ contain all positive RGA elements, and it is easy to verify that they all have positive NI (0.62 and 1.87, respectively), but because the RGA values of these two feasible pairings have similar deviations from unity, it is difficult to use RGA values to determine which pairing has fewer interactions. In such a case, the GIA-based criterion can make an effective selection, which is calculated as

$$\mathbf{\Omega} = \begin{pmatrix} 1.0251 & 3.2787 & \infty \\ 4.5081 & 0.6811 & \infty \\ 53.2591 & \infty & 0.5031 \end{pmatrix}$$

where the infinity elements ∞ of $\mathbf{\Omega}$ indicate that the elements of G have been filtered out by the RGA criteria (this representation is also used in the next example).

It can be easily seen from GIA that the pairing of $1-1/2-2/3-3$ has smaller values compared with the second pairing of $1-2/2-1/3-3$, which indicates less loop interaction from the first pairing structure than from the second.

3.4.2 Example 3.

A three-product (Petlyuk) distillation column was studied by Wolff and Skogestad [8]. The process gain at steady-state operating conditions is given by

$$\mathbf{G}(0) = \begin{pmatrix} 153.45 & -179.34 & 0.23 & 0.03 \\ -157.67 & 184.75 & -0.10 & 21.63 \\ 24.63 & -28.97 & -0.23 & -0.10 \\ -4.80 & 6.09 & 0.13 & -2.41 \end{pmatrix}$$

and the RGA is obtained as

$$\mathbf{\Lambda} = \begin{pmatrix} 24.5230 & -23.6378 & 0.1136 & 0.0012 \\ -48.9968 & 49.0778 & 0.0200 & 0.8990 \\ 38.5591 & -38.6327 & 1.0736 & 0.0000 \\ -13.0852 & 14.1927 & -0.2072 & 0.0998 \end{pmatrix}$$

It is easy to verify that there are six configurations that give positive values for both RGA and NI. According to the RGA-based loop-pairing criterion, the preferred control structure sequence is $1-1/2-4/3-3/4-2 > 1-3/2-4/3-1/4-2 > 1-1/2-2/3-3/4-4 > 1-3/2-2/3-1/4-4 > 1-1/2-3/3-4/4-2 > 1-4/2-3/3-1/4-2$; i.e., the first pairing structure $1-1/2-4/3-3/4-2$ is the most preferred. However, the pairing criterion based on GIA makes a very different selection. From algorithm 1, the GIA of that process is obtained as

$$\mathbf{\Omega} = \begin{pmatrix} 2.2032 & \infty & 771.3599 & 5.5671e+4 \\ \infty & 1.0259 & 2.9624e+3 & 75.4987 \\ 1.8562 & \infty & 44.8766 & 9.9018e+6 \\ \infty & 4.9251 & \infty & 193.7161 \end{pmatrix} \tag{3.19}$$

It can be easily seen that if loop pairings $\mathbf{y}_1-\mathbf{u}_4$, $\mathbf{y}_2-\mathbf{u}_3$, or $\mathbf{y}_3-\mathbf{u}_4$ are selected, the interactions between loops will be very large. Therefore, these pairing structures

should also be filtered out; i.e., these elements in eq 3.19 can be replaced by ∞, reducing the GIA to

$$\mathbf{\Omega} = \begin{pmatrix} 2.2032 & \infty & 771.3599 & \infty \\ \infty & 1.0259 & \infty & 75.4987 \\ 1.8562 & \infty & 44.8766 & \infty \\ \infty & 4.9251 & \infty & 193.7161 \end{pmatrix}$$

For the remaining four possible pairings, their corresponding products of GIs are calculated and listed in Table 3.5.

Table 3.5: Four possible pairings and their corresponding products of GI for Example 3

	feasible pairing			
	$1-1/2-4$ $/3-3/4-2$	$1-3/2-4$ $/3-1/4-2$	$1-1/2-2$ $/3-3/4-4$	$1-3/2-2$ $/3-1/4-4$
Product of GIs	36 764.5	532 397.9	19 649.2	284 546.1

Apparently, the third pairing of $1-1/2-2/3-3/4-4$ is the best one, with the smallest interactions between loops, and should be selected, which gives the same result as that in ref [8].

In this chapter, a new loop-pairing criterion based on a new interaction measures for the control structure configuration of the multivariable process was proposed. DRIA was defined to evaluate all possible interactions among loops, and GI based on the concept of interaction energy and DRIA was introduced for control-loop interaction measure. An effective algorithm that combines RGA, NI, and GI rules was developed that can accurately and systematically solve the loop configuration problem. Several examples were used to demonstrate the effectiveness of the new loop-pairing criterion.

Since the flexibility to bring subsystems in and out of service is very important also for the situations when actuators or sensors in some subsystems fail, how to

evaluate decentralized closed-loop integrity of the selected decentralized control configuration will be studied in next chapter.

Chapter 4

Evaluation of Decentralized Closed-loop Integrity for Multivariable Control Systems

In this chapter, through applying the left-right (LR) factorization to the Decomposed Relative Interaction Array (DRIA), the relative interaction (RI) is converted to the summation of a series of values as presented by the decomposed relative interaction sequence (DRIS). The DRIS provides important insights into the cause-effects of loop interaction due to the interactions are transferable through interactive loops. Subsequently, the maximum decomposed relative interaction factor (DRIF) of the loop providing the maximum interaction among the remaining loops is determined and used to analyze the RI of an individual loop in the face of single-loop failure or multiple-loop failure. Consequently, the necessary and sufficient conditions for the DCLI of an individual loop under both single- and multiple-loop failure are provided. Also a simple and effective algorithm for verifying the DCLI for multivariable processes is developed.

The structure of this chapter is as follows. In section 4.1, we revisit the DCLI as well as the necessary conditions provided by RGA and NI. In section 4.2, through

application of the LR factorization to DRIA, the RI is transformed to the DRIS. The necessary and sufficient conditions for an individual loop possessing single- and multiple-loop failure tolerance are derived based on the DRIS and are given in section 4.3. An effective algorithm for verifying the DCLI of multivariable processes is developed in section 4.4. The usefulness of the novel approach is illustrated by two classical examples in section 4.5.

4.1 Preliminaries

Throughout this chapter, it is assumed that the system is square ($n \times n$), open-loop-stable, strictly proper, nonsingular at steady state, and under a decentralized control configuration as shown in Figure 4.1. Here, $\mathbf{G}(s)$ is the transfer function matrix of the plant, and its steady-state gain matrix and individual elements are represented by $\mathbf{G}(0)$ (or simply $\mathbf{G}$) and g_{ij} , respectively. The decentralized controller $\mathbf{C}(s)$ can be decomposed into $\mathbf{C}(s) = \mathbf{N}(s)\mathbf{K}/s$, where $\mathbf{N}(s)$ is the transfer function matrix of the dynamic compensator, which is diagonal and stable and does not contain integral action, and $\mathbf{K} = diag\{k_i\}$, $i = 1, 2, \ldots, n$.

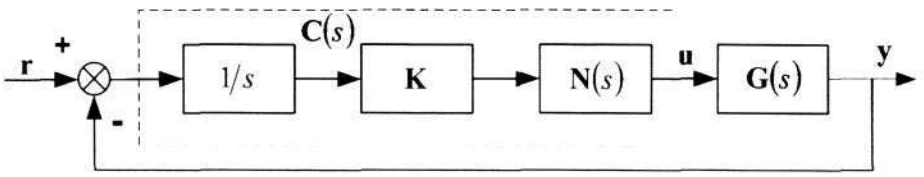

Figure 4.1: Decentralized integral control of multivariable systems

When loop failures of an arbitrary loop in system $\mathbf{G}(s)$ are investigated, all possible scenarios of the other $n-1$ loops in any failure order have to be considered, which are as many as $(n-1)!$. To effectively reflect these failed possibilities, we define a failure index M, which consist of $n-1$ different integers $M = \{(i_1, \cdots, i_m, \cdots, i_{n-1})\}$ where $m, i_m \in [1\ n-1]$.

The following definitions and theorems for loop pairing and DCLI for multivariable

control systems are needed in our development.

Definition 4.1.1 ([66]) *The RI for loop pairing* $\mathbf{y}_i - \mathbf{u}_j$ *is defined as the ratio of two elements: the increment of the process gain after all other control loops are closed, and the apparent gain in the same loop when all other control loops are open,*

$$\phi_{ij,n-1} = \frac{(\partial \mathbf{y}_i/\partial \mathbf{u}_j)_{\mathbf{y}_{k\neq i}\text{constant}} - (\partial \mathbf{y}_i/\partial \mathbf{u}_j)_{\mathbf{u}_{l\neq j}\text{constant}}}{(\partial \mathbf{y}_i/\partial \mathbf{u}_j)_{\mathbf{u}_{l\neq j}\text{constant}}} = \frac{1}{\lambda_{ij}} - 1, \tag{4.1}$$

where the subscript $ij, n-1$ *indicates that the RI is from the other* $n-1$ *loops to individual loop* $\mathbf{y}_i - \mathbf{u}_j$.

Even though the interpretations of RI and RGA are different, they are nevertheless equivalent, since one can be derived from another through simple transformation of coordinates. Therefore, the properties of RI can be easily derived from the RGA [66, 69, 70, 71]. Similarly to the RGA based loop pairing rule [6], one can obtain the following loop pairing rule in terms of the RI as:

$$\phi_{ij,n-1} \to 0, \qquad \text{and} \qquad \phi_{ij,n-1} > -1. \tag{4.2}$$

However, both RI- and RGA- based pairing rules do not offer any suggestion on the reverse effect of individual loop and loop-by-loop interactions, which may lead to undesirable loop pairing. To solve this problem, He and Cai decomposed the RI as DRIA to give important insights into the cause-effects of loop interactions [60].

Definition 4.1.2 ([60]) *The DRIA of* $n \times n$ *system is given as*

$$\mathbf{\Psi}_{ij,n-1} = \Delta\mathbf{G}_{ij,n-1} \otimes [\mathbf{G}^{ij}]^{-T}, \tag{4.3}$$

with its klth element

$$\psi_{ij,kl} = \phi_{ij,kl} * \lambda_{kl}^{ij}, \tag{4.4}$$

where $\mathbf{G}^{ij}$ *is the transfer function matrix* $\mathbf{G}$ *with its* i*th row and* j*th column removed,*

$$\Delta \mathbf{G}_{ij,n-1} = -\frac{1}{g_{ij}} g^{ij}_{\bullet j} g^{ij}_{i\bullet} \tag{4.5}$$

is the incremental process gain matrix of subsystem $\mathbf{G}^{ij}$ *when loop* $\mathbf{y}_i - \mathbf{u}_j$ *is closed,* $\phi_{ij,kl}$ *is the RI between loop* $\mathbf{y}_i - \mathbf{u}_j$ *and loop* $\mathbf{y}_k - \mathbf{u}_l$, λ^{ij}_{kl} *is relative gain of loop* $\mathbf{y}_k - \mathbf{u}_l$ *in subsystem* $\mathbf{G}^{ij}$, *and vectors* $g^{ij}_{i\bullet}$ *and* $g^{ij}_{\bullet j}$ *are the* i*th row and the* j*th column of* $\mathbf{G}$ *with the* ij*th element,* g_{ij}, *removed.*

Using DRIA, the RI, $\phi_{ij,n-1}$, can be decomposed according to the following theorem:

Theorem 4.1.1 ([60]) *For an arbitrary nonzero element* g_{ij} *of* $\mathbf{G}$, *the corresponding* $\phi_{ij,n-1}$ *is the sum of all elements of* $\mathbf{\Psi}_{ij,n-1}$,

$$\phi_{ij,n-1} = \|\mathbf{\Psi}_{ij,n-1}\|_{\Sigma} = \sum_{k=1,k\neq i}^{n} \sum_{l=1,l\neq j}^{n} \psi_{ij,kl},$$

where $\|\mathbf{A}\|_{\Sigma}$ is the summation of all elements in a matrix $\mathbf{A}$.

In the design of decentralized control system, it is desirable to choose input/output-pairings such that the system possesses the property of DCLI, which is defined as follows.

Definition 4.1.3 ([29]) *A stable plant is said to be DCLI, if it can be stabilized by a stable decentralized controller , which contains integral action shown as Figure 4.1, and if it remains stable after failure occurs in one or more of the feedback loops.*

The necessary conditions for a system to be DCLI is given as:

Theorem 4.1.2 (Necessary conditions for DCLI, [29, 30]) *Given an $n \times n$ stable process $\mathbf{G}(s)$, the closed-loop system of decentralized feedback structure possesses DCLI only if*

$$[\mathbf{\Lambda}(\mathbf{G}_m)]_{ii} > 0, \qquad \forall m = 1, \ldots, n;\ i = 1, \ldots, m \tag{4.6}$$

or

$$\mathbf{NI}[\mathbf{G}_m] > 0, \qquad \forall m = 1, \ldots, n. \tag{4.7}$$

where $\mathbf{A}_m$ is an arbitrary $m \times m$ principal submatrix of $\mathbf{A}$.

In theorem 4.1.2, either RGA or NI can be used as a necessary condition to examine the DCLI of decentralize control systems. However, the necessary and sufficient condition for DCLI with respect to single-and multi-loop failure are still unknown.

4.2 Decomposed Relative Interaction Sequence

We first reveal the relationship between DRIA and RGA, which is fundamental for the remaining developments.

Lemma 4.2.1 *For an arbitrary loop $\mathbf{y}_i - \mathbf{u}_i$ in system $\mathbf{G}$, the relationship between elements of $\mathbf{\Psi}_{ii,n-1}$ and elements of $\mathbf{\Lambda}$ satisfies,*

$$\frac{\lambda_{il}}{\lambda_{ii}} = \sum_{k=1, k\neq i}^{n} \psi_{ii,kl}, \qquad \forall i, l = 1, \cdots, n \text{ and } l \neq i, \tag{4.8}$$

and

$$\frac{\lambda_{ki}}{\lambda_{ii}} = \sum_{l=1, l\neq i}^{n} \psi_{ii,kl}, \qquad \forall i, k = 1, \cdots, n \text{ and } k \neq i. \tag{4.9}$$

Because the relationship provided by equation 4.9 is similar to that provided by equation 4.8, only the relationship given by equation 4.8 is proved here.

Proof. Because

$$\begin{aligned}\frac{\lambda_{il}}{\lambda_{ii}} &= \frac{(-1)^{i+l}g_{il} * \det[\mathbf{G}^{il}]/\det[\mathbf{G}]}{(-1)^{i+i}g_{ii} * \det[\mathbf{G}^{ii}]/\det[\mathbf{G}]} = \frac{(-1)^{i+l}g_{il} * \det[\mathbf{G}^{il}]}{(-1)^{i+i}g_{ii} * \det[\mathbf{G}^{ii}]} \\ &= (-1)^{l-i}\frac{g_{il}}{g_{ii}} * \frac{\sum_{k=1,k\neq i}^{n}[(-1)^{k+i-1}g_{ki} * \det[(\mathbf{G}^{ii})^{kl}]]}{\det[\mathbf{G}^{ii}]} \\ &= \sum_{k=1,k\neq i}^{n}[-\frac{g_{il}g_{ki}}{g_{ii}} * \frac{(-1)^{k+l}\det[(\mathbf{G}^{ii})^{kl}]}{\det[\mathbf{G}^{ii}]}],\end{aligned}$$

where $(\mathbf{G}^{ii})^{kl}$ is the transfer function matrix $\mathbf{G}$ with its ith, kth rows and jth, lth columns removed, using equation 4.4, we obtain,

$$\frac{\lambda_{il}}{\lambda_{ii}} = \sum_{k=1,k\neq i}^{n}(\phi_{ii,kl} * \lambda_{kl}^{ii}) = \sum_{k=1,k\neq i}^{n}\psi_{ii,kl}.$$

Remark 1. Lemma 4.2.1 presents an important relationship between the elements of DRIA and those of RGA. By the definition of RGA-number [23],

$$\text{RGAnumber} = \|\mathbf{\Lambda} - \mathbf{I}\|_{sum} = \sum_{i=1}^{n}[\lambda_{ii}|1 - 1/\lambda_{ii}| + \sum_{l=1,l\neq i}^{n}|\lambda_{il}/\lambda_{ii}|].$$

It is obvious that both $\lambda_{ii} \to 1$ and $|\lambda_{il}/\lambda_{ii}| \to 0$ are desired. As indicated by theorem 4.1.1 and lemma 4.2.1, this is consistent with the expectation that RI, ϕ_{ii}, and all elements of DRIA have smaller values. Furthermore, a smaller element $\psi_{ii,kl}$ means less interaction either between loop $\mathbf{y}_i - \mathbf{u}_i$ and loop $\mathbf{y}_k - \mathbf{u}_l$ or between loop $\mathbf{y}_k - \mathbf{u}_l$ and all the other loops in subsystem $\mathbf{G}^{ii}$. Therefore, the DRIA provides more information than RGA, and to select loop pairings that have smaller elements of DRIA is more effective than the RGA based loop pairing rules.

Using the LR matrix factorization method [67] to DRIA, $\mathbf{\Psi}_{ii,n-1}$ can be factorized as

$$\mathbf{\Psi}_{ii,n-1} = \mathbf{L}_{ii,n-1} \times \mathbf{R}_{ii,n-1}, \tag{4.10}$$

where $\mathbf{L}_{ii,n-1}$ is a $(n-1)\times(n-1)$ lower triangular matrix with its diagonal elements equal to unity and $\mathbf{R}_{ii,n-1}$ is a $n-1\times n-1$ upper triangular matrix. Then, we have the following lemma:

Lemma 4.2.2 *Given a subsystem $\mathbf{G}^{ii}$ of $\mathbf{G}$, if its first $n-m-1$ loops are removed, then the relative interaction to loop $\mathbf{y}_i - \mathbf{u}_i$ from the remaining m loops is the sum of all elements of the matrix that produced by the submatrices $\mathbf{L}_{ii,m}$ and $\mathbf{R}_{ii,m}$,*

$$\phi_{ii,m} = \|\mathbf{\Psi}_{ii,m}\|_\Sigma = \|\mathbf{L}_{ii,m} \times \mathbf{R}_{ii,m}\|_\Sigma. \tag{4.11}$$

Proof. According to the LR factorization algorithm, the DRIA $\mathbf{\Psi}_{ii,n-1}$ can be factorized step-by-step. The first step is given as:

$$\begin{aligned}
\mathbf{\Psi}_{ii,n-1} &= \begin{pmatrix} \psi_{ii,11} & \psi_{ii,12} & \cdots & \psi_{ii,1n} \\ \psi_{ii,21} & \psi_{ii,22} & \cdots & \psi_{ii,2n} \\ \vdots & \vdots & \ddots & \vdots \\ \psi_{ii,n1} & \psi_{ii,n2} & \cdots & \psi_{ii,nn} \end{pmatrix}_{n\neq i} \\
&= \begin{pmatrix} 1 & 0 & \cdots & 0 \\ \psi_{ii,21}/\psi_{ii,11} & 1 & & 0 \\ \vdots & & \ddots & \\ \psi_{ii,n1}/\psi_{ii,11} & 0 & & 1 \end{pmatrix}_{n\neq i} \\
&\quad \times \begin{pmatrix} \psi_{ii,11} & \psi_{ii,12} & \cdots & \psi_{ii,1n} \\ 0 & & & \\ \vdots & & \tilde{\mathbf{\Psi}}_{ii,n-2} & \\ 0 & & & \end{pmatrix}_{n\neq i},
\end{aligned} \tag{4.12}$$

where,

$$\tilde{\mathbf{\Psi}}_{ii,n-2} = \begin{pmatrix} \psi_{ii,22} - \psi_{ii,12}\psi_{ii,21}/\psi_{ii,11} & \cdots & \psi_{ii,2n} - \psi_{ii,1n}\psi_{ii,21}/\psi_{ii,11} \\ \vdots & \ddots & \vdots \\ \psi_{ii,n2} - \psi_{ii,12}\psi_{ii,n1}/\psi_{ii,11} & \cdots & \psi_{ii,nn} - \psi_{ii,1n}\psi_{ii,n1}/\psi_{ii,11} \end{pmatrix}_{n\neq i}.$$

In equation 4.12, the vectors $[1\ \psi_{ii,21}/\psi_{ii,11}\ \cdots\ \psi_{ii,n1}/\psi_{ii,11}]^T$ and $[\psi_{ii,11}\ \psi_{ii,12}\ \cdots\ \psi_{ii,1n}]$ are the first column and the first row of triangular matrices $\mathbf{L}_{ii,n-1}$ and $\mathbf{R}_{ii,n-1}$, respectively. On the basis of equation 4.4, the klth element $\tilde{\psi}_{ii,kl}$ of $\tilde{\mathbf{\Psi}}_{ii,n-2}$ can be simplified as,

$$\begin{aligned} \tilde{\psi}_{ii,kl} &= \psi_{ii,kl} - \psi_{ii,1l}\psi_{ii,k1}/\psi_{ii,11} \\ &= -\frac{g_{il}g_{ki}}{g_{ii}} \times \frac{\det[(\mathbf{G}^{ii})^{11}] * \det[(\mathbf{G}^{ii})^{kl}] - \det[(\mathbf{G}^{ii})^{1l}] * \det[(\mathbf{G}^{ii})^{i1}]}{\det[\mathbf{G}^{ii}]} \\ &= -\frac{g_{il}g_{ki}}{g_{ii}} \times \frac{\det[((\mathbf{G}^{ii})^{11})^{kl}]}{\det[\mathbf{G}^{ii}]} = \phi_{ii,kl} * \lambda_{kl}^{ii(11)} = \psi_{ii,kl}^{11}, \end{aligned}$$

where the superscript 11 means that loop $\mathbf{y}_1 - \mathbf{u}_1$ is removed. Obviously,

$$\begin{aligned} \tilde{\mathbf{\Psi}}_{ii,n-2} &= [\mathbf{\Psi}_{ii,n-1} - [\mathbf{\Psi}_{ii,n-1}]_{\bullet 1} \times [\mathbf{\Psi}_{ii,n-1}]_{1\bullet}/[\mathbf{\Psi}_{ii,n-1}]_{11}]^{11} \\ &= \mathbf{\Psi}_{ii,n-2}^{11} \end{aligned} \tag{4.13}$$

is the DRIA of loop $\mathbf{y}_i - \mathbf{u}_i$ in subsystem $\mathbf{G}^{11}$. Therefore based on theorem 4.1.1,

$$\phi_{ii,n-2} = \|\mathbf{\Psi}_{ii,n-2}\|_\Sigma = \|\mathbf{L}_{ii,n-2} \times \mathbf{R}_{ii,n-2}\|_\Sigma.$$

Above relationship can be applied straightforward to all loops of subsystem $\mathbf{G}^{ii}$. Consequently, the result given by equation 4.10 is obtained. If the top-left corner element of the matrix is not equal to zero, the similar factorization step can be continued loop-by-loop till m to result equation 4.11.

Remark 2. According to equation 4.12, since the top-left corner elements of DRIA such as $\psi_{ii,11}$ are applied in denominator in every step of factorization, they

must not be equal to zero, which requires all elements of $\mathbf{G}$ are not equal to zero. In practice, this problem can be easily solved by setting those zero elements to a very small value, say 10^{-9}. Our simulation results show that by using very small values to replace those zero elements do not avert the outcomes of failure tolerance property.

Theorem 4.2.3 *Suppose the control configuration of system* $\mathbf{G}$ *has been selected, for an arbitrary failure index* M*, the RI to loop* $\mathbf{y}_i - \mathbf{u}_i$ *from the other* $n-1$ *loops can be represented by the summation of* $n-1$ *elements,*

$$\phi^M_{ii,n-1} = \sum_{p=1}^{n-1} s^M_{ii,p}, \tag{4.14}$$

and,

$$s^M_{ii,p} = \sum [\mathbf{L}^M_{ii,n-1}]_{\bullet p} \times \sum [\mathbf{R}^M_{ii,n-1}]_{p\bullet} \tag{4.15}$$

where $\bullet p$ *and* $p\bullet$ *indicate the pth column and the pth row of matrix respectively.*

Proof.

Equation 4.14 can be derived straightforward from equation 4.11, since

$$\begin{aligned}
\phi^M_{ii,n-1} &= \|\mathbf{\Psi}^M_{ii,n-1}\|_\Sigma = \|\mathbf{L}^M_{ii,n-1} \times \mathbf{R}^M_{ii,n-1}\|_\Sigma \\
&= \underbrace{\begin{pmatrix} 1 & \cdots & 1 \end{pmatrix}}_{n-1} \times \mathbf{L}^M_{ii,n-1} \times \mathbf{R}^M_{ii,n-1} \times \underbrace{\begin{pmatrix} 1 & \cdots & 1 \end{pmatrix}^T}_{n-1} \\
&= \underbrace{\begin{pmatrix} \sum [\mathbf{L}^M_{ii,n-1}]_{\bullet 1} & \cdots & \sum [\mathbf{L}^M_{ii,n-1}]_{\bullet n-1} \end{pmatrix}}_{n-1} \\
&\quad \times \underbrace{\begin{pmatrix} \sum [\mathbf{R}^M_{ii,n-1}]_{1\bullet} & \cdots & \sum [\mathbf{R}^M_{ii,n-1}]_{n-1\bullet} \end{pmatrix}^T}_{n-1} \\
&= \sum_{p=1}^{n-1} [\sum [\mathbf{L}^M_{ii,n-1}]_{\bullet p}] \times [\sum [\mathbf{R}^M_{ii,n-1}]_{p\bullet}] \\
&= \sum_{p=1}^{n-1} s^M_{ii,p}.
\end{aligned}$$

Definition 4.2.1 *For individual loop* $\mathbf{y}_i - \mathbf{u}_i$ *in system* $\mathbf{G}$,

$$\mathbf{S}_{ii}^{M} = \{s_{ii,1}^{M}, \cdots s_{ii,p}^{M}, \cdots, s_{ii,n-1}^{M}\}, \tag{4.16}$$

and its individual element $s_{ii,p}^{M}$ *are defined as DRIS and DRIF to failure index* M, *respectively.*

To explain the physical meaning of DRIF, we analyze an arbitrary element in DRIS, say $s_{11,1}^{M}$, as an example. If all control loops of subsystem $(\mathbf{G}^{11})^{22}$ are closed, the subsystem including loop $\mathbf{y}_1 - \mathbf{u}_1$ and loop $\mathbf{y}_2 - \mathbf{u}_2$ are given as.

$$\tilde{\mathbf{G}}_{11-22} = \begin{pmatrix} \tilde{g}_{11} & \tilde{g}_{12} \\ \tilde{g}_{21} & \tilde{g}_{22} \end{pmatrix},$$

where $\sim$ indicates subsystem $(\mathbf{G}^{11})^{22}$ is closed and

$$\begin{aligned}
\tilde{g}_{11} &= g_{11}/\lambda_{11}^{22} = g_{11}/[g_{11}\det[(\mathbf{G}^{22})^{11}]/\det[\mathbf{G}^{22}]] = \det[\mathbf{G}^{22}]/\det[(\mathbf{G}^{22})^{11}], \\
\tilde{g}_{12} &= g_{12}/\lambda_{12}^{21} = g_{12}/[g_{12}\det[(\mathbf{G}^{21})^{12}]/\det[\mathbf{G}^{21}]] = \det[\mathbf{G}^{21}]/\det[(\mathbf{G}^{22})^{11}], \\
\tilde{g}_{21} &= g_{21}/\lambda_{21}^{12} = g_{21}/[g_{21}\det[(\mathbf{G}^{12})^{21}]/\det[\mathbf{G}^{12}]] = \det[\mathbf{G}^{12}]/\det[(\mathbf{G}^{22})^{11}], \\
\tilde{g}_{22} &= g_{22}/\lambda_{22}^{11} = g_{22}/[g_{22}\det[(\mathbf{G}^{11})^{22}]/\det[\mathbf{G}^{11}]] = \det[\mathbf{G}^{11}]/\det[(\mathbf{G}^{22})^{11}].
\end{aligned}$$

Now, if loop $\mathbf{y}_2 - \mathbf{u}_2$ is also closed, the incremental RI to loop $\mathbf{y}_1 - \mathbf{u}_1$ can be obtained as,

$$\begin{aligned}
\tilde{\phi}_{11,22} &= -\frac{\tilde{g}_{12}\tilde{g}_{21}}{g_{11}\tilde{g}_{22}} \\
&= -\frac{1}{g_{11}}\frac{\det[\mathbf{G}^{12}]\det[\mathbf{G}^{21}]/(\det[(\mathbf{G}^{22})^{11}])^2}{\det[\mathbf{G}^{11}]/\det[(\mathbf{G}^{22})^{11}]} \\
&= -\frac{1}{g_{11}}\frac{\det[\mathbf{G}^{12}]\det[\mathbf{G}^{21}]}{\det[\mathbf{G}^{11}]\det[(\mathbf{G}^{22})^{11}]} \\
&= \frac{g_{12}\det[\mathbf{G}^{12}]/\det[\mathbf{G}]g_{21}\det[\mathbf{G}^{21}]/\det[\mathbf{G}]}{-g_{12}g_{21}/(g_{11}g_{22})g_{22}\det[(\mathbf{G}^{22})^{11}]/\det[\mathbf{G}^{11}](g_{11}\det[\mathbf{G}^{11}]/\det[\mathbf{G}])^2} \\
&= \frac{1}{\psi_{22}^{11}}\frac{\lambda_{12}}{\lambda_{11}}\frac{\lambda_{21}}{\lambda_{11}}.
\end{aligned}$$

Then, from lemma 4.2.1,

$$\begin{aligned}\tilde{\phi}_{11,22} &= \frac{(\psi_{11,22}+\psi_{11,23}+\cdots+\psi_{11,2n})(\psi_{11,22}+\psi_{11,32}+\ldots+\psi_{11,n2})}{\psi_{11,22}} \\ &= s^M_{11,1}.\end{aligned}$$

which suggests the following:

(1) If subsystem $(\mathbf{G}^{11})^{22}$ is closed, closing loop $\mathbf{y}_2-\mathbf{u}_2$ will make the RI to loop $\mathbf{y}_1-\mathbf{u}_1$ increase by a value of $s^M_{11,1}$;

(2) Reversely, if loop $\mathbf{y}_2-\mathbf{u}_2$ is taken out of service, the RI to loop $\mathbf{y}_1-\mathbf{u}_1$ will decrease by a value of $s^M_{11,1}$.

To generalize the above explanation, we conclude that, for an arbitrary loop $\mathbf{y}_i-\mathbf{u}_i$, if the first $p-1$ loops of subsystem $\mathbf{G}^{ii}$ has already been taken out of service, the removal of the pth loop will decrease $\phi^M_{ii,n-p}$ by a value of $s^M_{ii,p}$.

The significance of the development in this section are as follows:

(1) The RI, $\phi^M_{ii,n-1}$, to individual control loop $\mathbf{y}_i-\mathbf{u}_i$ from all other $n-1$ control loops is decomposed as the DRIS, $\mathbf{S}^M_{ii}$, according to the failure index M, such that the interaction from an arbitrary loop of the remaining closed loops is represented by the DRIF;

(2) The DRIF, $s^M_{ii,p}$, indicates the interaction to individual control loop $\mathbf{y}_i-\mathbf{u}_i$ from the pth control loop of the remaining $n-p$ closed loops, which means when the pth control loop is put in or taken out of service, the corresponding DRIF should be added to or subtracted from the overall interaction RI;

(3) In terms of DRIS, not only the interactions between individual loop and the remaining loops but also the interactions to this individual loop from any combination of loops taken out of service can be reflected precisely.

4.3 Tolerance to Loops Failures

From equations 4.1 and 4.2, both large values and values close to -1 of RI imply significant interaction among individual loops. Because we are investigating the property of loop failure tolerance, only the lower boundary (-1) is considered. By selecting the maximum DRIF from all possible values, we can determine a failure index $\bar{M}$ corresponding DRIS $\mathbf{S}_{ii}^{\bar{M}}$ of individual loop $\mathbf{y}_i - \mathbf{u}_i$ as,

$$\mathbf{S}_{ii}^{\bar{M}} = \{s_{ii,p}^{\bar{M}} | s_{ii,p}^{\bar{M}} = \max\{s_{ii,p}^{M}\}, p = 1, 2, \ldots, n-1\}, \tag{4.17}$$

Therefore, taking the pth loop out of service according to failure index $\bar{M}$ will result

$$\phi_{ii,n-p-1}^{\bar{M}} = \min\{\phi_{ii,n-p-1}^{M}\}. \tag{4.18}$$

The value of RI is closest to -1, implying that the particular combination of loop failures has the most significant effect on the DCLI. On the basis of equations 4.2, 4.18, and Theorem 2 of ref [24], we now provide the necessary and sufficient conditions if individual loop $\mathbf{y}_i - \mathbf{u}_i$ is DCLI to single-loop failure.

Theorem 4.3.1 *For decentralized controlled multivariable process* $\mathbf{G}$*, individual loop* $\mathbf{y}_i - \mathbf{u}_i$ *is DCLI to single-loop failure, if and only if*

$$\phi_{ii,n-2}^{\bar{M}} > -1. \tag{4.19}$$

or

$$s_{ii,1}^{\bar{M}} < 1/\lambda_{ii}. \tag{4.20}$$

Proof.

Sufficient: In the case of an arbitrary loop failure, equations 4.14 and 4.17 gives the RI to individual loop $\mathbf{y}_i - \mathbf{u}_i$ as,

$$\phi^M_{ii,n-2} = \sum_{p=2}^{n-1} s^M_{ii,p} = \phi^M_{ii,n-1} - s^M_{ii,1} \geq \phi^{\bar{M}}_{ii,n-1} - s^{\bar{M}}_{ii,1} = \phi^{\bar{M}}_{ii,n-2}.$$

Obviously, when equation 4.19 holds, inequality $\phi^M_{ii,n-2} > -1$ holds. Therefore, the sign of steady-state gain for individual loop $\mathbf{y}_i - \mathbf{u}_i$ does not change in the face of single-loop failure.

Necessary: Because individual loop $\mathbf{y}_i - \mathbf{u}_i$ possesses single-loop failure tolerance, the sign of its steady-state loop gain does not change in the face of any single-loop failure,

$$\phi^M_{ii,n-2} > -1, \quad \forall M \Rightarrow \phi^{\bar{M}}_{ii,n-2} > -1.$$

Then, according to equations 4.1 and 4.14, inequality 4.20 can be obtained.

Similar as single-loop failure, on the basis of equations 4.2, 4.18, and Theorem 2 of ref [24], the necessary and sufficient condition for individual loop $\mathbf{y}_i - \mathbf{u}_i$ is DCLI for multiple-loop failures are given as follows.

Theorem 4.3.2 *For decentralized control multivariable process* $\mathbf{G}$, *individual loop* $\mathbf{y}_i - \mathbf{u}_i$ *is DCLI to multiple-loop failures if and only if*

$$\phi^{\bar{M}}_{ii,m_{min}} > -1, \tag{4.21}$$

where,

$$\phi^{\bar{M}}_{ii,m_{min}} = \min\{ \sum_{p=n-m_{min}}^{n-1} s^{\bar{M}}_{ii,p} | m_{min} = 1, \ldots, n-1\}. \tag{4.22}$$

Proof.

Sufficient: In the case of $n-m-1$ loops failure, equations 4.14 and 4.17 show that the RI to individual loop $\mathbf{y}_i - \mathbf{u}_i$ from the remaining m loops is,

$$\phi^M_{ii,m} = \sum_{p=n-m}^{n-1} s^M_{ii,p} = \phi^M_{ii,n-1} - \sum_{p=1}^{n-m-1} s^M_{ii,p} \geq \phi^{\bar{M}}_{ii,n-1} - \sum_{p=1}^{n-m_{min}-1} s^{\bar{M}}_{ii,p} = \phi^{\bar{M}}_{ii,m_{min}}.$$

Obviously, when equation 4.21 holds, inequality $\phi^M_{ii,m} > -1$ always holds. Therefore, the sign of the steady-state gain for individual loop $\mathbf{y}_i - \mathbf{u}_i$ does not change in the face of multiple-loop failure.

Necessary: Because individual loop $\mathbf{y}_i - \mathbf{u}_i$ possesses multiple-loop failure tolerance, the sign of its steady-state loop gain does not change in the face of any single-loop failure,

$$\phi^M_{ii,m} > -1, \quad \forall M \Rightarrow \phi^{\bar{M}}_{ii,m_{min}} > -1.$$

Remark 3. The significance of Theorems 4.1 and 4.2 are as follows:

(1) The necessary and sufficient conditions for both single- and multiple-loop failure tolerance are provided.

(2) In the case where two or more control structures are DCLI, the one with, $\phi^{\bar{M}}_{ii,m_{min}} \to 0$, should be preferred.

(3) Single-loop failure is a special case of multiple-loop failure.

4.4 Pairings Algorithm for DCLI

In subsystem $\mathbf{G}^{ii}$, the DRIF $s^M_{ii,p}$ may have as many as $n-p$ possible values according to different failure sequence of the remaining $n-p$ loops. Therefore, to find either $\phi^{\bar{M}}_{ii,m_{min}}$ or $\phi^{\bar{M}}_{ii,n-2}$, one is required first to determine the index $\bar{M}$ and to

calculate the DRIS $\mathbf{S}_{ii}^{\bar{M}}$, where $s_{ii,p}^{M}$ can be determined by the first row and column of $\mathbf{\Psi}_{ii,n-p}^{M}$ (equations 4.12 and 4.15),

$$s_{ii,p}^{M} = \sum_{k=1}^{n-p} [\mathbf{\Psi}_{ii,n-p}^{M}]_{1k} \times \sum_{k=1}^{n-p} [\mathbf{\Psi}_{ii,n-p}^{M}]_{k1} / [\mathbf{\Psi}_{ii,n-p}^{M}]_{11}.$$

However, there is no need to arrange elements of DRIA $\mathbf{\Psi}_{ii,n-p}^{M}$ $n-p$ times to calculate $s_{ii,p}^{\bar{M}}$, because the elements of DRIA are permutation- independent (equations 4.3 and 4.5). In fact, once the DRIA $\mathbf{\Psi}_{ii,n-p}$ for $p=1$ has been obtained (equation 4.3), the DRIF $s_{ii,p}^{\bar{M}}$ can be directly calculated from,

$$[s_{ii,p}^{\bar{M}}, l] = \max\{\mathrm{diag}[(\sum_{k=1}^{n-p} [\mathbf{\Psi}_{ii,n-p}]_{\bullet k} \times \sum_{k=1}^{n-p} [\mathbf{\Psi}_{ii,n-p}]_{k\bullet}) \odot \mathbf{\Psi}_{ii,n-p}]\} \tag{4.23}$$

where, function $\max[\mathbf{A}]$ finds the maximum diagonal element of matrix $\mathbf{A}$ and provides its row number l in matrix $\mathbf{\Psi}_{ii,n-p}$, $\mathrm{diag}[\mathbf{A}]$ is a diagonal matrix contains the diagonal elements of matrix $\mathbf{A}$. $\odot$ indicates element-by-element division.

For checking the DCLI of individual loop $\mathbf{y}_i - \mathbf{u}_i$ against failure of $p+1$ loops, the DRIA $\mathbf{\Psi}_{ii,n-p-1}$ can be recursively calculated as (equations 4.12 and 4.13),

$$\mathbf{\Psi}_{ii,n-p-1} = [\mathbf{\Psi}_{ii,n-p} - [\mathbf{\Psi}_{ii,n-p}]_{\bullet l} \times [\mathbf{\Psi}_{ii,n-p}]_{l\bullet} / [\mathbf{\Psi}_{ii,n-p}]_{ll}]^{ll}. \tag{4.24}$$

and the DRIF $s_{ii,p+1}^{\bar{M}}$ can be calculated by applying DRIA $\mathbf{\Psi}_{ii,n-p-1}$ to equation 4.23.

Therefore, for individual loop $\mathbf{y}_i - \mathbf{u}_i$ of $n \times n$ system $\mathbf{G}$, after $\mathbf{\Psi}_{ii,n-1}$ is obtained, its DRIS $\mathbf{S}_{ii}^{\bar{M}}$ can be calculated by using iterative equations 4.23 and 4.24 $n-2$ times which requires only one matrix inverse of $n-1$ order to calculated the DRIA as shown by equation 4.3, the computational load is much reduced compared with that of permutation methods.

For a given multivariable process $\mathbf{G}(s)$, its control configuration can be obtained based on its steady-state transfer function matrix $\mathbf{G}(0)$ by using the loop pairing

criterion such as the one developed in ref [60]. After all elements in matrix $\mathbf{G}(0)$ have been rearranged to place the gains of control loops in the diagonal position, the proposed method can be used to verify DCLI of the selected control configuration and an algorithm is given as follow.

Algorithm 1.

Step 1: Calculate $\mathbf{\Psi}_{ii,n-1}$ of loop $\mathbf{y}_i - \mathbf{u}_i$ by equations 4.3 and 4.5;

Step 2: Obtain $s^{\bar{M}}_{ii,p}$ and $\mathbf{S}^{\bar{M}}_{ii}$ of loop $\mathbf{y}_i - \mathbf{u}_i$ by equations 4.23 and 4.24;

Step 3: Verify single loop failure tolerance by equation 4.19;

Step 4: Obtain $\phi^{\bar{M}}_{ii,m_{min}}$ to loop $\mathbf{y}_i - \mathbf{u}_i$ form the other loops by equation 4.22;

Step 5: Verify multiple loop failure tolerance by referring to equation 4.21;

Step 6: Repeat the previous 5 steps loop-by-loop until any one loop fails or all loops pass;

Step 7: End.

The procedure for the determination of DCLI for a decentralized control system is illustrated by the flowchart shown in Figure 4.2.

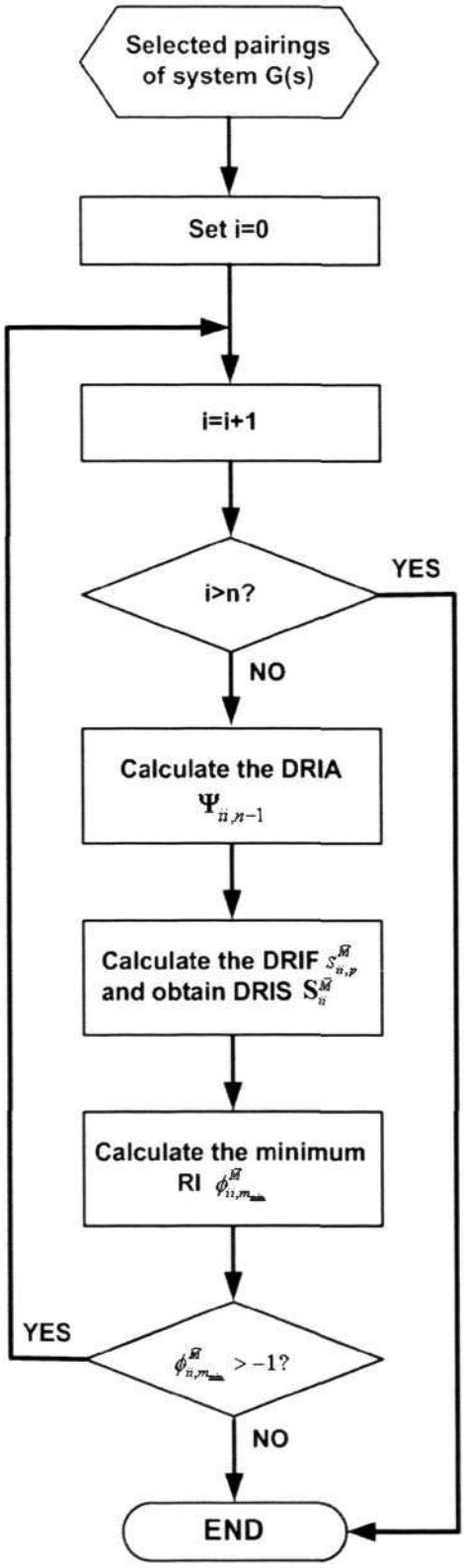

Figure 4.2: Flowchart for determining DCLI

4.5 Case Study

4.5.1 Example 1

Consider the following 4×4 process [31] with the process steady-state transfer function matrix given by,

$$\mathbf{G}(0) = \begin{pmatrix} 8.72 & -15.80 & 2.98 & 2.81 \\ 6.54 & -20.79 & 2.50 & -2.92 \\ -5.82 & -7.51 & -1.48 & 0.99 \\ -7.23 & 7.86 & 3.11 & 2.92 \end{pmatrix}.$$

To verify DCLI to single-loop failure of the first loop $\mathbf{y}_1 - \mathbf{u}_1$ by using RGA based criterion, three alternatives have to be tested, namely, calculation of RGAs of subsystems $\mathbf{G}^{22}$, $\mathbf{G}^{33}$ and $\mathbf{G}^{44}$ for single loop failure of $\mathbf{y}_2 - \mathbf{u}_2$, $\mathbf{y}_3 - \mathbf{u}_3$, and $\mathbf{y}_4 - \mathbf{u}_4$, respectively. Furthermore, to verify DCLI to multiple-loop failures, an additional three RGAs need to be calculated. Consequently, six inverse matrices have to be performed.

From application of Algorithm 1 and with one matrix inverse, the DRIA of control loop $\mathbf{y}_1 - \mathbf{u}_1$ is obtained, and DRIS is calculated through a series of vector operations. The results for DCLI to single- and multiple-loop failures are listed in Table 4.1.

Initially, when all control loops in subsystem $\mathbf{G}^{11}$ are closed, the RI $\phi^{\tilde{M}}_{11,3} = 1.4142 > -1$, implying that there is no sign change before and after subsystem $\mathbf{G}^{11}$ has been closed. Following Table 4.1, DCLI information of loop $\mathbf{y}_1 - \mathbf{u}_1$ can be obtained as follows:

(1) Loop $\mathbf{y}_4 - \mathbf{u}_4$ provides the maximum interaction, and if it fails, the RI of loop $\mathbf{y}_1 - \mathbf{u}_1$ will decrease in value of $s^{\tilde{M}}_{11,1} = 2.4095$ and is $\phi^{\tilde{M}}_{11,2} = -0.9953 > -1$, and for loop $\mathbf{y}_1 - \mathbf{u}_1$, the sign of its loop gain does not change for any single-loop failure. Therefore, loop $\mathbf{y}_1 - \mathbf{u}_1$ is DCLI for single loop failure.

Table 4.1: DCLI verification of control loop $\mathbf{y}_1 - \mathbf{u}_1$[a]

Loop	RI	DRIS	Failed Loop	DCLI-SLF	DCLI-MLF
$\mathbf{y}_1 - \mathbf{u}_1$	$\phi^{\bar{M}}_{11,3} = 1.4142$ $\downarrow$ $\phi^{\bar{M}}_{11,2} = -0.9953$ $\downarrow$ $\phi^{\bar{M}}_{11,1} = -1.3439$ $\downarrow$ 0	$s^{\bar{M}}_{11,1} = 2.4095$ $s^{\bar{M}}_{11,2} = 0.3486$ $s^{\bar{M}}_{11,3} = -1.3439$	$\mathbf{y}_4 - \mathbf{u}_4$ $\mathbf{y}_2 - \mathbf{u}_2$ $\mathbf{y}_3 - \mathbf{u}_3$	YES	NO

[a] SLF=single-loop failure. MLF=multi-loop failure.

(2) Loop $\mathbf{y}_2 - \mathbf{u}_2$ provides the maximum interaction among the two remaining loops after loop $\mathbf{y}_4 - \mathbf{u}_4$ has already been taken out of service. If loop $\mathbf{y}_2 - \mathbf{u}_2$ fails, the RI of loop $\mathbf{y}_1 - \mathbf{u}_1$ will decrease in a value of $s^{\bar{M}}_{11,2} = 0.3486$ and is $\phi^{\bar{M}}_{11,1} = -1.3439 < -1$. Hence, the process gain of loop $\mathbf{y}_1 - \mathbf{u}_1$ will change its sign and it is not DCLI when both $\mathbf{y}_4 - \mathbf{u}_4$ and $\mathbf{y}_2 - \mathbf{u}_2$ fail (implying that $\mathbf{G}$ is not DCLI for multiple loop failure).

To show how DCLI is pairing dependant, reconfigure the control structure using the loop pairing criterion proposed in ref [60] as follows

$$\mathbf{G}(0) = \begin{pmatrix} 2.81 & -15.80 & 8.72 & 2.98 \\ -2.92 & -20.79 & 6.54 & 2.50 \\ 0.99 & -7.51 & -5.82 & -1.48 \\ 2.92 & 7.86 & -7.23 & 3.11 \end{pmatrix}.$$

The DCLI results of $\mathbf{y}_1 - \mathbf{u}_1$ are listed in Table 4.2.

From Table 4.2, we observe the following

(1) When all control loops in subsystem $\mathbf{G}^{11}$ are closed, the RI $\phi^{\bar{M}}_{11,3} = 1.1237 > -1$, implying that there is no sign change before and after subsystem $\mathbf{G}^{11}$ has been closed.

Table 4.2: DCLI verification of control loop $\mathbf{y}_1 - \mathbf{u}_1$[a]

Loop	RI	DRIS	Failed Loop	DCLI-SLF	DCLI-MLF
$\mathbf{y}_1 - \mathbf{u}_1$	$\phi^{\bar{M}}_{11,3} = 1.1237$			YES	YES
	$\downarrow$	$s^{\bar{M}}_{11,1} = 0.6885$	$\mathbf{y}_2 - \mathbf{u}_2$		
	$\phi^{\bar{M}}_{11,2} = 0.4352$				
	$\downarrow$	$s^{\bar{M}}_{11,2} = 1.4309$	$\mathbf{y}_3 - \mathbf{u}_3$		
	$\phi^{\bar{M}}_{11,1} = -0.9957$				
	$\downarrow$	$s^{\bar{M}}_{11,3} = -0.9957$	$\mathbf{y}_4 - \mathbf{u}_4$		
	0				

[a] SLF=single-loop failure. MLF=multi-loop failure.

(2) Loop $\mathbf{y}_1 - \mathbf{u}_1$ can tolerate any single-loop failure because the minimal $\phi^{\bar{M}}_{11,2} = 0.4352 > -1$

(3) Loop $\mathbf{y}_1 - \mathbf{u}_1$ can tolerate any double-loop failure since the minimal $\phi^{\bar{M}}_{11,1} = -0.9957 > -1$

(4) Since $\phi^{\bar{M}}_{11,3} > \phi^{\bar{M}}_{11,2} > 0$, if loop $\mathbf{y}_2 - \mathbf{u}_2$ fails, interaction between loop $\mathbf{y}_1 - \mathbf{u}_1$ and the remaining loops will be smaller.

(5) If loop loop $\mathbf{y}_3 - \mathbf{u}_3$ also fails, interaction between loop $\mathbf{y}_1 - \mathbf{u}_1$ and loop $\mathbf{y}_4 - \mathbf{u}_4$ becomes significant for $\phi^{\bar{M}}_{11,1} = -0.9957 \rightarrow -1$, implying the equivalent process gain of loop $\mathbf{y}_1 - \mathbf{u}_1$ will undergo a big change in the case of where either loop $\mathbf{y}_4 - \mathbf{u}_4$ is closed first in system $\mathbf{G}$ or loop $\mathbf{y}_2 - \mathbf{u}_2$ and loop $\mathbf{y}_3 - \mathbf{u}_3$ fail first in closed subsystem $\mathbf{G}^{11}$.

Using algorithm 1, DRIS of the other 3 control loops can be obtained and list in Table 4.3, all control loops are DCLI to both single-loop and multiple-loop failures.

Table 4.3: DCLI verification of other three control loops[a]

Loop	RI	DRIS	Failed Loop	DCLI-SLF	DCLI-MLF
$\mathbf{y}_2 - \mathbf{u}_2$	$\phi^M_{11,3} = 1.2873$	$s^M_{22,1} = 0.7416$	$\mathbf{y}_1 - \mathbf{u}_1$	YES	YES
	$\phi^M_{11,2} = 0.5458$	$s^M_{22,2} = 0.2418$	$\mathbf{y}_3 - \mathbf{u}_3$		
	$\phi^M_{11,1} = 0.3039$	$s^M_{22,3} = 0.3039$	$\mathbf{y}_4 - \mathbf{u}_4$		
$\mathbf{y}_3 - \mathbf{u}_3$	$\phi^M_{11,3} = 1.4765$	$s^M_{33,1} = 0.8086$	$\mathbf{y}_4 - \mathbf{u}_4$	YES	YES
	$\phi^M_{11,2} = 0.6679$	$s^M_{33,2} = 0.2620$	$\mathbf{y}_1 - \mathbf{u}_1$		
	$\phi^M_{11,1} = 0.4059$	$s^M_{33,3} = 0.4059$	$\mathbf{y}_2 - \mathbf{u}_2$		
$\mathbf{y}_4 - \mathbf{u}_4$	$\phi^M_{11,3} = 0.7498$	$s^M_{44,1} = 0.5713$	$\mathbf{y}_3 - \mathbf{u}_3$	YES	YES
	$\phi^M_{11,2} = 0.1785$	$s^M_{44,2} = 1.1742$	$\mathbf{y}_2 - \mathbf{u}_2$		
	$\phi^M_{11,1} = -0.9957$	$s^M_{44,3} = -0.9957$	$\mathbf{y}_1 - \mathbf{u}_1$		

[a] SLF=single-loop failure. MLF=multi-loop failure.

4.5.2 Example 2

Consider the 4×4 distillation column studied by Chiang and Luyben (CL column) [73]. The steady state transfer function matrix is given as follow,

$$\mathbf{G}(0) = \begin{pmatrix} 4.45 & -7.4 & 0 & 0.35 \\ 17.3 & -41 & 0 & 9.2 \\ 0.22 & -4.66 & 3.6 & 0.042 \\ 1.82 & -34.5 & 12.2 & -6.92 \end{pmatrix}.$$

When the zero elements in $\mathbf{G}(0)$ are set to 1×10^{-9} to make the zero interaction a micro-interaction, the maximum DRIFs and DRIS of all control loops are obtained as listed in Table 4.4.

Obliviously, as Table 4.4 indicates, all four control loops are DCLI to multiple-loop failures.

In this chapter, a novel approach for evaluating DCLI for multivariable control systems was proposed. The DRIS was introduced to represent the RI to a particular loop from other loops. The maximum DRIF was used to find the maximum interaction from the remaining loops among all possible failure indexes. Consequently,

Table 4.4: DCLI verification of CL column[a]

Loop	RI	DRIS	Failed Loop	DCLI-SLF	DCLI-MLF
$\mathbf{y}_1 - \mathbf{u}_1$	$\phi^M_{11,3} = -0.5233$	$s^M_{11,1} = 0.1783$	$\mathbf{y}_4 - \mathbf{u}_4$	YES	YES
	$\phi^M_{11,2} = -0.7017$	$s^M_{11,2} = 0.0000$	$\mathbf{y}_3 - \mathbf{u}_3$		
	$\phi^M_{11,1} = -0.7017$	$s^M_{11,3} = -0.7017$	$\mathbf{y}_2 - \mathbf{u}_2$		
$\mathbf{y}_2 - \mathbf{u}_2$	$\phi^M_{11,3} = -0.2490$	$s^M_{22,1} = 0.4527$	$\mathbf{y}_4 - \mathbf{u}_4$	YES	YES
	$\phi^M_{11,2} = -0.7017$	$s^M_{22,2} = 0.0000$	$\mathbf{y}_3 - \mathbf{u}_3$		
	$\phi^M_{11,1} = -0.7017$	$s^M_{22,3} = -0.7017$	$\mathbf{y}_1 - \mathbf{u}_1$		
$\mathbf{y}_3 - \mathbf{u}_3$	$\phi^M_{11,3} = -0.3394$	$s^M_{33,1} = -0.1074$	$\mathbf{y}_1 - \mathbf{u}_1$	YES	YES
	$\phi^M_{11,2} = -0.2320$	$s^M_{33,2} = -0.2320$	$\mathbf{y}_4 - \mathbf{u}_4$		
	$\phi^M_{11,1} = 0.0000$	$s^M_{33,3} = 0.0000$	$\mathbf{y}_2 - \mathbf{u}_2$		
$\mathbf{y}_4 - \mathbf{u}_4$	$\phi^M_{11,3} = 1.6000$	$s^M_{44,1} = 1.5672$	$\mathbf{y}_2 - \mathbf{u}_2$	YES	YES
	$\phi^M_{11,2} = 0.0328$	$s^M_{44,2} = 0.0122$	$\mathbf{y}_1 - \mathbf{u}_1$		
	$\phi^M_{11,1} = 0.0206$	$s^M_{44,3} = 0.0206$	$\mathbf{y}_3 - \mathbf{u}_3$		

[a] SLF=single-loop failure. MLF=multi-loop failure.

the necessary and sufficient conditions for DCLI of an individual loop under both single- and multiple-loop failures were provided. A simple and effective algorithm for verifying DCLI for multivariable control systems was developed. Two classical examples were used to illustrate the effectiveness of the proposed approach.

With the determined decentralized control configuration, how to design the decentralized PID controller will be studied in the chapters.

Chapter 5

Simple Decentralized PID Controller Design Method Based on Dynamic Relative Interaction Analysis

This chapter extends the work of [60, 61] to develop a simple yet effective method for designing a decentralized PID controller based on dynamic interaction analysis. By implementation of a controller to each individual diagonal control loop using the SISO PID tuning rules, the dynamic relative interaction (dRI) to an individual control loop from all other loops is estimated. With the obtained dRI, the multiplicated model factor (MMF) is calculated and approximated by a time delay function at the neighborhood of the critical frequency to construct the equivalent transfer function for individual control loop. Subsequently, an algorithm for designing appropriate controller settings for the decentralized PID controllers is provided. The proposed method is very simple and effective and easily implemented especially for higher dimensional processes. Two examples, 2×2 process and 4×4 process are used to demonstrate the design procedures. The simulation results show that the

design method results favorable overall control performance, especially for higher dimensional processes.

5.1 Preliminaries

Consider an $n \times n$ system with a decentralized feedback control structure as shown in Figure 5.1, where, $\mathbf{r}$, $\mathbf{u}$ and $\mathbf{y}$ are vectors of references , inputs and outputs respectively, $\mathbf{G}(s) = [g_{ij}(s)]_{n\times n}$ is the system's transfer function matrix and its individual element $g_{ij}(s)$ described a second-order plus dead-time (SOPDT) model:

$$g_{ij}(s) = \frac{k_{ij}e^{-\theta_{ij}s}}{(\tau_{ij}s+1)(\tau'_{ij}s+1)}, \qquad \tau'_{ij} \leq \tau_{ij}. \tag{5.1}$$

and controller $\mathbf{C}(s) = \text{diag}\{c_1(s), \cdots, c_n(s)\}$ is the decentralized PID type with its individual element given in series form as

$$c_i(s) = k_{Pi}(1 + \frac{1}{\tau_{Ii}s})(\tau_{Di}s + 1). \tag{5.2}$$

It is assumed that $\mathbf{G}(s)$ has been arranged so that the pairings of the inputs and outputs in the decentralized feedback system correspond to the diagonal elements of $\mathbf{G}(s)$.

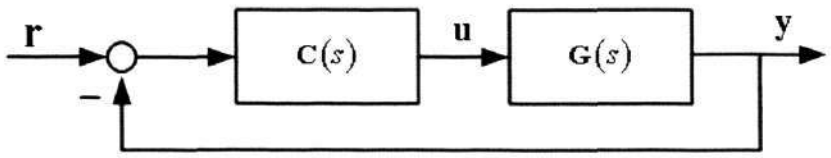

Figure 5.1: Block diagram of general decentralized control system

For the MIMO process, when one controller, $c_i(s)$, acting in response to the set-point change and/or the output disturbance, it affects the overall system through the off-diagonal elements of $\mathbf{G}(s)$, forcing other controllers to take actions as well, these controllers reversely influence the ith loop via other off-diagonal elements, and these interacting processes among control loops continue throughout the whole

transient until a steady state is reached. To examine the transmittance of interactions between an individual control loop and the others, the decentralized control system can be structurally decomposed into n individual SISO control loops, with the coupling among all loops explicitly exposed and embedded in each loop. Figure 5.2 shows the structure of an arbitrary control loop $y_i - u_i$ after the structural decomposition.

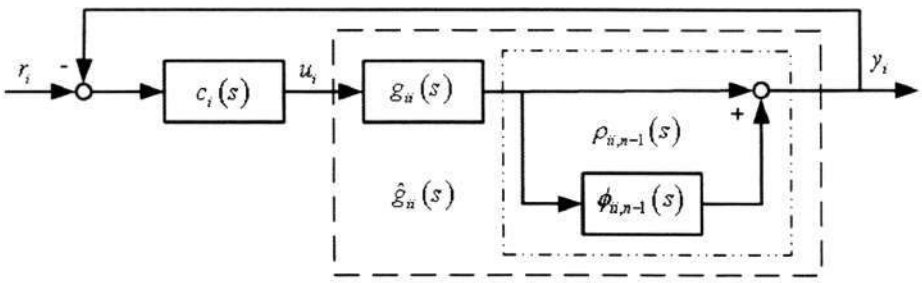

Figure 5.2: Structure of loop $y_i - u_i$ by structural decomposition

In Figure 5.2, the interaction to an individual control loop $y_i - u_i$ from the other $n-1$ control loops is represented by the RI $\phi_{ii,n-1}(s)$, and the equivalent transfer function of an individual control loop $y_i - u_i$, denoted by $\hat{g}_{ii}(s)$, can be obtained in terms of $\phi_{ii,n-1}(s)$ by

$$\hat{g}_{ii}(s) = g_{ii}(s)\rho_{ii,n-1}(s), \tag{5.3}$$

with

$$\rho_{ii,n-1}(s) = 1 + \phi_{ii,n-1}(s), \tag{5.4}$$

where $\rho_{ii,n-1}(s)$ is defined as the MMF to indicate the model change of an individual control loop $y_i - u_i$ after the other $n-1$ control loops are closed. Once the RI, $\phi_{ii,n-1}(s)$, is available, the corresponding MMF, $\rho_{ii,n-1}(s)$, and the equivalent process transfer function $\hat{g}_{ii}$ can be obtained which can be directly used to independently design the PID controller for each individual control loop $y_i - u_i$.

In the following development, we use RI as a basic interaction measure to investigate the interactions among control loops and derive equivalent transfer function

for each loop. Sometimes, we will omit the Laplace operator s for simplicity unless otherwise specified.

The RI for control loop $y_i - u_j$ is defined as the ratio of two elements [66]: the increment of the process gain after all other control loops are closed and the apparent gain in the same loop when all other control loops are open, i.e.

$$\phi_{ij,n-1} = \frac{(\partial y_i/u_j)_{y_{k\neq i}\text{constant}} - (\partial y_i/u_j)_{u_{l\neq j}\text{constant}}}{(\partial y_i/u_j)_{u_{l\neq j}\text{constant}}} \qquad k,l = 1,\cdots,n.$$

Because the RI cannot offer effective measure on the reverse effect of individual control loop and loop-by-loop interactions, He and Cai decomposed the RI at steady state as the element summation of DRIA to give important insights into the cause-effects of loop interactions [60]. However, the obtained results are limited to the steady state, which are less useful for controller design than the dynamic representations. Hence, it is necessary to derive the dynamic interaction among control loops represented explicitly by the process models and controllers.

5.2 Dynamic Relative Interaction

Because the dynamic interactions among control loops are controller dependent [17, 19, 74, 75], appropriate controllers have to be designed and implemented into the control system for investigation of the dynamic interactions. For an arbitrarily decentralized PID control system of a multivariable process, we can redraw Figure 5.1 as Figure 5.3 for the convenience of analyzing the interactions between an arbitrary control loop $y_i - u_i$ and the others, where $\underline{\mathbf{y}}_i$ is a vector indicating the effects of u_i on other outputs while $\bar{y}_i$ indicates the reverse effect of y_i by all of the other closed control loops; $\mathbf{r}^i$, $\mathbf{u}^i$, $\mathbf{y}^i$ and $\mathbf{C}^i(s)$ indicate $\mathbf{r}$, $\mathbf{u}$, $\mathbf{y}$ and $\mathbf{C}(s)$with their ith elements, r_i, u_i, y_i and $c_i(s)$, removed, respectively.

Because the dRIs are input independent, without loss of generality, the references

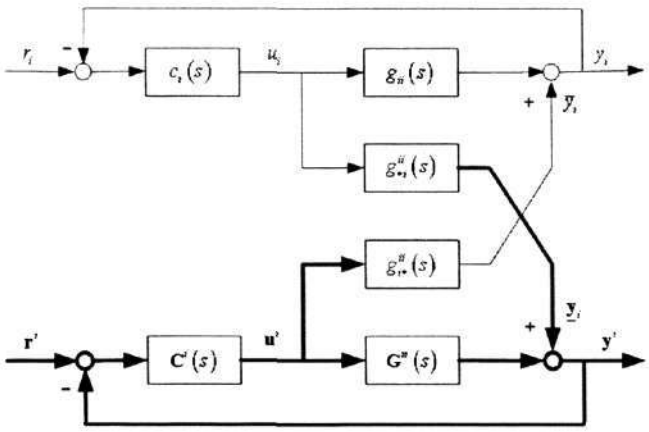

Figure 5.3: Closed-loop system with control loop $y_i - u_i$ presented explicitly

of the other $n-1$ control loops are set as constants, i.e.

$$\frac{d\mathbf{r}_k}{dt} = 0 \qquad \text{or} \qquad \mathbf{r}_k(s) = 0, \qquad k = 1, \cdots, n;\ k \neq i,$$

in the analysis of the dynamic interaction between control loop $y_i - u_i$ and the other controlled closed-loops. Then, we have

$$\mathbf{y}^i = \mathbf{G}^{ii}\mathbf{u}^i + \underline{\mathbf{y}}_i, \tag{5.5}$$

$$\mathbf{u}^i = -\mathbf{C}^i\mathbf{y}^i, \tag{5.6}$$

and

$$\underline{\mathbf{y}}_i = g^{ii}_{\bullet i}u_i, \tag{5.7}$$

$$\bar{y}_i = g^{ii}_{i\bullet}\mathbf{u}^i, \tag{5.8}$$

where $\mathbf{G}^{ii}$ is the transfer function matrix $\mathbf{G}$ with its ith row and the ith column removed, and $g^{ii}_{\bullet i}$ and $g^{ii}_{i\bullet}$ indicate the ith row and the ith column of $\mathbf{G}$ with the

iith element, g_{ii}, removed, respectively.

Combining equations 5.5 and 5.6, we can write

$$\mathbf{u}^i = -(\bar{\mathbf{G}}^{ii})^{-1}\underline{\mathbf{y}}_i, \tag{5.9}$$

where

$$\bar{\mathbf{G}} = \mathbf{G} + \mathbf{C}^{-1}. \tag{5.10}$$

Furthermore, $\bar{y}_i$ in equation 5.8 can be represented by the summation of the following row vector

$$\bar{y}_i = \|[\ g_{i1}u_1 \ \cdots \ g_{ik}u_k \ \cdots \ g_{in}u_n\ ]\|_\Sigma, \qquad k = 1, \cdots, n;\ k \neq i. \tag{5.11}$$

where $\|\mathbf{A}\|_\Sigma$ is the summation of all elements in a matrix $\mathbf{A}$.

Using equations 5.7 - 5.11, we obtain

$$\begin{aligned}
\bar{y}_i &= \| - g^{ii}_{i\bullet}(\bar{\mathbf{G}}^{ii})^{-1}g^{ii}_{\bullet i}\|_\Sigma u_i \\
&= \| - g^{ii}_{\bullet i}g^{ii}_{i\bullet} \otimes (\bar{\mathbf{G}}^{ii})^{-T}\|_\Sigma u_i \\
&= \| - \frac{g^{ii}_{\bullet i}g^{ii}_{i\bullet}}{g_{ii}} \otimes (\bar{\mathbf{G}}^{ii})^{-T}\|_\Sigma g_{ii}u_i.
\end{aligned}$$

Consequently, those steady state relationships provided in reference 20 can be extended as follows.

Define

$$\triangle\mathbf{G}_{ii,n-1} = -\frac{1}{g_{ii}}g^{ii}_{\bullet i}g^{ii}_{i\bullet}$$

as the incremental process gain matrix of subsystem $\mathbf{G}^{ii}$ when control loop $y_i - u_i$ is closed, then the dynamic DRIA (dDRIA) of individual control loop $y_i - u_i$ in an $n \times n$ system can be described as

$$\mathbf{\Psi}_{ii,n-1} = \triangle\mathbf{G}_{ii,n-1} \otimes (\bar{\mathbf{G}}^{ii})^{-T}, \tag{5.12}$$

and the dRI, $\phi_{ii,n-1}$, is the summation of all elements of $\mathbf{\Psi}_{ii,n-1}$, i.e.

$$\phi_{ii,n-1} = \|\mathbf{\Psi}_{ii,n-1}\|_{\Sigma} = \|\triangle\mathbf{G}_{ii,n-1} \otimes (\bar{\mathbf{G}}^{ii})^{-T}\|_{\Sigma}, \tag{5.13}$$

where $\otimes$ is the Hadamard product and $[\mathbf{G}^{ij}]^{-T}$ is the transpose of the inverse of matrix $\mathbf{G}^{ij}$.

From equation 5.10, $\bar{\mathbf{G}}$ can be factorized as

$$\begin{aligned}\bar{\mathbf{G}} &= \begin{pmatrix} g_{11}+1/c_1 & g_{12} & \cdots & g_{1n} \\ g_{21} & g_{22}+1/c_2 & \cdots & g_{2n} \\ \vdots & \vdots & \ddots & \vdots \\ g_{n1} & g_{n2} & \cdots & g_{nn}+1/c_n \end{pmatrix} \\ &= \mathbf{G} \otimes \mathbf{P},\end{aligned}$$

where

$$\mathbf{P} = \begin{pmatrix} \dfrac{1+g_{11}c_1}{g_{11}c_1} & 1 & \cdots & 1 \\ 1 & \dfrac{1+g_{22}c_2}{g_{22}c_2} & \cdots & 1 \\ \vdots & \vdots & \ddots & \vdots \\ 1 & 1 & \cdots & \dfrac{1+g_{nn}c_n}{g_{nn}c_n} \end{pmatrix}.$$

Hence, the dDRIA and dRI can be obtained respectively by,

$$\mathbf{\Psi}_{ii,n-1} = \triangle\mathbf{G}_{ii,n-1} \otimes (\mathbf{G}^{ii} \otimes \mathbf{P}^{ii})^{-T}, \tag{5.14}$$

and

$$\phi_{ii,n-1} = \|\triangle\mathbf{G}_{ii,n-1} \otimes (\mathbf{G}^{ii} \otimes \mathbf{P}^{ii})^{-T}\|_{\Sigma}. \tag{5.15}$$

Remark 1: In dDRIA and dRI of equations 5.14 and 5.15, there exists an additional matrix $\mathbf{P}$, which explicitly reveals interactions to an arbitrary loop by all the

other $n-1$ closed loops under band-limited control conditions. Thus, for the given decentralized PID controllers, the dynamic interaction among control loops at an arbitrary frequency can be easily investigated through the matrix $\mathbf{P}$, moreover, the calculation remains simple even for high dimensional processes.

Remark 2: For decentralized PI or PID control, we have

$$\mathbf{C}^{-1}(j0) = \mathbf{0},$$

and

$$\bar{\mathbf{G}}(j0) = \mathbf{G}(j0)$$

which implies that the RI and the dRI are equivalent at steady state. However, because the dRI measure interactions under practical unperfect control conditions at some specified frequency points, it is more accurate in estimating the dynamic loop interactions and more effective in designing decentralized controllers.

The significance of above development are as follows:

(1) The interaction to an individual control loop from the other loops is derived in matrix form, and the relationship between RI and DRIA is extended to the whole frequency domain from the steady state;

(2) Equations 5.12 and 5.13 indicate that the dRI is a combination of the interactions to individual control loops from the others; there may exist cause-effect cancelation among them such that selecting of loop pairings by dRI may be inaccurate [60].

(3) Because interactions among control loops are controllers dependent, the dDRIA represents how the decentralized controllers interact with each other, while the dRI provides the overall effect to an individual control loop from the others;

(4) The dRI can be obtained easily once process transfer function elements and controllers are available, which is not limited by the system dimension.

5.3 Determination of Multiplicated Model Factor

The proposed method of designing decentralized controllers for multivariable processes involves three main steps:

(1) the design of individual controllers by ignoring the loop interactions;

(2) the determination of the equivalent transfer function for each individual loop through use of the dRI;

(3) the fine-tuning of each controller parameter based on the equivalent transfer function.

Because the interactions among control loops are ignored in the first step, all available SISO PID controller design techniques can be applied to the design of the initial individual controllers for the diagonal elements. Thus, according to the expected control performance, one can select the most suitable tuning rules, such as Ziegler and Nichols tuning [35], IMC tuning [36], and some other optimal design methods [76]. Obviously, different tuning rules provide different controller settings and, correspondingly, different estimations of loop interactions. Even these different estimations will affect the decentralized controllers designed in the third step; they have no influence on the design mechanism of our method. Because our main objective in this chapter is to propose a much simpler method for designing decentralized PID controller based on the dynamic interaction analysis, the SIMC-PID tuning rule, which is derived from IMC theory, is applied in the following development because of its very simple and better tradeoff between disturbance

response and robustness, especially for the lag-dominant processes ($\tau_{ii} \gg \theta$ in equation 5.1) [38].

For the SOPDT SISO system given by equation 5.1, the SIMC-PID settings in the form of equation 5.2 was suggested as

$$k_{Pi} = \frac{1}{k_{ii}} \frac{\tau_{ii}}{\tau_{Ci} + \theta_{ii}}, \tag{5.16}$$

$$\tau_{Ii} = \min\{\tau_{ii}, 4(\tau_{Ci} + \theta_{ii})\}, \tag{5.17}$$

$$\tau_{Di} = \tau_{ii}^{'}, \tag{5.18}$$

where, τ_{Ci} is the desired closed-loop time constant. It is recommended to select the value of τ_{Ci} as θ_{ii} for a tradeoff between:

(1) the fast speed of the response and good disturbance rejection (favored by a small value of τ_{Ci});

(2) the stability, robustness, and small input variation (favored by a large value of τ_{Ci}).

Let $\tilde{\mathbf{G}} = \text{diag}\{\mathbf{G}\}$, the initial controllers $\tilde{\mathbf{C}}$ can be designed for $\tilde{\mathbf{G}}$ through the SIMC-PID tuning rules, such that

$$\tilde{\mathbf{G}}\tilde{\mathbf{C}} = \begin{pmatrix} g_{11}\tilde{c}_1 & 0 & \cdots & 0 \\ 0 & g_{22}\tilde{c}_2 & \cdots & 0 \\ \vdots & \vdots & \ddots & \vdots \\ 0 & 0 & \cdots & g_{nn}\tilde{c}_n \end{pmatrix},$$

with the open-loop transfer function for each individual control loop is

$$g_{ii}\tilde{c}_i = \frac{1}{(\tilde{\tau}_{Ci} + \theta_{ii})s} e^{-\theta_{ii}s}. \tag{5.19}$$

Using first order Taylor series expansion for equation 5.19, the closed-loop transfer function, open-loop gain crossover frequency ω_{ci} and matrix $\mathbf{P}$, can be obtained

respectively by,

$$\frac{y_i}{r_i} = \frac{1}{\tilde{\tau}_{Ci}s + 1} e^{-\theta_{ii}s},$$

$$\tilde{\omega}_{ci} = \frac{1}{\tilde{\tau}_{Ci} + \theta_{ii}}, \tag{5.20}$$

and

$$\mathbf{P} = \begin{pmatrix} (\tilde{\tau}_{C1}s + 1)e^{\theta_{11}s} & 1 & \cdots & 1 \\ 1 & (\tilde{\tau}_{C2}s + 1)e^{\theta_{22}s} & \cdots & 1 \\ \vdots & \vdots & \ddots & \vdots \\ 1 & 1 & \cdots & (\tilde{\tau}_{Cn}s + 1)e^{\theta_{nn}s} \end{pmatrix}. \tag{5.21}$$

Because each controller is designed around the critical frequency of its transfer function, the dRI of individual control loop $\mathbf{y}_i - \mathbf{u}_i$ can be estimated at the critical frequency $j\omega_{cri}$

$$\phi_{ii,n-1}(j\omega_{cri}) = \|\triangle \mathbf{G}_{ii,n-1}(j\omega_{cri}) \otimes (\mathbf{G}^{ii}(j\omega_{cri}) \otimes \mathbf{P}^{ii}(j\omega_{cri}))^{-T}\|_{\Sigma}. \tag{5.22}$$

For interactive multivariable process $\mathbf{G}$, it is desirable to have the same open-loop transfer function as multivariable control system $\tilde{\mathbf{G}}\tilde{\mathbf{C}}$ [20]. Because controller $\tilde{\mathbf{C}}$ is designed for the diagonal elements of $\mathbf{G}$ without considering the couplings between control loops, the designed controller should be detunned by

$$c_i = \frac{\tilde{c}_i}{\rho_{ii,n-1}} = \frac{\tilde{c}_i}{1 + \phi_{ii,n-1}} \tag{5.23}$$

to result in approximately the same closed-loop control performance. However, it is impractical to use $\rho_{ii,n-1}$ directly to fine-tune the controller because it has different values at different frequencies. To solve this problem, one possible way is to use some appropriate transfer functions to identify those MMFs. Because at the neighborhood of the critical point the transmission interaction can be considered as a linear function, it is reasonable to represent the MMF by a low-order transfer

function involving the first two items of its Taylor series, which can be further simplified for controller design by a pure time-delay transfer function as

$$\rho_{ii,n-1} = k_{\rho i,n-1} e^{-\theta_{\rho i,n-1} s}, \tag{5.24}$$

where,

$$k_{\rho i,n-1} = |\rho_{ii,n-1}(j\omega_{cri})| = |1 + \phi_{ii,n-1}(j\omega_{cri})| \tag{5.25}$$

and

$$\theta_{\rho i,n-1} = -\frac{\arg(\rho_{ii,n-1}(j\omega_{cri}))}{\omega_{cri}} = -\frac{\arg(1 + \phi_{ii,n-1}(j\omega_{cri}))}{\omega_{cri}}, \tag{5.26}$$

with ω_{cri} indicating the critical frequency of the ith control loop $y_i - u_i$. Obviously, the positive/negative $\theta_{\rho i,n-1}$ indicates that the interactions from other control loops bring a phase lag/lead of individual control loops.

From equations 5.1 and 5.3, the equivalent transfer function for loop $y_i - u_i$ can be expressed by

$$\hat{g}_{ii}(s) = \frac{f_{ki} k_{ii}}{(\tau_{ii} s + 1)(\tau'_{ii} s + 1)} e^{-f_{\theta i}\theta_{ii} s}, \tag{5.27}$$

where,

$$f_{ki} = \max\{1, k_{\rho i,n-1}\}, \tag{5.28}$$

and

$$f_{\theta i} = \max\{1, 1 + \frac{\theta_{\rho i,n-1}}{\theta_{ii}}\}. \tag{5.29}$$

Remark 3: The open-loop transfer function for each individual control loop given by equation 5.19 is determined by the SIMC-PID tuning settings. If other tuning

rules are applied, some different forms may be derived, and $g_{ii}\tilde{c}_i$ always has the form

$$g_{ii}\tilde{c}_i = \tilde{h}(s)\frac{ke^{-\theta s}}{s},$$

where, $\tilde{h}(s)$ is proper and rational with $\tilde{h}(j0) = 0$ [76].

Remark 4: Because the region between $\tilde{\omega}_{ci}$ ($|g_{ii}\tilde{c}_i| = 1$) and $\tilde{\omega}_{180}$ [$\arg(g_{ii}\tilde{c}_i) = -180^o$] is most critical for individual control loop design, the crossover frequency of $g_{ii}\tilde{c}_i$ can be adopted as the critical frequency point for determining the dRI to the particular loop $y_i - u_i$ to obtain $\hat{g}_{ii}$ [23].

Remark 5: In equations 5.28 and 5.29, the factors f_{ki} and $f_{\theta i}$ are selected to be not smaller than 1, such that the equivalent open loop gain and the time delay of $\hat{g}_{ii}$ are no smaller than those of g_{ii}. The reason for such a selection is to make the resultant controller settings more conservative than those of $\hat{g}_{ii}$ so that loop failure tolerance property can be preserved.

5.4 Design of a Decentralized Controller

Using tuning rules of equations 5.16-5.18, the controller parameters for the individual equivalent transfer function of equation 5.27 can be determined as,

$$k_{Pi} = \frac{1}{f_{ki}k_{ii}}\frac{\tau_{ii}}{\tau_{Ci} + f_{\theta i}\theta_{ii}}, \tag{5.30}$$

$$\tau_{Ii} = \min\{\tau_{ii}, 4(\tau_{Ci} + f_{\theta i}\theta_{ii})\}, \tag{5.31}$$

$$\tau_{Di} = \tau'_{ii}. \tag{5.32}$$

Furthermore, by selecting the desired closed-loop time constant τ_{Ci} to be the same value as the time delay $f_{\theta i}\theta_{ii}$, we can obtain a set of simple rules for designing the

parameters of a decentralized PID controller as,

$$k_{Pi} = \frac{1}{f_{ki}} \frac{1}{2f_{\theta i}} \frac{1}{k_{ii}} \frac{\tau_{ii}}{\theta_{ii}}, \tag{5.33}$$

$$\tau_{Ii} = \min\{\tau_{ii}, 8f_{\theta i}\theta_{ii}\}, \tag{5.34}$$

$$\tau_{Di} = \tau'_{ii}. \tag{5.35}$$

Once the closed-loop properties of the diagonal elements and the critical frequencies of all individual control loops are determined, the dRI and MMF can be obtained through calculation of the matrix P and dDRIA. Then, the parameters of the PID controllers can be calculated based on the equivalent transfer function of each control loop and the SIMC-PID tuning rules. In such a design procedure, the overall control system stability is assured if the loop pairing is structurally stable, which can be explained as follows:

(1) Each $\tilde{c}_i$ is designed without considering loop interaction; it is more aggressive to control loop $y_i - u_i$ than the final control setting c_i. Generally, we have $\bar{\sigma}(\mathbf{\Delta}_1) \leq \bar{\sigma}(\mathbf{\Delta}_2)$ as $\max\{1, |\rho_{ii,n-1}|\} \geq 1$, where $\bar{\sigma}(\mathbf{A})$ is the maximum singular value of matrix $\mathbf{A}$, $\mathbf{\Delta}_1 = \tilde{\mathbf{G}}\mathbf{C}(1+\tilde{\mathbf{G}}\mathbf{C})^{-1}$ and $\mathbf{\Delta}_2 = \tilde{\mathbf{G}}\tilde{\mathbf{C}}(1+\tilde{\mathbf{G}}\tilde{\mathbf{C}})^{-1}$.

(2) Let $\mathbf{M} = -(\mathbf{G} - \tilde{\mathbf{G}})\tilde{\mathbf{G}}^{-1}$, and following the definition of the structured singular value (SSV) [56]:

$$\mu_{\mathbf{\Delta}}(\mathbf{M}) \equiv \frac{1}{\min\{\bar{\sigma}(\mathbf{\Delta}) | \det(I - k_m\mathbf{M}\mathbf{\Delta}) = 0 \text{ for structured } \mathbf{\Delta}\}},$$

we have $\mu_{\mathbf{\Delta}_1}(\mathbf{M}) \leq \mu_{\mathbf{\Delta}_2}(\mathbf{M})$, which implies there exist smaller interactions among control loops when the detunned controller $\mathbf{C}$ is applied [20].

(3) Because the bigger dRI $\phi_{ii,n-1}$ is used to determine the detunning factors and f_{ki} and $f_{\theta i}$ are no smaller than 1, the resultant controller c_i will be more conservative, with a smaller gain and crossover frequency compared with $\tilde{c}_i$.

(4) Conservative control action in each loop presents smaller interaction to other loops. Because the design based on $\hat{g}_{ii}$ for loop $y_i - u_i$ will end up with a more conservative c_i. the stability margin for each individual loop will be further increased compared with that using the true $\phi_{ii,n-1}$.

As a summary of the above results, an algorithm for the design of a decentralized PID controller for general multivariable processes is given as below.

Algorithm 1:

Step 1. For multivariable process **G**, pair the inputs and outputs based on the method given in ref [60];

Step 2. Design an individual controller for the diagonal elements of the process transfer function matrix following equations 5.16 - 5.18;

Step 3. Use equation 5.21 to construct matrix **P**;

Step 4. Let $i = 1$, go to step 5;

Step 5. Calculate critical frequency ω_{cri}, dRI and $\phi_{ii,n-1}(j\omega_{cri})$, by equations 5.20 and 5.22, respectively;

Step 6. Determine $k_{\rho i,n-1}$ and $\theta_{\rho i,n-1}$ for MMF, $\rho_{ii,n-1}$, by equations 5.24-5.26;

Step 7. Obtain the factors f_{ki} and $f_{\theta i}$ by equations 5.28 and 5.29;

Step 8. Fine-tune the controller parameters following equations 5.30 - 5.32 or 5.33 - 5.35;

Step 9. If $i < n$, $i = i + 1$, go to step 5. Otherwise, go to step 10;

Step 10. End.

The procedure for the independent design of a decentralized PID controller by using the proposed method is illustrated in Figure 5.4.

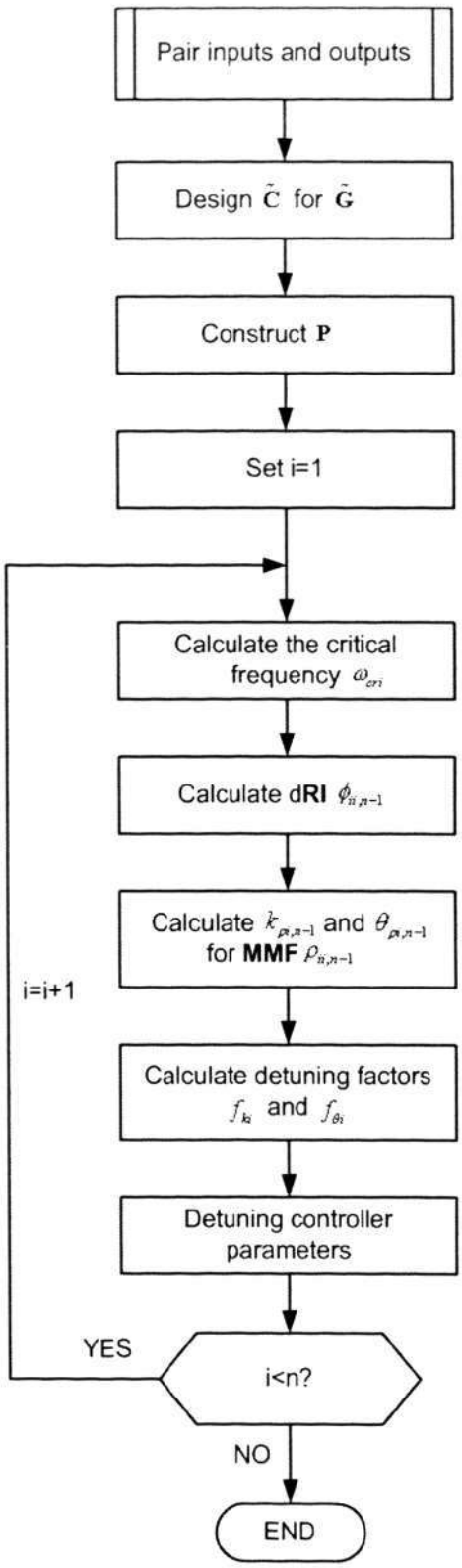

Figure 5.4: Procedure for the independent design of a decentralized PID controller

5.5 Examples

The main advantage of the proposed method is to provide a simple yet effective way to design decentralized PID controller especially for a high-dimension process (a process larger than 2×2 process). Many 2×2, 3×3 and 4×4 processes have been tested on the closed-loop performance of the proposed method. In the following, we will present the results on a 2 × 2 Vinante and Luyben (VL) column process and a 4 × 4 Alatiqi(A1) column process, of which the VL case is used to illustrate the step-by-step design procedures while the A1 case is used to demonstrate the effectiveness of the proposed method for higher dimensional processes.

5.5.1 Example 1. VL Column

The VL column system with its transfer function matrix was given by Luyben [39]:

$$\mathbf{G} = \begin{pmatrix} \frac{2.2e^{-s}}{7s+1} & \frac{1.3e^{-0.3s}}{7s+1} \\ \frac{2.8e^{-1.8s}}{9.5s+1} & \frac{4.3e^{-0.35s}}{9.2s+1} \end{pmatrix}.$$

According to equations 5.16 - 5.18 and selecting $\tau_{Ci} = \theta_{ii}$, the SIMC-PID controller for diagonal system $\tilde{\mathbf{G}}$ is obtained as,

$$\tilde{\mathbf{C}} = \begin{pmatrix} -1.5909(1+\frac{1}{7s}) & 0 \\ 0 & 3.0565(1+\frac{1}{2.8s}) \end{pmatrix}$$

resulting in the critical frequencies for control loops $y_1 - u_1$ and $y_2 - u_2$ as $\omega_{cr1} = \tilde{\omega}_{cr1} = 0.5\ rad/s$ and $\omega_{cr2} = \tilde{\omega}_{cr2} = 1.4286\ rad/s$, respectively (equation 5.20). Then from equations 5.21 and 5.22, we have

$$\mathbf{P} = \begin{pmatrix} (s+1)e^{s} & 1 \\ 1 & (0.35s+1)e^{0.35s} \end{pmatrix}.$$

and

$$\begin{aligned}\phi_{11,1}(j0.5) &= -0.2739 + j0.2451,\\ \phi_{22,1}(j1.4286) &= 0.2026 - j0.0674.\end{aligned}$$

Subsequently,

$$\begin{aligned}\rho_{11,1} &= 0.7663e^{-(-0.6510)s},\\ \rho_{22,1} &= 1.2047e^{-0.0392s},\end{aligned}$$

and the equivalent transfer functions of both control loops are constructed as

$$\begin{aligned}\hat{g}_{11} &= -\frac{2.2e^{-s}}{7s+1},\\ \hat{g}_{22} &= \frac{5.1802e^{-0.3892s}}{9.2s+1}.\end{aligned}$$

It is noted that because $k_{\rho 1,1} < 1$ and $\theta_{\rho 1,1} < 0$, both f_{k1} and $f_{\theta 1}$ are set to 1 such that $\hat{g}_{11} = g_{11}$ to guarantee the loop failure tolerance of control loop $y_1 - u_1$. While $f_{k2} = 1.2047$ and $f_{\theta 2} = 1.1120$ are used to fine-tune the PI controller setting of control loop $y_2 - u_2$. Consequently, the decentralized PI controller parameters are determined as $k_{P1} = -1.5909, \tau_{I1} = 7.0000$, and $k_{P2} = 2.2817, \tau_{I2} = 3.1135$.

Figure 5.5 shows the system inputs and responses for step changes in the set-points for y_1 and y_2. The simulation results indicate that both setpoint responses and magnitude of inputs of the proposed PI controllers are comparable with those of the BLT PI controller ($k_{P1} = -1.0700, \tau_{I1} = 7.1000$, and $k_{P2} = 1.9700, \tau_{I2} = 2.5800$) [39].

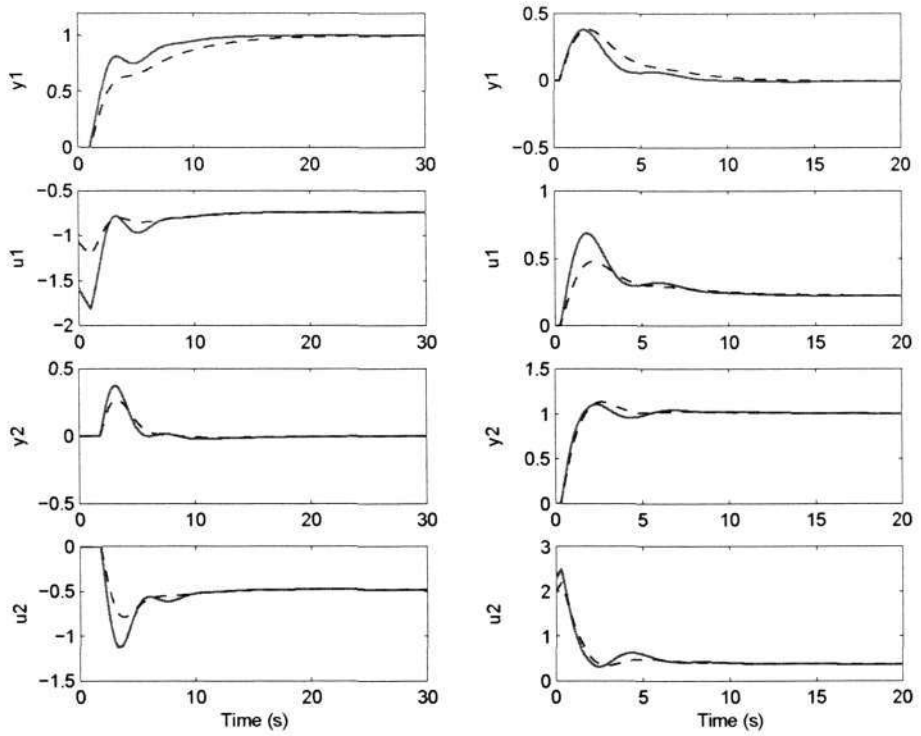

Figure 5.5: Setpoint change response for the Vinante and Luyben column (solid line, Proposed design; dashed line, BLT design).

5.5.2 Example 2. Alatiqi Column (A1)

The transfer function matrix for the A1 column system is given by

$$\mathbf{G} = \begin{pmatrix} \frac{2.22e^{-2.5s}}{(36s+1)(25s+1)} & \frac{-2.94(7.9s+1)e^{-0.05s}}{(23.7s+1)^2} & \frac{0.017e^{-0.2s}}{(31.6s+1)(7s+1)} & \frac{-0.64e^{-20s}}{(29s+1)^2} \\ \frac{-2.33e^{-5s}}{(35s+1)^2} & \frac{3.46e^{-1.01s}}{32s+1} & \frac{-0.51e^{-7.5s}}{(32s+1)^2} & \frac{1.68e^{-2s}}{(28s+1)^2} \\ \frac{-1.06e^{-22s}}{(17s+1)^2} & \frac{3.511e^{-13s}}{(12s+1)^2} & \frac{4.41e^{-1.01s}}{16.2s+1} & \frac{-5.38e^{-0.5s}}{17s+1} \\ \frac{-5.73e^{-2.5s}}{(8s+1)(50s+1)} & \frac{4.32(25s+1)e^{-0.01s}}{(50s+1)(5s+1)} & \frac{-1.25e^{-2.8s}}{(43.6s+1)(9s+1)} & \frac{4.78e^{-1.15s}}{(48s+1)(5s+1)} \end{pmatrix}.$$

According to Algorithm 1, the resulting decentralized controllers and those obtained by using the BLT method of Luyben [39], the trial-and-error method [51], and an independent design method of Chen and Seborg [50] are shown in table 5.1.

Table 5.1: Proposed PID controllers for Alatiqi column

loop	proposed design			BLT design		ICC design		Chen's design	
	k_{Pi}	τ_{Ii}	τ_{Di}	k_{Pi}	τ_{Ii}	k_{Pi}	τ_{Ii}	k_{Pi}	τ_{Ii}
1	2.1822	29.7250	25	2.28	72.2	0.385	34.72	0.176	62.9
2	4.4807	8.0800	0	2.94	7.48	6.190	21.80	0.220	31.0
3	1.6656	8.0800	0	1.18	7.39	2.836	19.22	3.15	8.03
4	4.3660	9.2000	5	2.02	27.8	0.732	36.93	0.447	47.5

The closed-loop responses as well as system inputs for unit step changes of the setpoints $r_1 - r_4$ are shown in Figures 5.6 - 5.9. The simulation results indicate that the control performance is better than those of the other three design methods.

In this chapter, a simple yet effective method was proposed to design a decentralized PID controller for multivariable processes. The design obtains the MMF at an arbitrary frequency by using the dRI. Through approximating the MMF by a time-delay function at the neighborhood of the critical frequency, the equivalent transfer function of an individual control loop was constructed. Subsequently, the appropriate controller settings can be determined by applying the SISO controller tuning rules to the equivalent transfer function. An algorithm for using the proposed method to design a decentralized PID controller was also provided. The application of the design method to 2×2 system and 4×4 systems showed that it results in a better overall control performance than those of other design methods such as the BLT method, the trial and error method, and the independent design method based on Nyquist stability analysis.

Since most industrial processes can be represented by low order transfer functions, how to apply the proposed design procedure to the low order process will be studied in the following chapter.

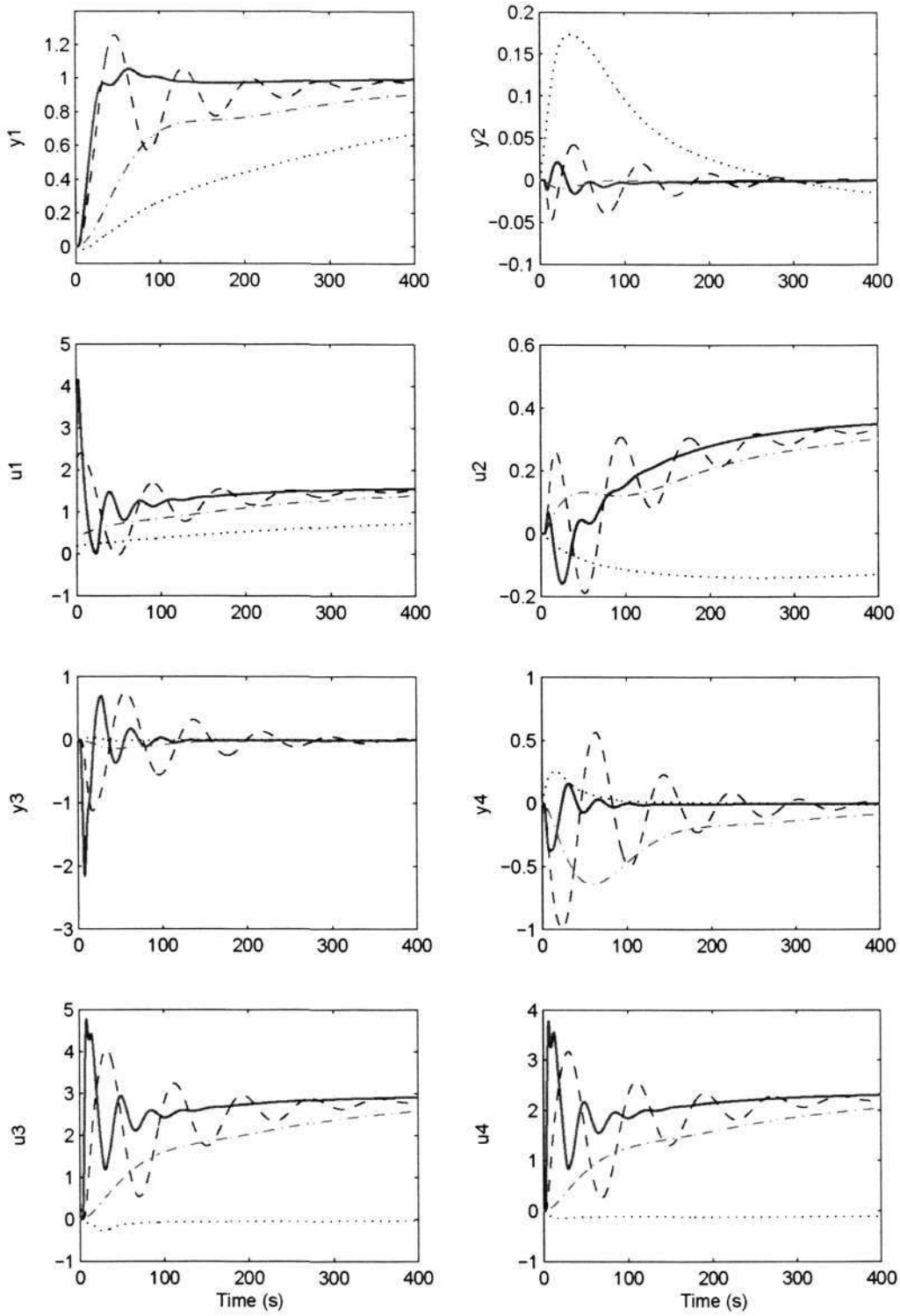

Figure 5.6: Setpoint change response of y_1 for the A1 column example (solid line, proposed design; dashed line, BLT design; dashed-dotted line, Lee at el.; dotted line, Chen at el.).

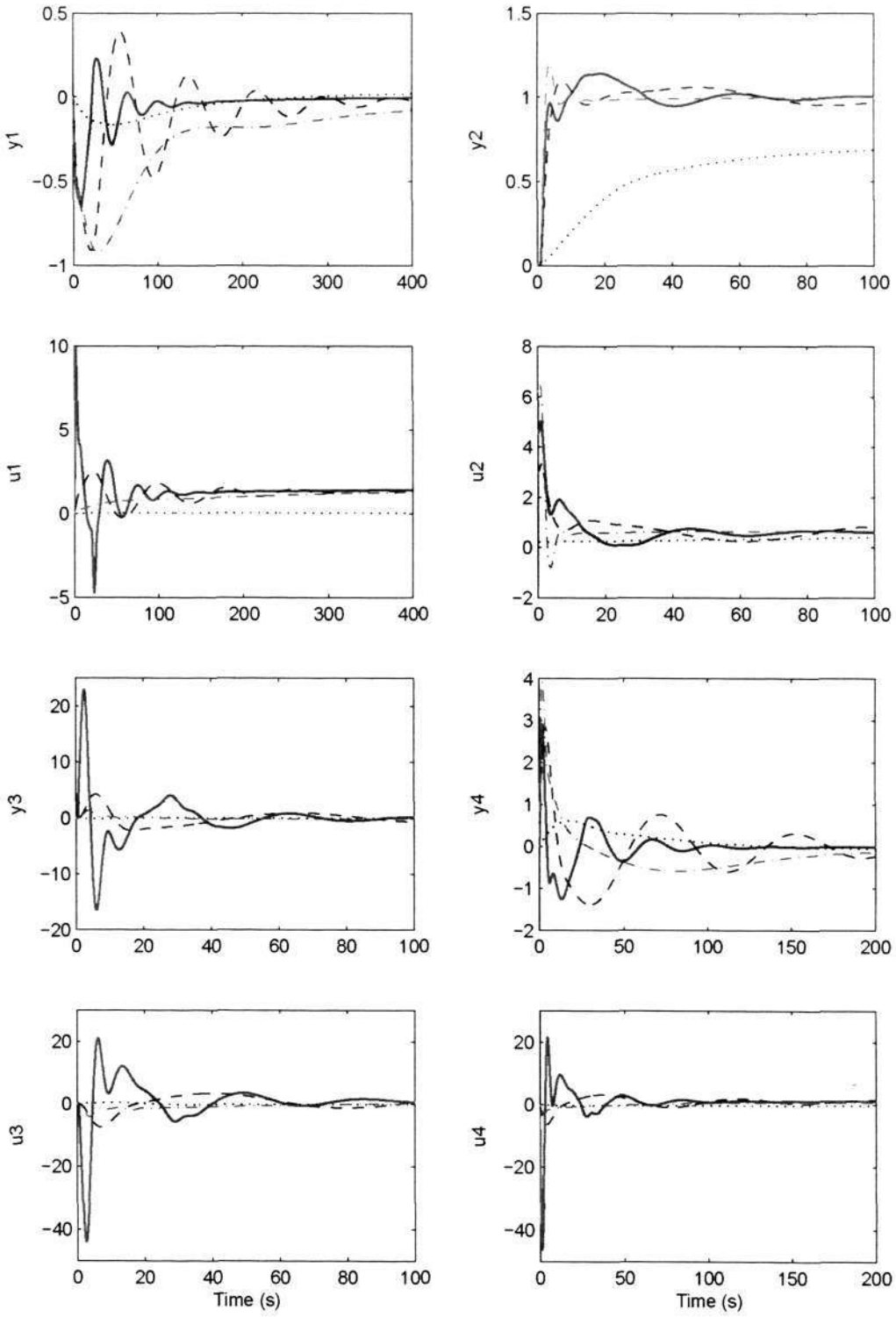

Figure 5.7: Setpoint change response of y_2 for the A1 column example (solid line, proposed design; dashed line, BLT design; dashed-dotted line, Lee at el.; dotted line, Chen at el.).

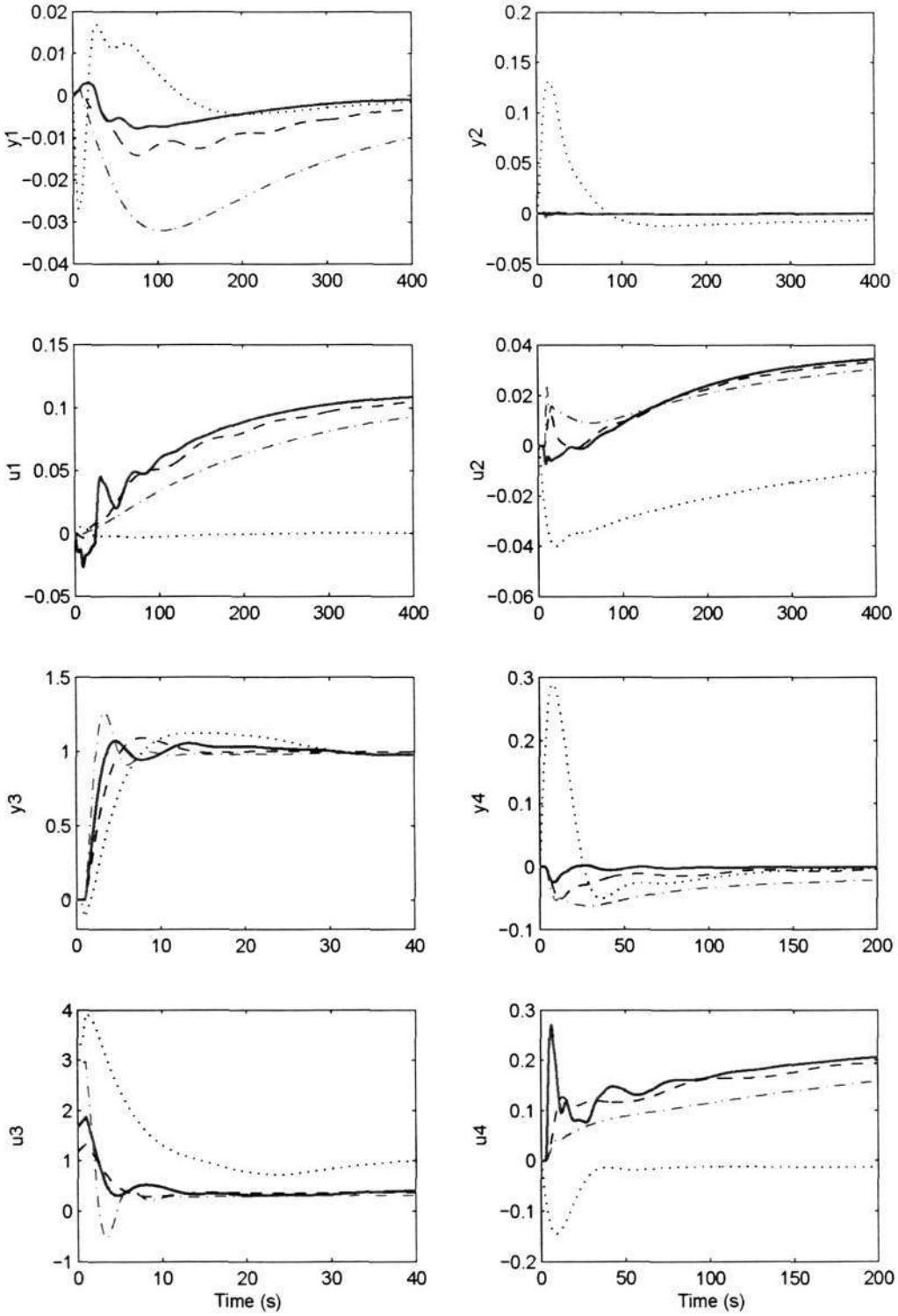

Figure 5.8: Setpoint change response of y_3 for the A1 column example (solid line, proposed design; dashed line, BLT design; dashed-dotted line, Lee at el.; dotted line, Chen at el.).

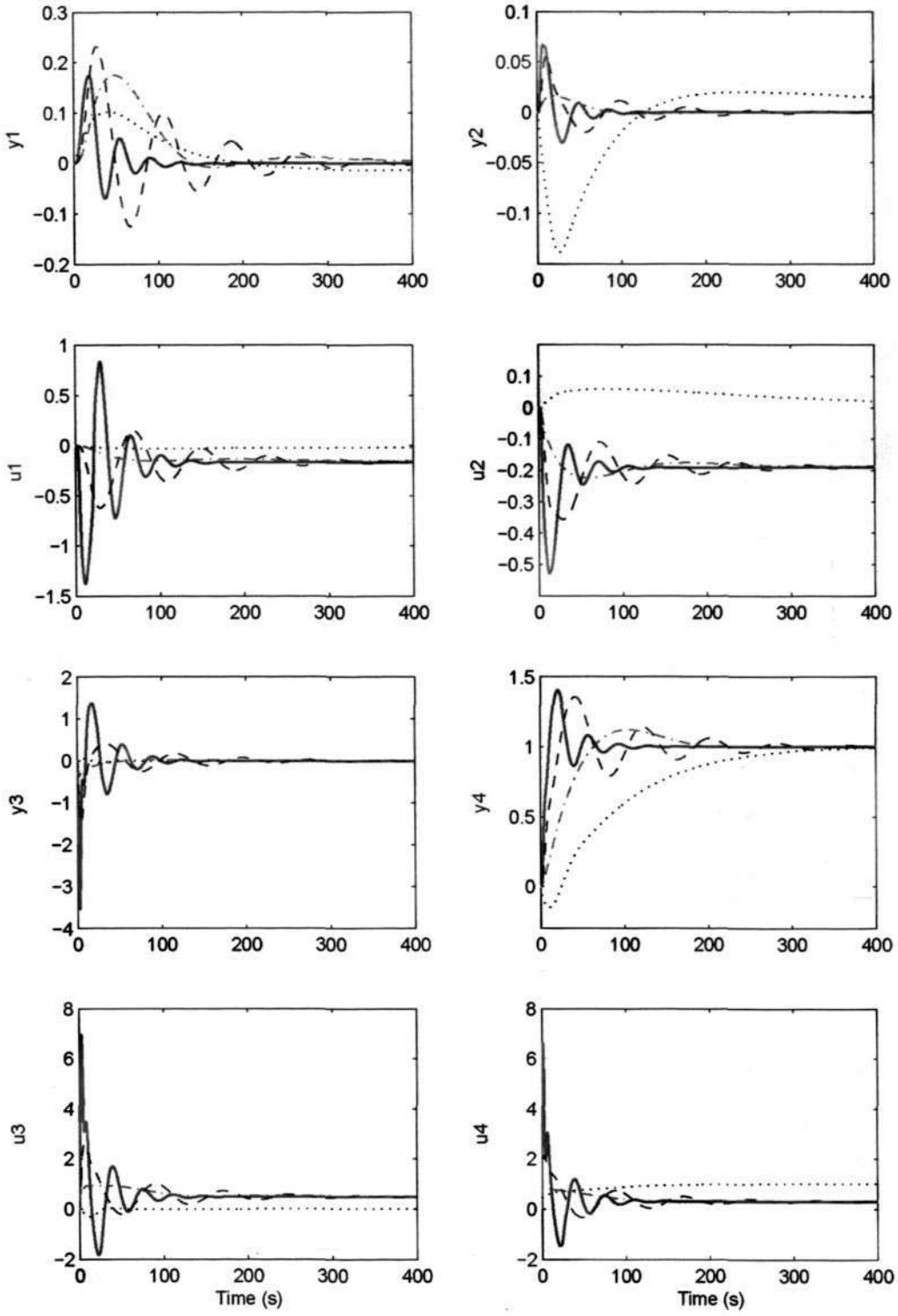

Figure 5.9: Setpoint change response of y_4 for the A1 column example (solid line, proposed design; dashed line, BLT design; dashed-dotted line, Lee at el.; dotted line, Chen at el.).

Chapter 6

Design of Decentralized IMC-PID Controller Based on dRI Analysis

In this chapter, a simple yet effective decentralized PID controller design methodology is proposed based on dynamic interaction analysis and internal model control principle. On the basis of structure decomposition, the dynamic relative interaction is defined and represented by the process model and controller explicitly. An initial decentralized controller is designed first by using the diagonal elements and then implemented to estimate the dynamic relative interaction (dRI) to individual control loop from all others. With the obtained dRI, the multiplicate model factor is derived and then simplified to a pure time delay function at the neighborhood of each control loop critical frequency to obtain the equivalent transfer function for the particular control loop. Consequently, appropriate controller parameters for individual control loop are determined by applying the IMC-PID tuning rules for the equivalent transfer function. Examples for a variety of 2×2, 3×3 and 4×4 systems are used to demonstrate that the overall control system performance is much better than that of other tuning methods, such as the BLT method [39, 40], the trial and error method [51], and the independent design method based on Nyquist stability analysis [50], especially for higher dimensional processes.

6.1 Preliminaries

Consider an $n \times n$ system with a decentralized feedback control structure as shown in Figure 6.1, where, $\mathbf{r}$, $\mathbf{u}$ and $\mathbf{y}$ are vectors of references , inputs and outputs respectively, $\mathbf{G}(s) = [g_{ij}(s)]_{n\times n}$ is system's transfer function matrix with its individual element $g_{ij}(s)$ described by the common used models, as given by the second column in Table 6.1, and controller $\mathbf{C}(s) = \text{diag}\{c_1(s), \cdots, c_n(s)\}$ is the decentralized PID type with its individual element given in parallel form as

$$c_i(s) = k_{Pi}(1 + \frac{1}{\tau_{Ii}s} + \tau_{Di}s). \tag{6.1}$$

It is assumed that $\mathbf{G}(s)$ has been arranged so that the pairings of the inputs and outputs in the decentralized feedback system correspond to the diagonal elements of $\mathbf{G}(s)$.

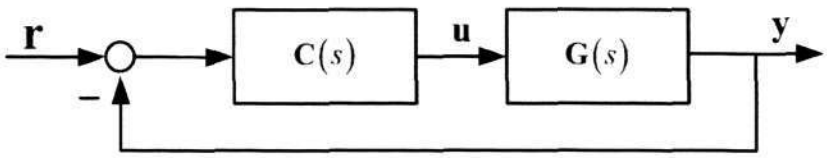

Figure 6.1: General decentralized control system.

For multi-input multi-output (MIMO) process, when one controller, $c_i(s)$, acting in response to the setpoint change and/or the output disturbance, it affects the overall system through the off-diagonal elements of $\mathbf{G}(s)$, forcing other controllers to take actions, as well, these controllers reversely influence the ith loop via other off-diagonal elements, and this interacting processes among control loops continue throughout the whole transient until a steady state is reached. To examine the transmittance of interactions between an individual control loop and the others, the decentralized control system can be structurally decomposed into n individual SISO control loops with the coupling among all loops explicitly exposed and embedded in each loop. Figure 6.2 shows the structure of an arbitrary control loop $y_i - u_i$ after the structural decomposition.

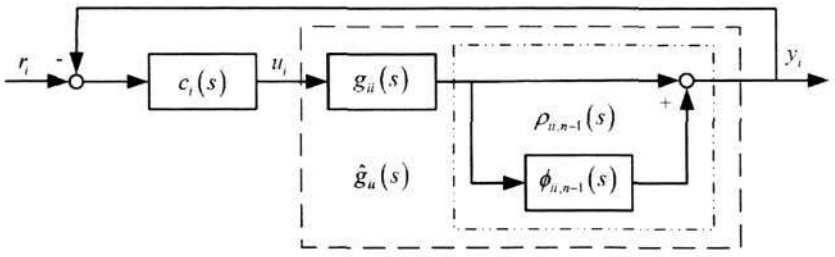

Figure 6.2: Structure of loop $y_i - u_i$ by structural decomposition

In Figure 6.2, the interaction to an individual control loop $y_i - u_i$ from the other $n-1$ control loops is represented by the Relative Interaction (RI) $\phi_{ii,n-1}(s)$, and the equivalent transfer function of an individual control loop $y_i - u_i$, denoted by $\hat{g}_{ii}(s)$, can be obtained in terms of $\phi_{ii,n-1}(s)$ by

$$\hat{g}_{ii}(s) = g_{ii}(s)\rho_{ii,n-1}(s), \tag{6.2}$$

with

$$\rho_{ii,n-1}(s) = 1 + \phi_{ii,n-1}(s), \tag{6.3}$$

where $\rho_{ii,n-1}(s)$ is defined as multiplicate model factor (MMF) to indicate the model change of an individual control loop $y_i - u_i$ after the other $n-1$ control loops are closed. Once the RI, $\phi_{ii,n-1}(s)$, is available, the corresponding MMF, $\rho_{ii,n-1}(s)$, and the equivalent process transfer function $\hat{g}_{ii}$ can be obtained, which can be directly used to independently design the PID controller for each individual control loop $y_i - u_i$.

In the following development, we use RI as a basic interaction measure to investigate the interactions among control loops and derive equivalent transfer function for each loop. Sometimes, we will omit the Laplace operator s for simplicity unless otherwise specified.

The RI for control loop $y_i - u_j$ is defined as the ratio of two elements [66]: the increment of the process gain after all other control loops are closed, and the

apparent gain in the same loop when all other control loops are open, that is

$$\phi_{ij,n-1} = \frac{(\partial y_i/u_j)_{y_{k\neq i}\text{constant}} - (\partial y_i/u_j)_{u_{l\neq j}\text{constant}}}{(\partial y_i/u_j)_{u_{l\neq j}\text{constant}}} \qquad k,l = 1,\cdots,n.$$

Since the RI cannot offer effective measure on the reverse effect of individual control loop and loop-by-loop interactions, He and Cai decomposed the RI as the elements summation of decomposed relative interaction array (DRIA) to give important insights into the cause-effects of loop interactions [60]. However, the obtained results are limited to the steady state, which are less useful for controller design than the dynamic representations. Hence, it is necessary to derive the dynamic interaction among control loops represented explicitly by the process models and controllers.

6.2 Dynamic Relative Interaction

As the dynamic interactions among control loops are controller dependent [17, 19, 74, 75], appropriate controllers have to be designed and implemented into the control system for investigating the dynamic interactions. For an arbitrarily decentralized PID control system, we can redraw Figure 6.1 as Figure 6.3 for the convenience of analyzing the interactions between an arbitrary control loop $y_i - u_i$ and the others, where $\underline{\mathbf{y}}_i$ is a vector indicating the effects of u_i to other outputs, while $\bar{y}_i$ indicates the reverse effect of y_i by all the other closed control loops, $\mathbf{r}^i$, $\mathbf{u}^i$, $\mathbf{y}^i$ and $\mathbf{C}^i(s)$ indicate $\mathbf{r}$, $\mathbf{u}$, $\mathbf{y}$ and $\mathbf{C}(s)$with their ith elements, r_i, u_i, y_i and $c_i(s)$, been removed, respectively.

Since the dynamic relative interaction are input independent, without loss of generality, the references of the other $n-1$ control loops are set as constants, that is

$$\frac{d\mathbf{r}_k}{dt} = 0 \qquad \text{or} \qquad \mathbf{r}_k(s) = 0, \qquad k = 1,\cdots,n;\ k \neq i,$$

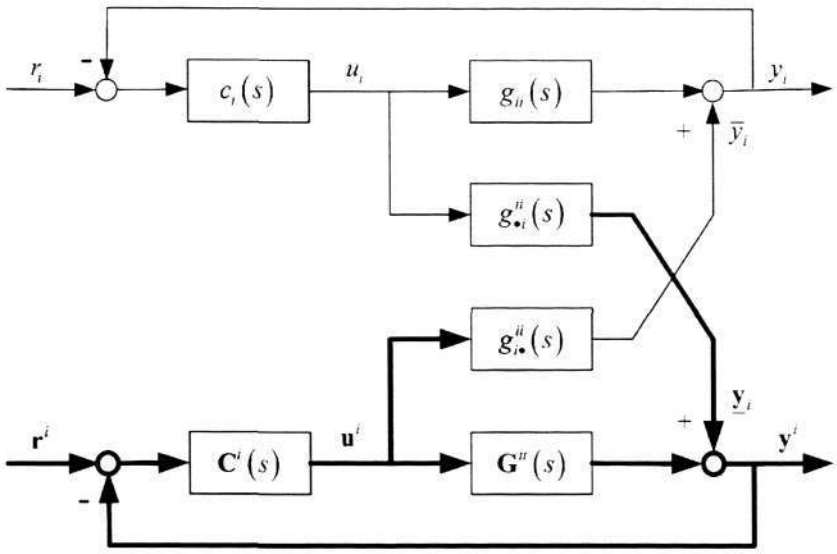

Figure 6.3: Closed-loop system with control loop $y_i - u_i$ presented explicitly

in analysis of the dynamic interaction between control loop $y_i - u_i$ and the other controlled closed-loops. Then, we have

$$\mathbf{y}^i = \mathbf{G}^{ii}\mathbf{u}^i + \underline{\mathbf{y}}_i, \tag{6.4}$$

$$\mathbf{u}^i = -\mathbf{C}^i\mathbf{y}^i, \tag{6.5}$$

and

$$\underline{\mathbf{y}}_i = g^{ii}_{\bullet i}u_i, \tag{6.6}$$

$$\bar{y}_i = g^{ii}_{i\bullet}\mathbf{u}^i, \tag{6.7}$$

where $\mathbf{G}^{ii}$ is the transfer function matrix $\mathbf{G}$, with its ith row and the ith column removed, and $g^{ii}_{\bullet i}$ and $g^{ii}_{i\bullet}$ indicate the ith row, and the ith column of $\mathbf{G}$ with the iith element, g_{ii} removed, respectively.

Combining equations 6.4 and 6.5, we can write

$$\mathbf{u}^i = -(\bar{\mathbf{G}}^{ii})^{-1}\underline{\mathbf{y}}_i, \tag{6.8}$$

where

$$\bar{\mathbf{G}} = \mathbf{G} + \mathbf{C}^{-1}. \tag{6.9}$$

Furthermore, $\bar{y}_i$ in equation 6.7 can be reprented by the summation of the following row vector

$$\bar{y}_i = |||[\ g_{i1}u_1 \quad \cdots \quad g_{ik}u_k \quad \cdots \quad g_{in}u_n\ ]|||_\Sigma, \qquad k = 1, \cdots, n;\ k \neq i. \tag{6.10}$$

where $\|\mathbf{A}\|_\Sigma$ is the summation of all elements in a matrix $\mathbf{A}$.

Using equations 6.6 - 6.10, we obtain

$$\begin{aligned} \bar{y}_i &= \| - g^{ii}_{i\bullet}(\bar{\mathbf{G}}^{ii})^{-1}g^{ii}_{\bullet i}\|_\Sigma * u_i \\ &= \| - g^{ii}_{\bullet i}g^{ii}_{i\bullet} \otimes (\bar{\mathbf{G}}^{ii})^{-T}\|_\Sigma * u_i \\ &= \| - \frac{g^{ii}_{\bullet i}g^{ii}_{i\bullet}}{g_{ii}} \otimes (\bar{\mathbf{G}}^{ii})^{-T}\|_\Sigma * g_{ii}u_i. \end{aligned}$$

Consequently, those steady state relationships provided in reference 20 can be extended as following.

Define

$$\triangle\mathbf{G}_{ii,n-1} = -\frac{1}{g_{ii}}g^{ii}_{\bullet i}g^{ii}_{i\bullet}$$

as the incremental process gain matrix of subsystem $\mathbf{G}^{ii}$ when control loop $y_i - u_i$ is closed, then the dynamic DRIA (dDRIA) of individual control loop $y_i - u_i$ in $n \times n$ system can be described as

$$\mathbf{\Psi}_{ii,n-1} = \triangle\mathbf{G}_{ii,n-1} \otimes (\bar{\mathbf{G}}^{ii})^{-T}, \tag{6.11}$$

and the corresponding dynamic relative interaction (dRI), $\phi_{ii,n-1}$, is the summation of all elements of $\mathbf{\Psi}_{ii,n-1}$, that is

$$\phi_{ii,n-1} = \|\mathbf{\Psi}_{ii,n-1}\|_{\Sigma} = \|\triangle\mathbf{G}_{ii,n-1} \otimes (\bar{\mathbf{G}}^{ii})^{-T}\|_{\Sigma}, \tag{6.12}$$

where $\otimes$ is the Hadamard product and $[\mathbf{G}^{ij}]^{-T}$ is the transpose of the inverse of matrix $\mathbf{G}^{ij}$.

From equation 6.9, $\bar{\mathbf{G}}$ can be factorized as

$$\begin{aligned}\bar{\mathbf{G}} &= \begin{pmatrix} g_{11}+1/c_1 & g_{12} & \cdots & g_{1n} \\ g_{21} & g_{22}+1/c_2 & \cdots & g_{2n} \\ \vdots & \vdots & \ddots & \vdots \\ g_{n1} & g_{n2} & \cdots & g_{nn}+1/c_n \end{pmatrix} \\ &= \mathbf{G} \otimes \mathbf{P},\end{aligned}$$

where

$$\mathbf{P} = \begin{pmatrix} \frac{1+g_{11}c_1}{g_{11}c_1} & 1 & \cdots & 1 \\ 1 & \frac{1+g_{22}c_2}{g_{22}c_2} & \cdots & 1 \\ \vdots & \vdots & \ddots & \vdots \\ 1 & 1 & \cdots & \frac{1+g_{nn}c_n}{g_{nn}c_n} \end{pmatrix}. \tag{6.13}$$

Hence, the dDRIA and dRI can be obtained respectively by,

$$\mathbf{\Psi}_{ii,n-1} = \triangle\mathbf{G}_{ii,n-1} \otimes (\mathbf{G}^{ii} \otimes \mathbf{P}^{ii})^{-T}, \tag{6.14}$$

and

$$\phi_{ii,n-1} = \|\triangle\mathbf{G}_{ii,n-1} \otimes (\mathbf{G}^{ii} \otimes \mathbf{P}^{ii})^{-T}\|_{\Sigma}. \tag{6.15}$$

Remark 1: In dDRIA and dRI of equations 6.14 and 6.15, there exists an additional matrix $\mathbf{P}$, which explicitly reveals interactions to an arbitrary loop by all the

other $n-1$ closed loops under band limited control conditions. Thus, for the given decentralized PID controllers, the dynamic interaction among control loops at an arbitrary frequency can be easily investigated through the matrix $\mathbf{P}$, moreover, the calculation remains simple even for high dimensional processes.

Remark 2: For decentralized PI or PID control, we have

$$\mathbf{C}^{-1}(j0) = \mathbf{0},$$

and

$$\bar{\mathbf{G}}(j0) = \mathbf{G}(j0)$$

which implies that the RI and the dRI are equivalent at steady state. However, since the dRI measure interactions under practical unperfect control conditions at some specified frequency points, it is more accurate in estimating the dynamic loop interactions and more effective in designing decentralized controllers.

The significance of above development are:

(1) The interaction to individual control loop from the other loops is derived in matrix form, and the relationship between RI and DRIA is extended to the whole frequency domain from the steady state;

(2) Equations 6.11 and 6.12 indicate that the dRI is a combination of the interactions to individual control loop from the others, and loop pairings selected based on the dRI may be inaccurate as there may exist cause-effect cancelation among them such that [60].

(3) As interactions among control loops are controllers dependent, the dDRIA represents how the decentralized controllers interact with each other, while the dRI provides the overall effect to individual control loop from the others;

(4) The dRI can be obtained easily once process transfer function elements and controllers are available, which is not limited by the system dimension.

6.3 Estimation of Equivalent Transfer Function

The proposed method of designing decentralized controllers for multivariable processes involves three main steps:

(1) Design individual controllers by ignoring the loop interaction;

(2) Estimate the equivalent transfer function for each individual loop through dynamic interaction analysis;

(3) Design decentralized controller based on the equivalent transfer function.

Let $\tilde{\mathbf{G}} = \text{diag}\{\mathbf{G}\}$ and ignore the interaction effect among control loops, the initial controller $\tilde{\mathbf{C}}$ can be designed by applying the well known IMC tunning rules to each element in $\tilde{\mathbf{G}}$ [36]. The IMC design procedure is brief studied as follows. The process model $\tilde{g}$ is factorized into an all-pass portion $\tilde{g}_+$ and minimum phase portion $\tilde{g}_-$, that is

$$\tilde{g} = \tilde{g}_+ \tilde{g}_-.$$

The all-pass portion $\tilde{g}_+$ includes all the open right-half-plane zeros and delays of $\tilde{g}$ and has the form

$$\tilde{g}_+ = e^{-\theta s} \prod_i (-\beta_i s + 1)^{\cdot} \qquad \text{Re}\{\beta_i\} > 0,$$

where $\theta > 0$ is the tim delay and β_i^{-1} is the right-half-plane zero in the process model.

Then the IMC controller and the complementary sensitivity function are derived respectively as

$$g_c = \tilde{g}_-^{-1} f,$$

and

$$T = \tilde{g}_+ f,$$

where f is the IMC filter and has the form

$$f = \frac{1}{(\tau_C s + 1)^r},$$

where the filter order r is selected large enough to make g_c proper, and the adjustable filter parameter τ_C provides the tradeoff between performance and robustness. The key advantage of the IMC design procedure is that all controller parameters are related in a unique, straightforward manner to the model parameters. There is only one adjustable parameter τ_C which has intuitive appeal because it determines the speed of response of the system. Furthermore, τ_C is approximately proportional to the closed-loop bandwidth which must always be smaller than the bandwidth over which the process model is valid.

Table 6.1: Parameters of IMC-PID controller for typical low order systems[a]

	g	g_{CL}	ω_c	k_P	τ_I	τ_D [b]
A[c]	$ke^{-\theta s}$			$-$	k_I	$-$
B	$\frac{ke^{-\theta s}}{s}$			$\frac{1}{k(\tau_C+\theta)}$	$-$	$-$
C	$\frac{ke^{-\theta s}}{\tau s+1}$	$\frac{e^{-\theta s}}{\tau_C s+1}$	$\frac{1}{\tau_C+\theta}$	$\frac{\tau}{k(\tau_C+\theta)}$	τ	$-$
D	$\frac{ke^{-\theta s}}{s(\tau s+1)}$			$\frac{1}{k(\tau_C+\theta)}$	$-$	τ
E	$\frac{ke^{-\theta s}}{(\tau s+1)(\tau' s+1)}$			$\frac{\tau+\tau'}{k(\tau_C+\theta)}$	$\tau+\tau'$	$\frac{\tau\tau'}{\tau+\tau'}$
F	$\frac{ke^{-\theta s}}{\tau^2 s+2\xi\tau s+1}$			$\frac{2\xi\tau}{k(\tau_C+\theta)}$	$2\xi\tau$	$\frac{\tau}{2\xi}$

[a] The given settings are IAE and ISE optimal for step setpoint changes when $\tau_C = 0$ and $\tau_C = \theta$ respectively. It is recommended to select $\tau_C > \theta$ for practical design.

[b] To achieve much better performance, the derivation can be added by following tranditional rule [77]

[c] For pure time delay system, the pure integral controller $c(s) = (k_I/s)$ is applied and $k_I \equiv (k_P/\tau_I) = [1/k(\tau_C + \theta)]$ [38].

Even though more precise higher order process models can be obtained by either physical model construction (following the mass and energy balance principles) or the classical parameter identification methods, from a practical point of view, the lower order process model is more convenient for controller design. Six commonly used low order process models and parameters of their IMC-PID controllers are listed in Table 6.1, where g_{CL} and ω_c are the close-loop transfer function and the crossover frequency of gc, respectively.

From equation 6.13 and according to Table 6.1, we have

$$\begin{aligned}
\mathbf{P} &= \begin{pmatrix} \frac{1+g_{11}\tilde{c}_1}{g_{11}\tilde{c}_1} & 1 & \cdots & 1 \\ 1 & \frac{1+g_{22}\tilde{c}_2}{g_{22}\tilde{c}_2} & \cdots & 1 \\ \vdots & \vdots & \ddots & \vdots \\ 1 & 1 & \cdots & \frac{1+g_{nn}\tilde{c}_n}{g_{nn}\tilde{c}_n} \end{pmatrix} \\
&= \begin{pmatrix} g_{11,CL}^{-1} & 1 & \cdots & 1 \\ 1 & g_{22,CL}^{-1} & \cdots & 1 \\ \vdots & \vdots & \ddots & \vdots \\ 1 & 1 & \cdots & g_{nn,CL}^{-1} \end{pmatrix} \\
&= \begin{pmatrix} (\tilde{\tau}_{C1}s+1)e^{\theta_{11}s} & 1 & \cdots & 1 \\ 1 & (\tilde{\tau}_{C2}s+1)e^{\theta_{22}s} & \cdots & 1 \\ \vdots & \vdots & \ddots & \vdots \\ 1 & 1 & \cdots & (\tilde{\tau}_{Cn}s+1)e^{\theta_{nn}s} \end{pmatrix}.
\end{aligned} \tag{6.16}$$

Since each controller is designed around the critical frequency of its transfer function, the dRI of individual control loop $\mathbf{y}_i - \mathbf{u}_i$ can be estimated at the critical frequency $j\omega_{cri}$

$$\phi_{ii,n-1}(j\omega_{cri}) = \|\triangle\mathbf{G}_{ii,n-1}(j\omega_{cri}) \otimes (\mathbf{G}^{ii}(j\omega_{cri}) \otimes \mathbf{P}^{ii}(j\omega_{cri}))^{-T}\|_{\Sigma}. \tag{6.17}$$

For interactive multivariable process $\mathbf{G}$, it is desirable to have the same open-loop transfer function as multivariable control system $\tilde{\mathbf{G}}\tilde{\mathbf{C}}$ [20]. As controller $\tilde{\mathbf{C}}$ is designed for the diagonal elements of $\mathbf{G}$ without considering the couplings between control loops, the designed controller should be detuned by

$$c_i = \frac{\tilde{c}_i}{\rho_{ii,n-1}} = \frac{\tilde{c}_i}{1+\phi_{ii,n-1}}$$

to result approximately the same closed-loop control performance. However, it is impractical to use $\rho_{ii,n-1}$ directly to fine-tune the controller, because it has different values at different frequencies. To solve this problem, one possible way is to use some appropriate transfer functions to identify those MMFs. Since at the neighborhood of the critical point, the transmission interaction can be considered as a linear function, it is reasonable to represent the MMF by a low order transfer function involved the first two items of its Taylor series, which can be further simplified for controller design by a pure time delay transfer function as

$$\rho_{ii,n-1} = k_{\rho i,n-1} e^{-\theta_{\rho i,n-1} s}, \tag{6.18}$$

where,

$$k_{\rho i,n-1} = |\rho_{ii,n-1}(j\omega_{cri})| = |1+\phi_{ii,n-1}(j\omega_{cri})| \tag{6.19}$$

and

$$\theta_{\rho i,n-1} = -\frac{\arg(\rho_{ii,n-1}(j\omega_{cri}))}{\omega_{cri}} = -\frac{\arg(1+\phi_{ii,n-1}(j\omega_{cri}))}{\omega_{cri}}, \tag{6.20}$$

with ω_{cri} indicates the critical frequency of the ith control loop $y_i - u_i$. Then for individual control loop $y_i - u_i$ with an arbitrary process model listed in Table 6.1, its equivalent transfer function can be represented as showed by the third column in Table 2, where

$$f_{ki} = \max\{1, k_{\rho i,n-1}\}, \tag{6.21}$$

and

$$f_{\theta i} = \max\{1, 1 + \frac{\theta_{\rho i,n-1}}{\theta_{ii}}\}. \tag{6.22}$$

Remark 3: Since the region between $\tilde{\omega}_{ci}$ ($|g_{ii}\tilde{c}_i| = 1$) and $\tilde{\omega}_{180}$ ($\arg(g_{ii}\tilde{c}_i) = -180^o$)is most critical for individual control loop design, the crossover frequency of $(g_{ii}\tilde{c}_i)$ can be adopted as the critical frequency point for determining the dRI to the particular loop $y_i - u_i$ to obtain $\hat{g}_{ii}$ [23].

Remark 4: In equations 6.21 and 6.22, the factors f_{ki} and $f_{\theta i}$ are selected to be not smaller than 1, such that the equivalent open loop gain and the time delay of $\hat{g}_{ii}$ are no smaller than that of g_{ii}. The reason for such selection is to make the resultant controller settings more conservative than that of $\hat{g}_{ii}$, such that loop failure tolerance property can be preserved.

6.4 Design of Decentralized Controller

Once the closed-loop properties of the diagonal elements and the critical frequencies of all individual control loops are determined, the dRI and MMF can be obtained through calculating the matrix $\mathbf{P}$ and dDRIA. Then, the parameters of decentralized controllers can be calculated based on the equivalent transfer function of each control loop and the IMC-PID tuning rules as shown in Table 6.2.

In such design procedure, the overall control system stability is assured if the loop pairing is structurally stable which can be explained as follows:

(1) Each $\tilde{c}_i$ designed without considering loop interaction is more aggressive to control loop $y_i - u_i$ than that of the final control setting c_i. Generally, we have $\bar{\sigma}(\mathbf{\Delta}_1) \leq \bar{\sigma}(\mathbf{\Delta}_2)$ as $\max\{1, |\rho_{ii,n-1}|\} \geq 1$, where $\bar{\sigma}(\mathbf{A})$ is the maximum singular value of matrix $\mathbf{A}$, $\mathbf{\Delta}_1 = \tilde{\mathbf{G}}\mathbf{C}(1+\tilde{\mathbf{G}}\mathbf{C})^{-1}$ and $\mathbf{\Delta}_2 = \tilde{\mathbf{G}}\tilde{\mathbf{C}}(1+\tilde{\mathbf{G}}\tilde{\mathbf{C}})^{-1}$.

Table 6.2: PID controllers of the equivalent processes for typical low order systems

	g_{ii}	$\hat{g}_{ii}$	k_P	τ_I	τ_D
A[a]	$k_{ii}e^{-\theta_{ii}s}$	$f_{ki}k_{ii}e^{-f_{\theta i}\theta_{ii}s}$	–	k_{Ii}	–
B	$\frac{k_{ii}e^{-\theta_{ii}s}}{s}$	$\frac{f_{ki}k_{ii}e^{-f_{\theta i}\theta_{ii}s}}{s}$	$\frac{1}{f_{ki}k_{ii}(\tau_{Ci}+f_{\theta i}\theta_{ii})}$	–	–
C	$\frac{k_{ii}e^{-\theta_{ii}s}}{\tau_{ii}s+1}$	$\frac{f_{ki}k_{ii}e^{-f_{\theta i}\theta_{ii}s}}{\tau_{ii}s+1}$	$\frac{\tau_{ii}}{f_{ki}k_{ii}(\tau_{Ci}+f_{\theta i}\theta_{ii})}$	τ_{ii}	–
D	$\frac{k_{ii}e^{-\theta_{ii}s}}{s(\tau_{ii}s+1)}$	$\frac{f_{ki}k_{ii}e^{-f_{\theta i}\theta_{ii}s}}{s(\tau_{ii}s+1)}$	$\frac{1}{f_{ki}k_{ii}(\tau_{Ci}+f_{\theta i}\theta_{ii})}$	–	τ_{ii}
E	$\frac{k_{ii}e^{-\theta_{ii}s}}{(\tau_{ii}s+1)(\tau'_{ii}s+1)}$	$\frac{f_{ki}k_{ii}e^{-f_{\theta i}\theta_{ii}s}}{(\tau_{ii}s+1)(\tau'_{ii}s+1)}$	$\frac{\tau_{ii}+\tau'_{ii}}{f_{ki}k_{ii}(\tau_{Ci}+f_{\theta i}\theta_{ii})}$	$\tau_{ii}+\tau'_{ii}$	$\frac{\tau_{ii}\tau'_{ii}}{\tau_{ii}+\tau'_{ii}}$
F[b]	$\frac{k_{ii}e^{-\theta_{ii}s}}{\tau_{ii}^2s^2+2\xi_{ii}\tau_{ii}s+1}$	$\frac{f_{ki}k_{ii}e^{-f_{\theta i}\theta_{ii}s}}{\tau_{ii}^2s^2+2\xi_{ii}\tau_{ii}s+1}$	$\frac{2\xi_{ii}\tau_{ii}}{f_{ki}k_{ii}(\tau_{Ci}+f_{\theta i}\theta_{ii})}$	$2\xi_{ii}\tau_{ii}$	$\frac{\tau_{ii}}{2\xi_{ii}}$

[a] For pure time delay system, the pure integral controller $c(s) = (k_{Ii}/s)$ is applied and $k_{Ii} \equiv (k_{Pi}/\tau_{Ii}) = [1/f_{ki}k_{ii}(\tau_C + f_{\theta i}\theta_{ii})]$.

(2) Let $\mathbf{M} = -(\mathbf{G} - \tilde{\mathbf{G}})\tilde{\mathbf{G}}^{-1}$, and following the definition of the Structured Singular Value (SSV) [56]:

$$\mu_{\mathbf{\Delta}}(\mathbf{M}) \equiv \frac{1}{\min\{\bar{\sigma}(\mathbf{\Delta})|\det(I - k_m\mathbf{M}\mathbf{\Delta}) = 0 \text{ for structured } \mathbf{\Delta}\}},$$

we have $\mu_{\mathbf{\Delta}_1}(\mathbf{M}) \leq \mu_{\mathbf{\Delta}_2}(\mathbf{M})$, which implies there exist smaller interactions among control loops when the detuned controller $\mathbf{C}$ is applied [20].

(3) Since the bigger dRI $\phi_{ii,n-1}$ is used to determine the detuning factors, and f_{ki} and $f_{\theta i}$ are no smaller than 1, the resultant controller c_i will be more conservative with smaller gain and crossover frequency compared with $\tilde{c}_i$.

(4) Conservative control action in each loop presents smaller interaction to other loops. As the design based on $\hat{g}_{ii}$ for loop $y_i - u_i$ will end up with a more conservative c_i. the stability margin for each individual loop will be further increased compared with using the true $\phi_{ii,n-1}$.

Summarize the above results, a procedure for designing decentralized PID controller for general multivariable processes is illustrated as in Figure 6.4.

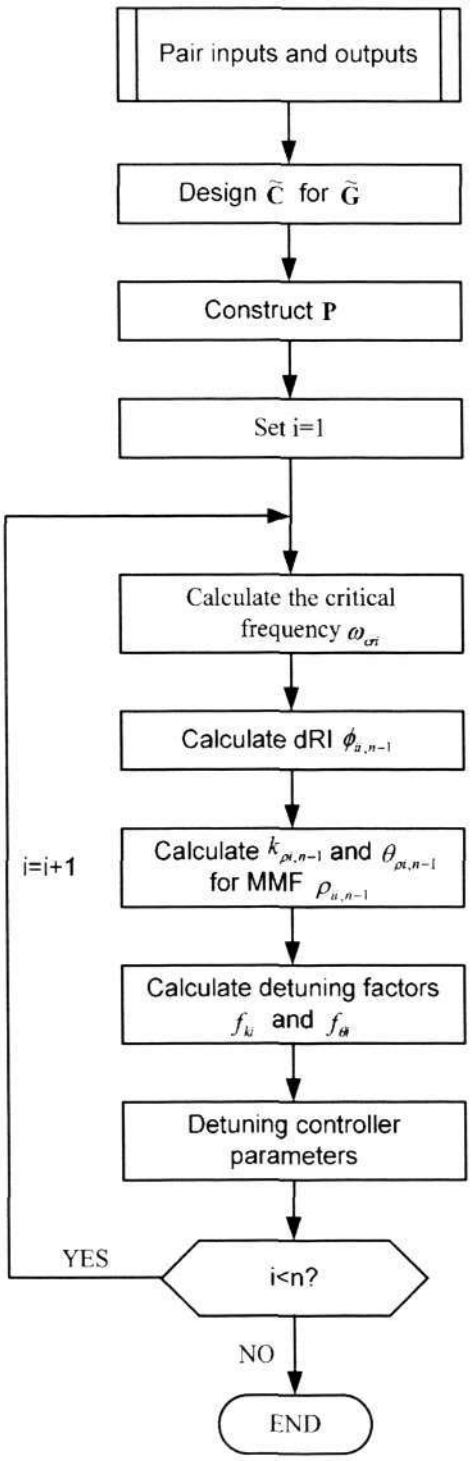

Figure 6.4: The procedure for designing decentralized PID controller

Remark 5: As the interactions among control loops are ignored in both the dynamic interaction estimation step and the PID controller designing step, all

available SISO PID controller design techniques can be adopted. Thus, according to the expected control performance, one can select the most suitable tuning rules, such as Ziegler and Nichols tuning rule [35], IMC tuning rule [36], and some other optimal design methods [37] for each step independently. Apparently, applying various tuning rules must lead to various interaction estimations, initial controller settings, final controller settings as well as overall control performance. However, has no influence to the design mechanism of our method. In the present chapter, the IMC-PID tuning rule is adopted because of its robust, generally good responses for setpoint changes and widely accepted.

6.5 Simulation Examples

To evaluate effectiveness of the proposed decentralized PID controller design method, 10 multivariable processes in reference [39] are studied:

- 2×2 systems: (1) Tyreus stabilizer — TS; (2) Wood and Berry — WB; (3) Vinante and Luyben — VL; (4) Wardle and Wood — WW.
- 3×3 systems: (5) Ogunnaike and Ray — OR; (6) Tyreus case 1 — T1; (7) Tyreus case 4 — T4.
- 4×4 systems: (8) Doukas and Luyben — DL; (9) Alatiqi case 1 — A1; (10) Alatiqi case 2 — A2.

The process open-loop transfer function matrices of these systems are listed by Tables **A1**, **A2** and **A3**, respectively in Appendix. As some process models, such as g_{11} in TS case, are in higher order (higher than second-order), the standard order reduction method is used to make them have the forms as those presented in table 6.1. The controller parameters are listed in Table 6.3 together with those obtained by using other three design methods: the biggest log-modulus tuning (BLT) method of Luyben [39], the trial-and-error method [51], and an independent design method based on Nyquist stability analysis [50]. It should be pointed out that the Gershorin circle and Gershorin band are utilized to determine the stability region in the last method, a static decoupler is required if the processes is not open-loop column diagonal dominance.

To evaluate the output control performance, we consider a unit step setpoint change ($r_i = 1$) of all control loops one-by-one, and the integral square error (ISE) of $e_i = y_i - r_i$ is used to evaluate the control performance,

$$J_i = \int_0^\infty e_i^2 dt.$$

The simulation results and ISE values are given in Figures 6.5 -6.14. The results show that, for some of the 2×2 processes, the proposed design provides better per-

Table 6.3: Parameters of the decentralized PID controllers for 10 classical systems[a]

	BLT design		Lee design		Chen design		Proposed design		
	k_P	τ_I	k_P	τ_I	k_P	τ_I	k_P	τ_I	τ_D
TS	−16.6	20.6					−149.0	3.460	2.300
	70.6	80.1					769.5	64.00	13.75
WB	0.375	8.29	0.850	7.21	0.436	11.0	0.932	16.70	–
	−0.075	23.6	−0.0885	8.86	−0.0945	15.5	−0.124	14.40	–
VL	−1.07	7.1	−1.31	2.26	1.21	4.64	−2.121	7.000	–
	1.97	2.58	3.97	2.42	3.74	1.10	3.951	9.200	–
WW	27.4	41.4	53.8	31.1			52.52	60.00	–
	−13.3	52.9	−20.3	29.7			−24.52	35.00	–
OR	1.51	16.4					1.676	6.700	–
	−0.295	18					−0.353	5.000	–
	2.63	6.61					4.385	8.620	–
T1	−17.8	4.5					−20.85	66.67	–
	0.749	5.61					1.168	2.860	0.715
	−0.261	139					−0.088	33.30	–
T4	−11.26	7.09					−23.64	66.67	–
	−3.52	14.5					0.622	2.860	0.715
	−0.182	15.1					−0.515	46.48	11.57
DL	−0.118	23.5					−0.410	43.48	10.87
	−7.26	11					−23.64	66.67	–
	0.429	12.1					0.589	2.860	0.715
	0.743	7.94					0.028	1.000	–
A1	2.28	72.2	0.385	34.72	0.176	62.9	3.698	61.00	14.75
	2.94	7.48	6.190	21.80	0.220	31.0	4.481	32.00	–
	1.18	7.39	2.836	19.22	3.150	8.03	1.666	16.20	–
	2.02	27.8	0.732	36.93	0.447	47.5	4.821	53.00	4.528
A2	0.923	61.7					3.884	41.30	6.632
	1.16	13.2					2.549	44.60	–
	0.727	13.2					1.311	18.50	–
	2.17	40					4.233	54.30	5.569

[a] In the proposed design, the control configurations of both Tyreus case 4 and Doukas and Luyben systems are re-selected as $y_1 - u_1/y_2 - u_3/y_3 - u_2$ and $y_1 - u_4/y_2 - u_2/y_3 - u_1/y_4 - u_3$, respectively, by using the pairing method proposed in ref [60].

formance than both BLT method and Chen et al. method, and is quite competitive with Lee et al. method, but for higher dimensional processes, the proposed design provides less conservative controller settings as well as better control performance.

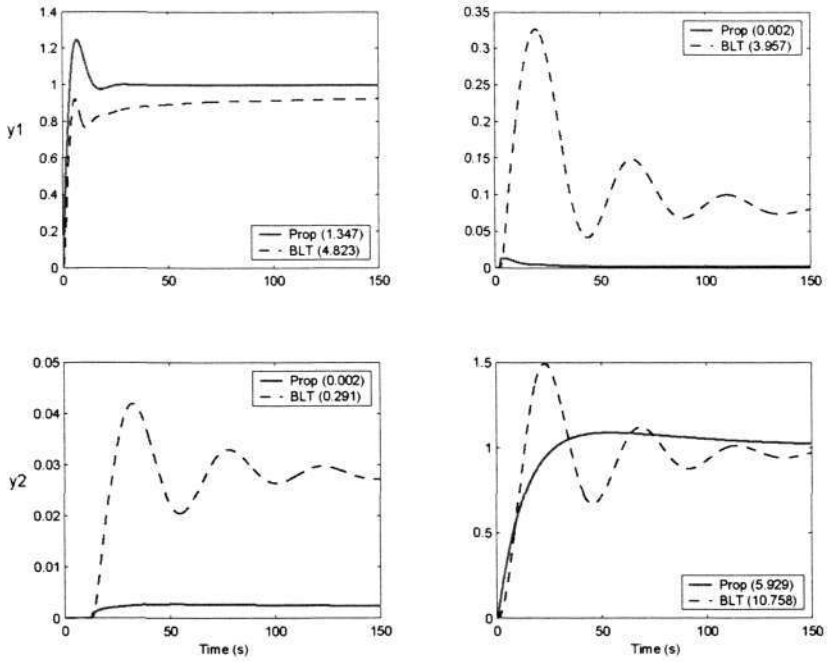

Figure 6.5: Step response and ISE values of decentralized control for Tyreus stabilizer (solid line: Proposed design, dashed line: BLT design, dashed-dotted line: Lee at el., dotted line: Chen at el.)

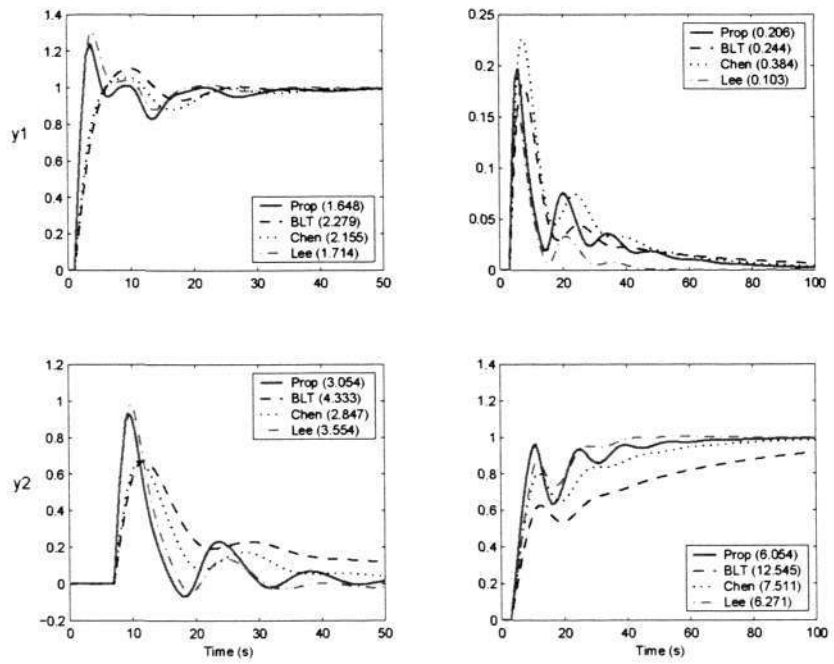

Figure 6.6: Step response and ISE values of decentralized control for Wood and Berry (lower) systems (solid line: Proposed design, dashed line: BLT design, dashed-dotted line: Lee at el., dotted line: Chen at el.)

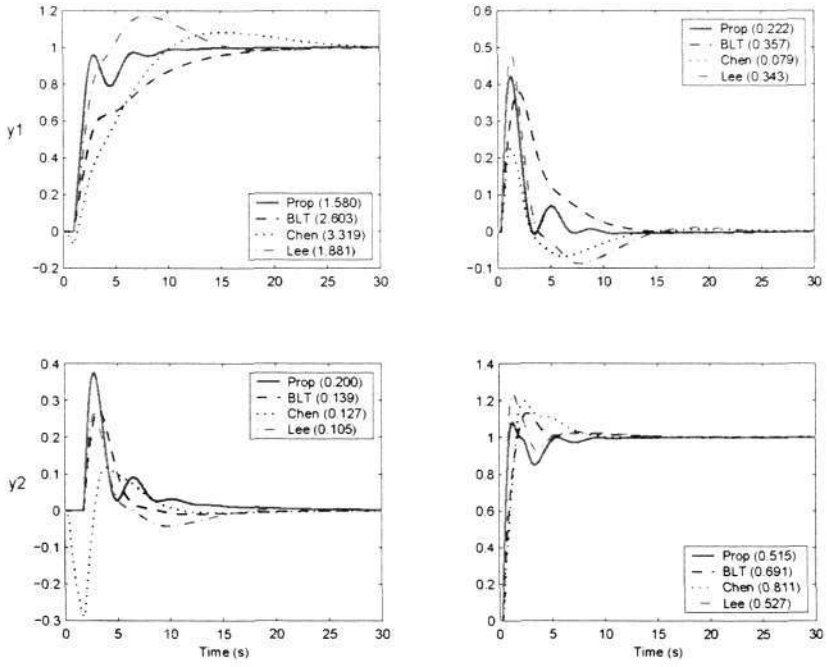

Figure 6.7: Step response and ISE values of decentralized control for Vinate and Luyben system (solid line: Proposed design, dashed line: BLT design, dashed-dotted line: Lee at el., dotted line: Chen at el.)

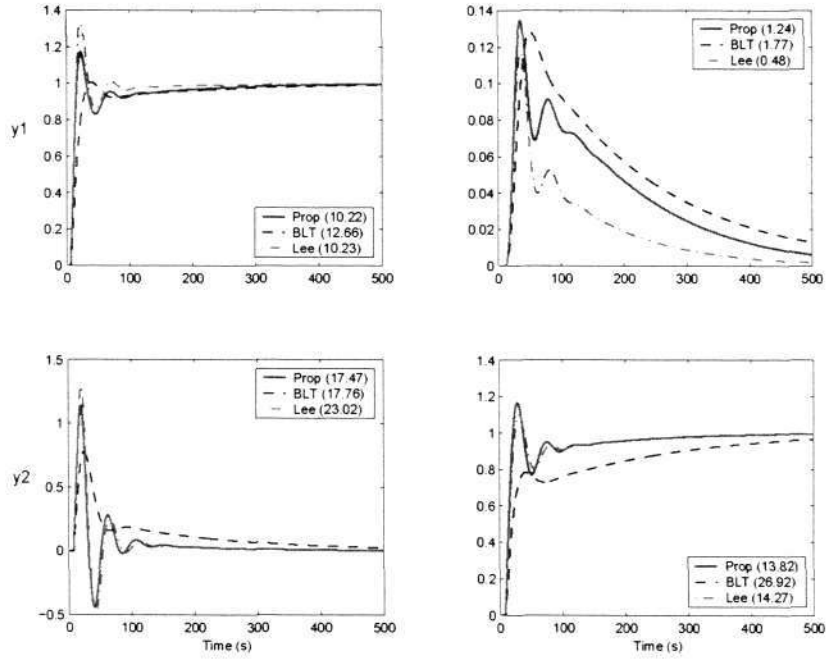

Figure 6.8: Step response and ISE values of decentralized control for Wardle and Wood system (solid line: Proposed design, dashed line: BLT design, dashed-dotted line: Lee at el., dotted line: Chen at el.)

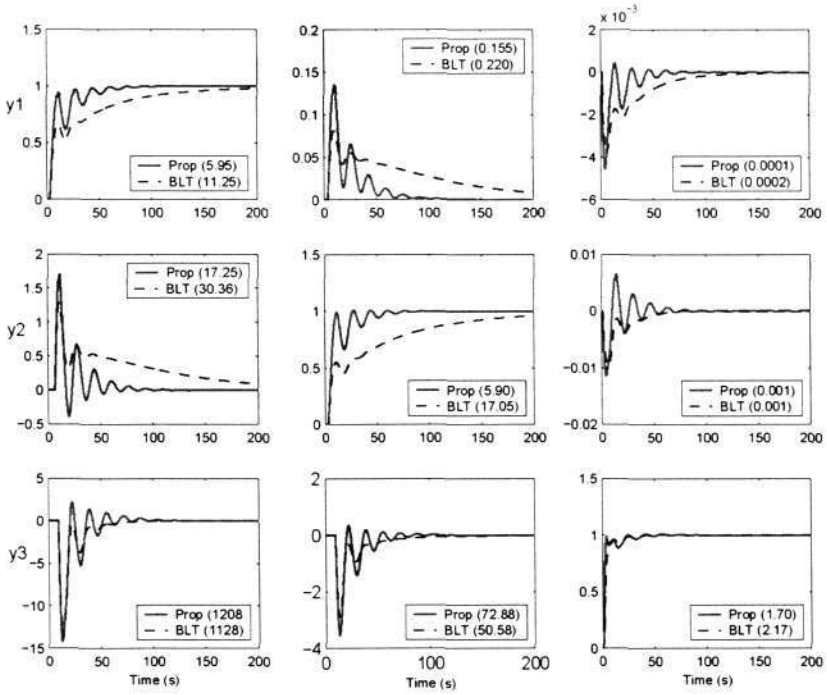

Figure 6.9: Step response and ISE values of decentralized control for Ogunnaile and Ray system (solid line: Proposed design, dashed line: BLT design)

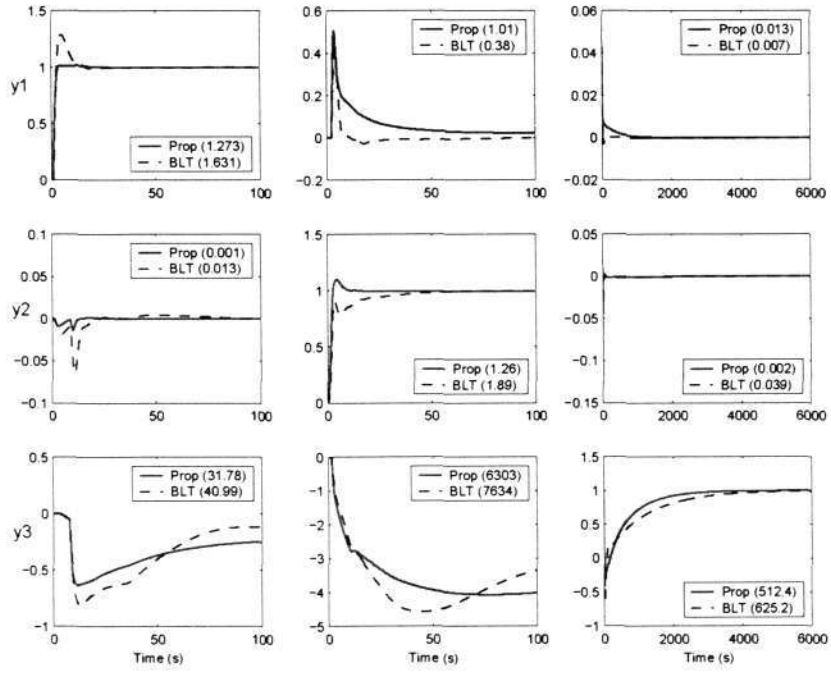

Figure 6.10: Step response and ISE values of decentralized control for Tyreus case 1 systems (solid line: Proposed design, dashed line: BLT design)

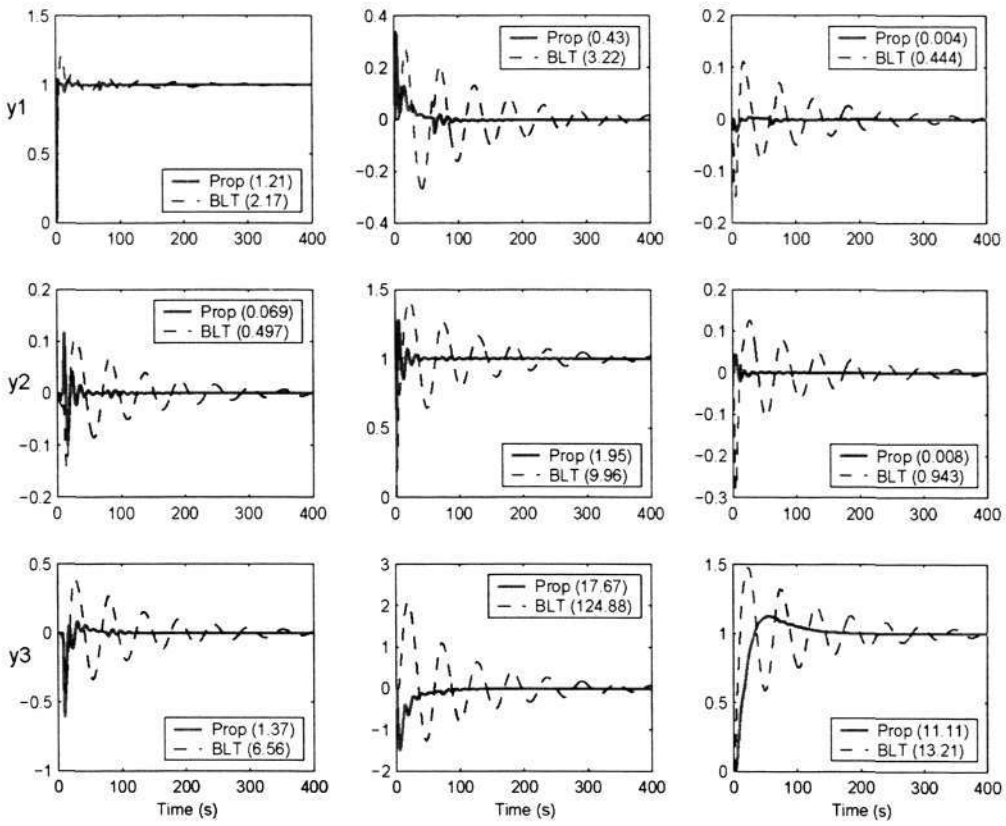

Figure 6.11: Step response and ISE values of decentralized control for Tyreus case 4 system (solid line: Proposed design, dashed line: BLT design)

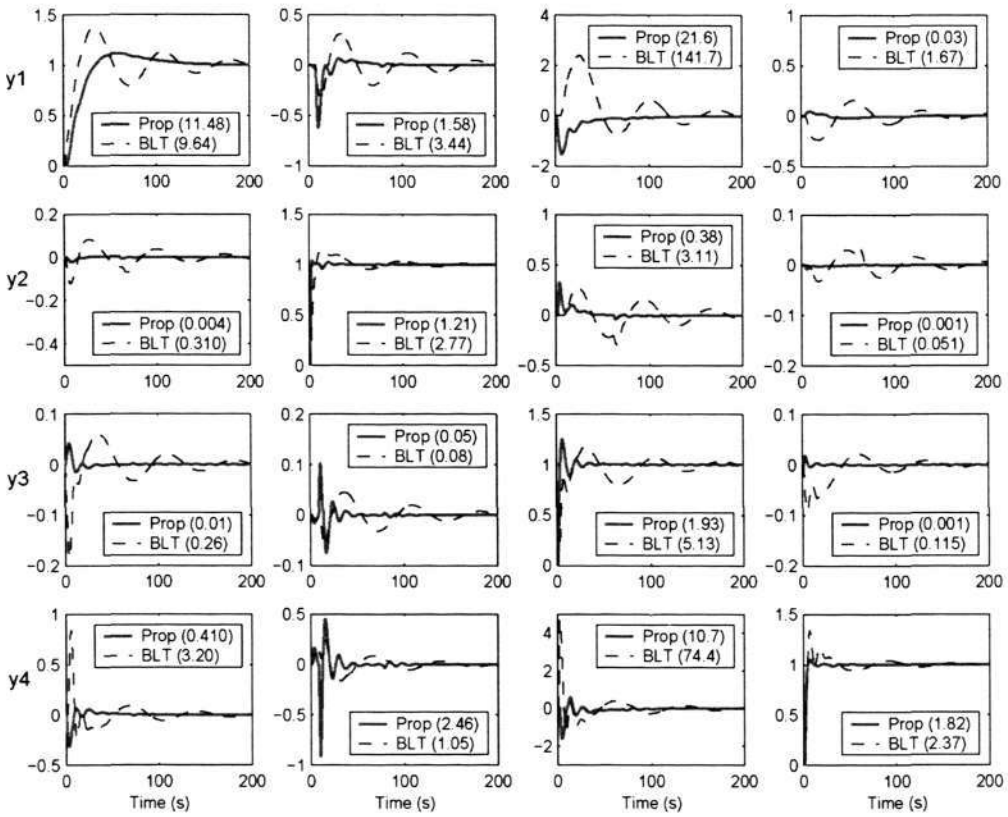

Figure 6.12: Step response and ISE values of decentralized control for Doukas and Luyben system (solid line: Proposed design, dashed line: BLT design)

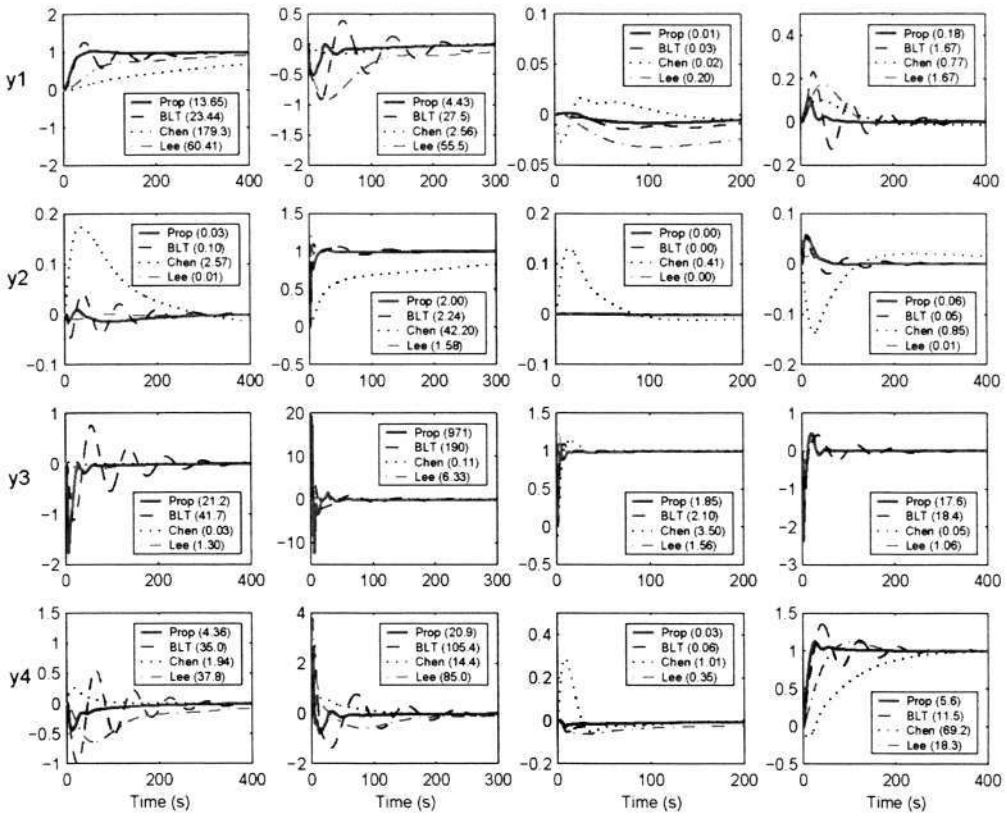

Figure 6.13: Step response and ISE values of decentralized control for Alatiqi case 1 system (solid line: Proposed design, dashed line: BLT design, dashed-dotted line: Lee at el., dotted line: Chen at el.)

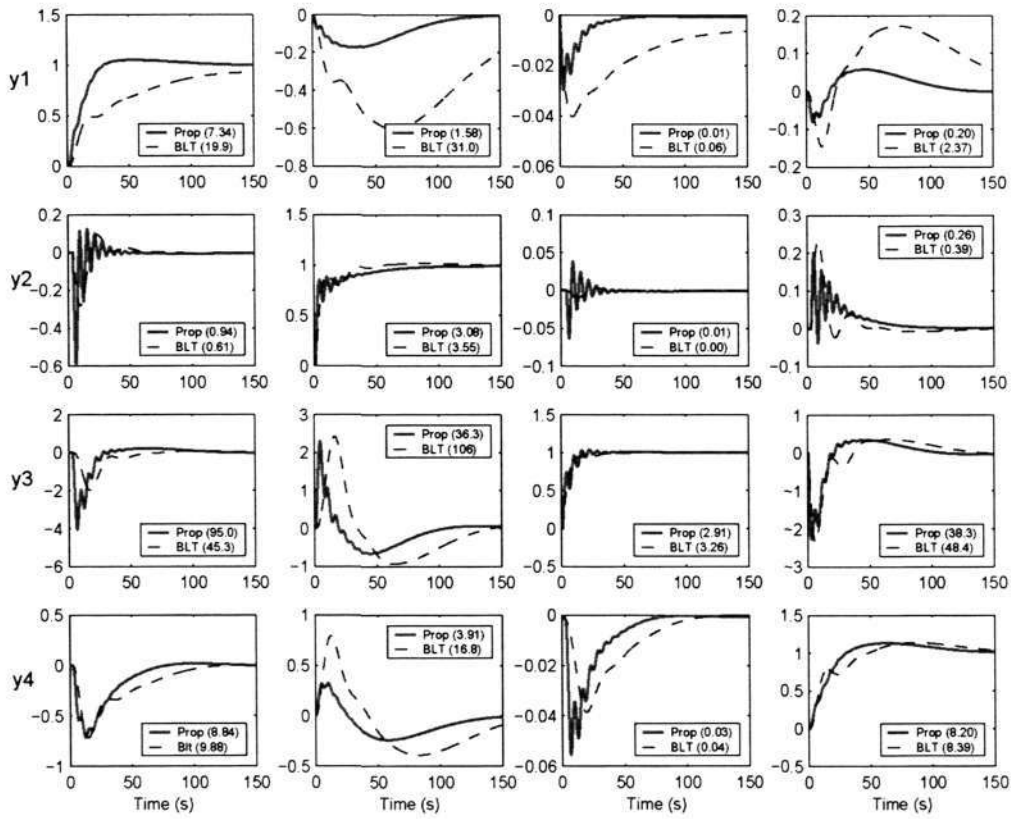

Figure 6.14: Step response and ISE values of decentralized control for Alatiqi case 2 system (solid line: Proposed design, dashed line: BLT design)

A simple yet effective design method for decentralized PID controller design method was proposed based on dynamic interaction analysis and internal model control principle. On the basis of structure decomposition, the dynamic relative interaction was defined and represented by the process model and controller explicitly. An initial decentralized controller was designed first by using the diagonal elements and then implemented to estimate the dRI to individual control loop from all others. By using the dRI, the MMF was derived and simplified to a pure time delay function at the neighborhood of each control loop critical frequency to obtain the equivalent transfer function. Consequently by applying the IMC-PID tuning rules for the equivalent transfer function, appropriate controller parameters for individual control loop were determined. The proposed technique is very simple and effective, and has been applied to a variety of 2×2, 3×3 and 4×4 systems. Simulation results showed that the overall control system performance is much better than that of other tuning methods, such as the BLT method, the trial and error method, and the independent design method based on Nyquist stability analysis, especially for higher-dimensional processes.

In case of severe interactions existing between control loops, decentralized control might not meet up the control objectives. In this case, a block-diagonal control structure would be a better alternative. How to determine the block-diagonal control structure will be studied in the following chapter.

Chapter 7

Control Structure Selection Based on Relative Interaction Decomposition

In this chapter, a simple yet effective approach for control structure selection of multivariable processes is proposed based on element decomposition of relative interaction (RI) [66]. On the basis of structure decomposition, the interaction transmitted to and from a subsystem is examined. By employing the decomposed relative interaction array (DRIA), all interaction transmitting channels to individual control loop from all the other closed control loops are decoupled. Furthermore, the decomposed relative gain array (DRGA) can be constructed to evaluate the comprehensive transmitting interaction to an individual control loop from another one. Consequently, the synthesis of the control structure can be dealt with in a straightforward manner using structure interaction acceptable index (SIAI). A C-H diagram is proposed to facilitate control structure selection process. Two examples are used to demonstrate that the proposed approach is simple, effective and very easy to be implemented.

7.1 Preliminaries

Throughout this chapter, it is assumed that the system we are dealing with is square ($n \times n$), open loop stable, and non-singular at steady state with a multivariable feedback control structure as shown in figure 7.1, where, $\mathbf{G}(s)$ is system's transfer function matrix with its steady-state gain matrix and individual elements represented by $\mathbf{G}(0)$ (or simply $\mathbf{G}$) and g_{ij}, respectively. $\mathbf{C}(s)$ is the multivariable controller to be selected in form of all types of controller ranging from full decentralized controller to centralized controller including block diagonal controller and sparse controller. $\mathbf{r}$, $\mathbf{u}$ and $\mathbf{y}$ are vectors of references, manipulated and controlled variables with their ith elements represented by $\mathbf{r}_i$, $\mathbf{u}_i$ and $\mathbf{y}_i$, respectively.

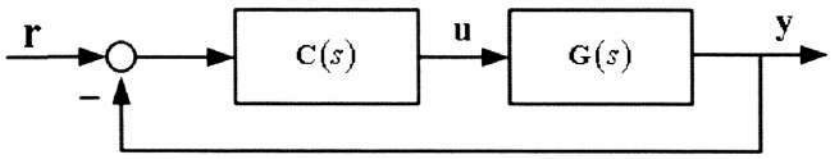

Figure 7.1: Block diagram of general multivariable control system

7.2 Relative Interaction Decomposition

In the following development, it is assumed that:

(1) a full decentralized control structure for process $\mathbf{G}$ has been determined according to the RGA-NI-GI based criterion; and

(2) all elements of matrix $\mathbf{G}$ have been re-arranged so that the pairings of the inputs and outputs in the decentralized feedback system correspond to the diagonal elements of $\mathbf{G}$.

To examine the interactions between an arbitrary control loop and the others, the decentralized feedback control system can be structurally decomposed into n

individual SISO control loops with the coupling among all loops explicitly exposed and embedded in each loop. As shown in figure 7.2, the interactions between individual control loop $\mathbf{y}_i - \mathbf{u}_i$ and other $n-1$ control loops are divided into three portions with respect to their directions.

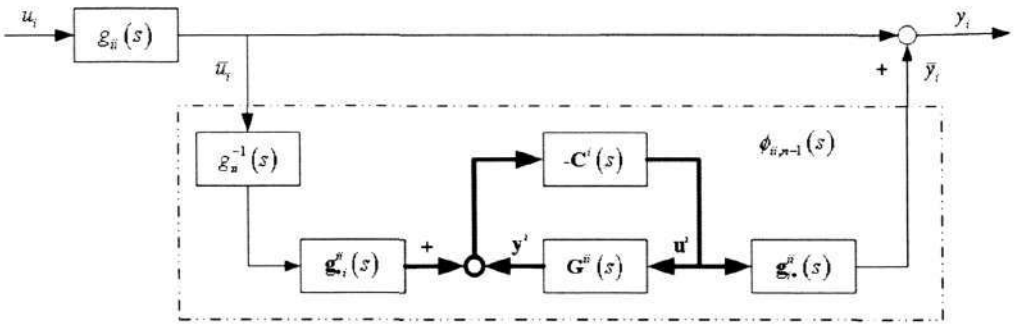

Figure 7.2: Structure of loop $\mathbf{y}_i - \mathbf{u}_i$ by structural decomposition

(i) *One-way interactions from control loop* $\mathbf{y}_i - \mathbf{u}_i$ *to other* $n-1$ *loops.*

These one-way interactions are introduced by column vector $\mathbf{g}_{\bullet i}^{ii}$ through transmitting the changes of input u_i to other $n-1$ outputs $\mathbf{y}^i$. Since the value of column vector $g_{ii}^{-1}\mathbf{g}_{\bullet i}^{ii}$ indicates the relative change of $\mathbf{y}^i$ with respect to unity change of output $\mathbf{y}_i$, it is desirable that all elements in $g_{ii}^{-1}\mathbf{g}_{\bullet i}^{ii}$ are small. Moreover, column diagonal dominance would be achieved if all elements of $g_{ii}^{-1}\mathbf{g}_{\bullet i}^{ii}$ have the absolute value less than 1 for all i.

(ii) *Internal interactions among the closed subsystem* $\mathbf{G}^{ii}$.

By considering the one-way interactions from control loop $\mathbf{y}_i - \mathbf{u}_i$ to $\mathbf{G}^{ii}$ as disturbance, all $n-1$ controllers for subsystem $\mathbf{G}^{ii}$ must regulate their outputs to counter the effect. In addition, all control loops in subsystem $\mathbf{G}^{ii}$ interact with each other due to the existing non-zero off-diagonal elements in $\mathbf{G}^{ii}$. Consequently, both the one-way interaction transmitted from control loop $\mathbf{y}_i - \mathbf{u}_i$ to outputs of subsystem $\mathbf{G}^{ii}$ and the internal interaction among control loops in closed subsystem $\mathbf{G}^{ii}$ contribute to the changes of $\mathbf{u}^i$. Thus, it is desirable for all loop pairings that $\mathbf{G}^{ii}$ has small off-diagonal elements.

(iii) *One-way interaction from closed subsystem* $\mathbf{G}^{ii}$ *to control loop* $\mathbf{y}_i - \mathbf{u}_i$.

With all inputs of subsystem $\mathbf{G}^{ii}$ updated to reject the disturbance from control loop $\mathbf{y}_i - \mathbf{u}_i$, their changes are transmitted and combined as a whole to affect the output $\mathbf{y}_i$ through the row vector $\mathbf{g}_{i\bullet}^{ii}$. Since the value of row vector $g_{ii}^{-1}\mathbf{g}_{i\bullet}^{ii}$ indicates the relative change of $u_{j,j\neq i}$ with respect to unity change of output u_i, it is desirable for loop pairing $\mathbf{y}_i - \mathbf{u}_i$ that all elements in $g_{ii}^{-1}\mathbf{g}_{i\bullet}^{ii}$ are small. Moreover, row diagonal dominance would be achieved in the case that all elements of $g_{ii}^{-1}\mathbf{g}_{i\bullet}^{ii}$ have the absolute value less than 1 for all i.

Now, rewrite equation 2.14 as

$$\phi_{ii,n-1} = \mathbf{P}[\mathbf{\Psi}_{ii}]^T\mathbf{P}^T, \tag{7.1}$$

where row vector $\mathbf{P} = [1 \ \cdots \ 1]_{1\times n-1}$. According to equation (7), the decomposed structure of control loop $y_i - u_i$ can also be expressed as shown in figure 7.3, where β_{ki} indicates the relative interaction transmitted by individual element g_{ik} and the matrix $[\mathbf{\Psi}_{ii}]^{-T}$ relates inputs $[\bar{u}_i \ \cdots \ \bar{u}_i]_{1\times n-1}^T$ to outputs $[\beta_{1i} \ \cdots \ \beta_{ni}]_{n\neq i}^T$. Comparing figure 7.3 with figure 7.2 reveals that the klth element $\psi_{ii,kl}$ in $\mathbf{\Psi}_{ii}$ is the relative interaction transmitted by channel $g_{ki} - ([\mathbf{G}^{ii}]^{-T})_{kl} - g_{il}$, of which g_{ki}, $([\mathbf{G}^{ii}]^{-T})_{kl}$ and g_{il} indicate the three potions of interactions between control loop $\mathbf{y}_i - \mathbf{u}_i$ and closed subsystem $\mathbf{G}^{ii}$, respectively. Clearly, all of three portions of interactions between one individual control loop and the others are reflected by the DRIA.

To effectively evaluate the interaction effects to an individual control loop from the others, we need to consider the following two cases:

Case (i). Rewrite equation 7.1 as,

$$\phi_{ii,n-1} = \mathbf{A}_i\mathbf{P}^T$$

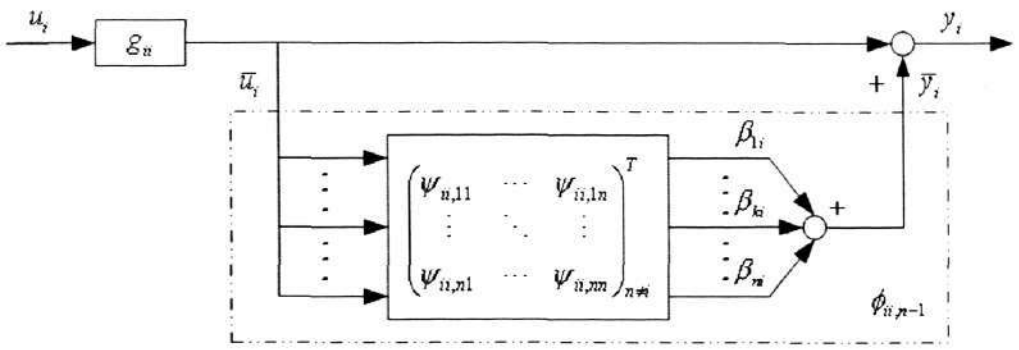

Figure 7.3: All interaction transmitting channels in closed subsystem $\mathbf{G}^{ii}$ are decoupled by DRIA

where $\mathbf{A}_i$ is a $1 \times n-1$ vector with its individual element

$$\alpha_{ik} = [\mathbf{A}_i]_{1k} = \sum_{m=1, m\neq i}^{n} [\mathbf{\Psi}_{ii}]_{mk}, \qquad k = 1, \cdots, n;\ k \neq i. \tag{7.2}$$

As a summation of all elements in the kth row of $\mathbf{\Psi}_{ii}$, α_{ik} represents the relative interaction transmitted by element g_{ki} and can be regarded as an output disturbance to the output of the kth control loop. Clearly, the larger the value of α_{ik} is, the bigger one-way interaction will be introduced to the kth control loop from the ith ***one***.

Case (ii). Rewrite equation 7.1 as

$$\phi_{ii,n-1} = \mathbf{P}\mathbf{B}_i,$$

where $\mathbf{B}_i^T$ is a $1 \times (n-1)$ vector with its individual element

$$\beta_{ki} = [\mathbf{B}_i]_{k1} = \sum_{m=1, m\neq i}^{n} [\mathbf{\Psi}_{ii}]_{km}, \qquad k = 1, \cdots, n;\ k \neq i. \tag{7.3}$$

Similarly, as the summation of all elements in the the kth column of $\mathbf{\Psi}_{ii}$, β_{ki} represents the relative interaction transmitted by element g_{ik} and can be regarded as an output disturbance to the output of the ith control loop. Clearly, the larger the value of β_{ki} is, the bigger one-way interaction will be introduced to the ith control loop from the kth one.

Since both α_{ik} and β_{ki} reflect the relative interactions between the ith and the kth control loops, they are desired to have small value for loop pairing, which is consistent with the requirement in the RGA-NI-GI based loop pairing criterion. Moreover, from ref [61](**Lemma 3.1**), we have

$$\alpha_{ik} = \sum_{m=1,m\neq i}^{n} [\mathbf{\Psi}_{ii}]_{mk} = \frac{\lambda_{ik}}{\lambda_{ii}}, \tag{7.4}$$

and

$$\beta_{ki} = \sum_{m=1,m\neq i}^{n} [\mathbf{\Psi}_{ii}]_{km} = \frac{\lambda_{ki}}{\lambda_{ii}}. \tag{7.5}$$

Equations (7.4) and (7.5) both use RGA information in which smaller value of the off-diagonal elements in RGA results smaller α_{ik} and β_{ki}. This relative values between the off-diagonal elements and the diagonal ones is very important in determining the interaction to an individual control loop from another individual control loop. To effectively measure the interaction to the control loop $\mathbf{y}_i - \mathbf{u}_i$ from kth control loop in closed subsystem $\mathbf{G}^{ii}$, a decomposed relative gain (DRG) and corresponding decomposed relative gain array (DRGA) is defined based on α_{ik} and β_{ki} as follows.

Definition 7.2.1 *The DRGA, $\mathbf{\Gamma}$, is an $n \times n$ matrix with its element, γ_{ik}, determined by*

$$\mathbf{\Gamma} \triangleq \{\gamma_{ik} | \gamma_{ik} = \begin{cases} \frac{1}{2}(\alpha_{ik} + \beta_{ki}) & k \neq i \\ 1 & k = i \end{cases}, \qquad i = 1, 2, \cdots, n\}. \tag{7.6}$$

Clearly, γ_{ik} comprehensively reflects the interaction from the kth control loop in the closed subsystem $\mathbf{G}^{ii}$ to the control loop $\mathbf{y}_i - \mathbf{u}_i$. Furthermore, figure 7.4 shows the control structure of control loop $\mathbf{y}_i - \mathbf{u}_i$ in which the relative interaction transmitted by individual control loop in closed subsystem $\mathbf{G}^{ii}$ can be explicitly represented in terms of γ_{ik}.

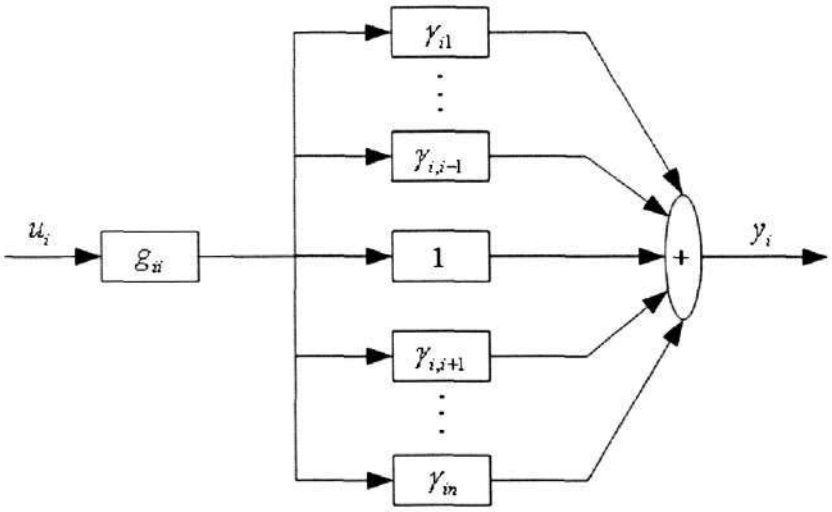

Figure 7.4: Decomposed structure of loop $y_i - u_i$ represented by DRG.

Using equations (2.2), (7.4) – (7.6), the DRGA can be calculated easily by

$$\mathbf{\Gamma} = \frac{1}{2}[\text{diag}\{\mathbf{\Lambda}\}^{-1}\mathbf{\Lambda} + \mathbf{\Lambda}\text{diag}\{\mathbf{\Lambda}\}^{-1}], \tag{7.7}$$

where $\text{diag}\{\mathbf{\Lambda}\}$ is a diagonal matrix containing the diagonal elements of matrix $\mathbf{\Lambda}$.

Remark 1. Since DRGA is calculated from RGA, it has the following interesting properties:

(i) DRGA only depends on the steady-state gain of the system;

(ii) individual element of DRGA is not affected by any permutation of $\mathbf{G}$;

(iii) DRGA is scaling independent (e.g. independent of units chosen for $\mathbf{u}$ and $\mathbf{y}$);

(iv) the summation of all off-diagonal elements in the ith row is equal to the RI of that control loop, i.e. $\phi_{ii,n-1} = \sum_{k=1,k\neq i}^{n} \mathbf{\Gamma}_{ik}$;

(v) if the transfer function matrix is diagonal or triangular, the corresponding DRGA is a zero matrix.

Remark 2. For the system that has pure integral element, RGA and DRGA can be calculated by using a method similar to that proposed by Arkun and Downs [72].

Since the DRGA, Γ, highlights the interactions from one individual control loop to another loop, it is more significant in describing interactions for multivariable processes. In the following, we will use DRGA to select control structures.

7.3 Control Structure Selection

Proper control structure selection is to find a fine balance between the control system complexity and the performance. If tight control system performance is required, a more complex control structure would be necessary. Otherwise, if the system does not require very tight control, simpler control structure would be preferred.

To provide a feasible method for performance based control structure selection, we now define a structure interaction acceptable index:

Definition 7.3.1 *The structure interaction acceptable index (SIAI), ε, is selected between 0 and 1 and indicates the confidence level on loop interactions with respect to the promising control structures. By control structure selection criterion, it leads to a dominant model as*

$$\mathbf{G}_o \triangleq \{g_{ik} | g_{ik} = 0, \quad \text{if } |\gamma_{ik}| < \varepsilon, \qquad i,k = 1,2,\cdots,n\} \tag{7.8}$$

i.e. the element of which the DRG is smaller than ε has so weak interactions with other loops that it can be ignored with confidence level ε.

The specification of ε is a designer's choice, it follows that:

(i) if the best overall control system performance is desired, $\varepsilon = 0$, so that all interactions among control loops are deemed to be severe and should be

counted for. Hence, centralized or full decoupling control structure is preferred regardless of complexity of the processes;

(ii) if selecting $\varepsilon = 1$, the simplest controller structure is called for rather than best overall control system performance so that the interactions to an individual control loop from the others are deemed to be small and can be ignored, hence, full decentralized controller would be preferred;

(iii) for $0 < \varepsilon < 1$, the smaller value of ε is, the better overall control system performance will be achievable and the more interactions among control loop are deemed to be severe and should be considered, hence, block diagonal controller or sparse controller would be preferred, and vice versa.

(iv) if all off-diagonal elements of Γ are less than 0.5, the main loops are dominant and good designed decentralized control can generally results in satisfactory performances. Otherwise, if all or some off-diagonal elements of Γ are close to 1, the interactions are considered to be severe and block diagonal controller or sparse controller would be preferred.

For the control structure selection, if we gradually increase the value of ε from 0 to 1, a unique series of control structures will be generated from full centralized control to block diagonal control, and to full decentralized control. Correspondingly, the control system performance also degrades gradually. On the basis of conventional visualization, we introduce a simple diagram, which we will call Cai-He (C-H) diagram, to facilitate the control structure selection procedure. The C-H diagram contains only two elements:

(i) n nodes are used to represent those n decentralized control loops of system $\mathbf{G}$, each node has a value of 1 to represent individual decentralized control loop has a unity DRG;

(ii) an arrow drawn from one node to another one is used to indicate the interaction from one individual control loop to another one.

By taking the ith and the kth control loops as an example, elements of the C-H diagram are shown in figure 7.5 and explained as follows:

(i) if no interaction exists between the ith and the kth control loops, i.e. $\gamma_{ik} < \varepsilon$ and $\gamma_{ki} < \varepsilon$, no connections between the two nodes, as shown in figure 7.5(a);

(ii) if only the interaction from the ith control loop to the kth one exists, i.e. $\gamma_{ik} < \varepsilon$, and $\gamma_{ki} \geq \varepsilon$, an arrow is drawn from the ith node to the kth node, as shown in figure 7.5(b);

(iii) if only the interaction from the kth control loop to the ith one exists, i.e. $\gamma_{ik} \geq \varepsilon$, and $\gamma_{ki} < \varepsilon$, an arrow is drawn from the kth node to the ith node, as shown in figure 7.5(c);

(iv) if the interaction is on both directions of the ith and the kth control loops, i.e. $\gamma_{ik} \geq \varepsilon$, and $\gamma_{ki} \geq \varepsilon$, two arrows are drawn between the ith and the kth nodes, as shown in figure 7.5(d).

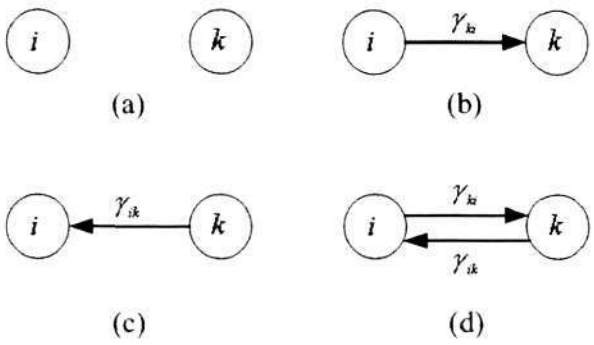

Figure 7.5: The typical representations in C-H diagram

Remark 3. As the configuration of C-H diagram strictly depends on the value of ε, which can be set arbitrarily ranging from 0 to 1, it is sufficient to select a certain element of $\mathbf{\Gamma}$ as the ε. Let ε_m be the selected SIAI that leads to the m blocks control configurations, then the m blocks C-H diagram can be obtained, and for $n \times n$ system, the maximal number of blocks control configurations is n.

Based on the calculation of DRGA and C-H diagram, an algorithm for selecting the control structure is given in Algorithm 1:

Algorithm 1.

Step 1. Calculate the RGA, NI, DRIA and GIA by equations (2.2)-(2.13) and (2.16) and determine the best loop pairing following to the RGA-NI-GI based criterion;

Step 2. Re-arrange process **G** so that the pairing of input and output correspond to the diagonal elements of **G** and adjust the corresponding elements in RGA;

Step 3. Calculate the DRGA by equation (7.7);

Step 4. Select SIAI ε and draw the C-H diagram;

Step 6. Determine the controller structure;

Step 7. If the resulting control performance is not satisfactory, decrease ε and go to Step 4;

Step 8. End.

The significance of above development is as follows:

(1) since only the steady state gain matrix is required in the calculations, Algorithm 1 is very simple and easy to be implemented;

(2) through increase or decrease the SIAI gradually, one can obtain a unique series of control structure;

(3) the C-H diagram provides an easy understandable and useful way to examine the interaction among control loops.

7.4 Case Study

To illustrate the power and the validity of the DRGA concept in control structure selection, we present the results on two industrial processes: a 3×3 Ogunnaike and Ray (OR) system and a 4×4 Alatiqi case 2 (A2) column process in the following.

7.4.1 Example 1.

Consider the OR system [39] with the transfer function matrix given by

$$\mathbf{G}(s)=\begin{pmatrix} \frac{0.66e^{-2.6s}}{6.7s+1} & \frac{-0.61e^{-3.5s}}{8.64s+1} & \frac{-0.0049e^{-s}}{9.06s+1} \\ \frac{1.11e^{-6.5s}}{3.25s+1} & \frac{-2.36e^{-3s}}{5s+1} & \frac{-0.01e^{-1.2s}}{7.09s+1} \\ \frac{-34.68e^{-9.2s}}{8.15s+1} & \frac{46.2e^{-9.4s}}{10.9s+1} & \frac{0.87(11.61s+1)e^{-s}}{(3.89s+1)(18.8s+1)} \end{pmatrix}.$$

According to the RGA-NI-GI loop pairing criterion, the diagonal pairing is preferred for full decentralized control, and from equations (2.2) and (7.7), both RGA and DRGA are obtained as

$$\mathbf{\Lambda}=\begin{pmatrix} 2.0370 & -0.7571 & -0.2799 \\ -0.6774 & 1.8647 & -0.1872 \\ -0.3596 & -0.1076 & 1.4671 \end{pmatrix},$$

and

$$\mathbf{\Gamma}=\begin{pmatrix} 1.0000 & -0.3521 & -0.1570 \\ -0.3847 & 1.0000 & -0.0791 \\ -0.2179 & -0.1005 & 1.0000 \end{pmatrix}.$$

By selecting ε in values of 0, 0.2, 0.3, and 1, respectively, the C-H diagrams for these four cases are as shown in figure 7.6 which are explained as follows:

(1) $\varepsilon=0$, figure 7.6(a). All interactions are to be considered, centralized control or full decoupling control is preferred;

(2) $\varepsilon = 0.2$, figure 7.6(b). Those interactions between control loops with $|\gamma_{ik}| \geq 0.2$ are deemed to be severe. In this case, a dominant model can be obtained by equation (7.8). Then according to the internal model control (IMC) theory [78], the controller structure can be determined as

$$\text{structure}(\mathbf{C}(s)) = \text{structure}(\mathbf{G}_o^{-1}).$$

In fact, one can easily find this control structure is still complex, it is recommended to select centralized/full decoupling control rather than this structure;

(3) $\varepsilon = 0.3$, figure 7.6(c). Only the interactions between the first loop and the second loop are deemed to be severe, hence, block diagonal control is preferred. Obviously, the controller must have the structure as

$$\mathbf{C}(s) = \begin{pmatrix} c_{11}(s) & c_{12}(s) & 0 \\ c_{21}(s) & c_{22}(s) & 0 \\ 0 & 0 & c_{33}(s) \end{pmatrix}.$$

Moreover, this obtained control structure is the best alternative for two blocks control.

(4) $\varepsilon = 1$, figure 7.6(d). As interactions among all control loops are ignored, a full decentralized control structure will be the option.

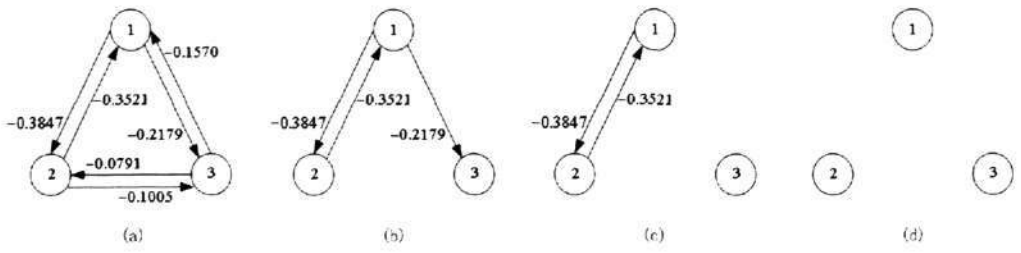

Figure 7.6: The C-H diagram for OR system: (a) $\varepsilon = 0$, centralized control/full decoupling control; (b) $\varepsilon = 0.2$, sparse control; (c) $\varepsilon = 0.3$, two blocks control, and (d) $\varepsilon = 1$, full decentralized control.

Above analysis suggests that pairing $\{(\mathbf{y}_1,\ \mathbf{y}_2) - (\mathbf{u}_1,\ \mathbf{u}_2)),\ (\mathbf{y}_3 - \mathbf{u}_3)\}$ is a better block control structure among all alternatives.

To illustrate the validity of the above results, decentralized controls with decoupling compensators for different block control structures are designed following the block diagram as shown in figure 7.7, where $\mathbf{C}(s)$ and $\mathbf{D}(s)$ are decentralized controller and decoupling compensator respectively.

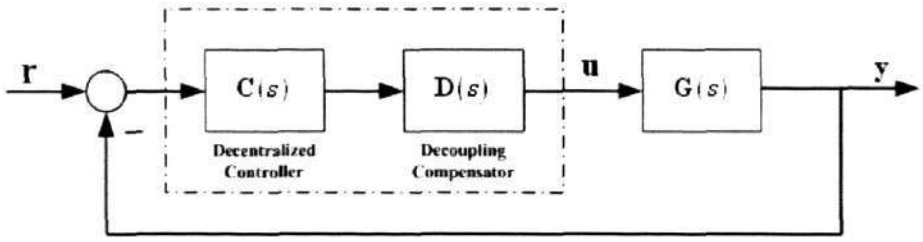

Figure 7.7: The block diagram of decentralized controller with decoupling compensator control system

The designed decoupling compensators are listed as following,

$$\mathrm{PD}_{12}(s) = \begin{pmatrix} 1 & \dfrac{0.9242(6.7s+1)e^{-0.9s}}{8.64s+1} & 0 \\ \dfrac{0.4703(5s+1)e^{-3.5s}}{3.25s+1} & 1 & 0 \\ 0 & 0 & 1 \end{pmatrix},$$

$$\mathrm{PD}_{13}(s) = \begin{pmatrix} 1 & 0 & 1 \\ 0 & 1 & 0 \\ \dfrac{39.86(3.89s+1)(18.8s+1)e^{-8.2s}}{(8.15s+1)(11.61s+1)} & 0 & \dfrac{134.69(9.06s+1)e^{-1.6s}}{6.7s+1} \end{pmatrix},$$

$$\mathrm{PD}_{23}(s) = \begin{pmatrix} 1 & 0 & 0 \\ 0 & 1 & 1 \\ 0 & \dfrac{-53.10(3.89s+1)(18.8s+1)e^{-8.4s}}{(10.9s+1)(11.61s+1)} & \dfrac{-236(7.09s+1)e^{-1.8s}}{5s+1} \end{pmatrix},$$

$$\mathrm{FD}(s) =$$

$$\begin{pmatrix} 1 & \frac{0.753(30.41s^2+12.08s+1)e^{-0.9s}}{30.98s^2+11.61s+1} & \frac{-4.45(6.47s^2+2.88s+1)e^{-0.2s}}{25.89s^2+11.67s+1} \\ \frac{0.402(24.75s^2+11.0s+1)e^{-3.5s}}{15.39s^2+8.03s+1} & 1 & 1 \\ \frac{18.51(24.75s^2+11.0s+1)e^{-8.2s}}{13.38s^2+6.54s+1} & \frac{-23.1(30.41s^2+12.08s+1)e^{-8.4s}}{31.68s^2+18.96s+1} & \frac{-724.3(6.47s^2+2.88s+1)e^{-1.8s}}{16.31s^2+8.06s+1} \end{pmatrix},$$

where "$\mathrm{PD}_{ij}(s)$" and "$\mathrm{FD}(s)$" indicate "partial decoupling with the ith and the jth control loops in one block" and "full decoupling" respectively. The decentralized controller for each loop are tuned by the method proposed in ref [62] and the parameters are given in Table 7.1.

Table 7.1: Parameters of the decentralized PID controllers for different block control structures of OR system[a,b]

	K_p	T_i	T_d
He[b]	1.676, −0.353, 4.385	6.70, 5.00, 8.62	–
PD_{12}	1.521, −0.244, 3.967	3.137, 2.016, 8.186	0.176, 0.266, 0.232
PD_{13}	1.510, −0.353, 0.007	3.851, 5.000, 3.022	0.040, 0, 0.257
PD_{23}	1.773, −0.290, −0.004	6.700, 3.181, 3.492	0, 0.177, 0.175
FD	1.427, −0.248, −0.00484	2.405, 1.920, 11.632	0.255, 0.312, 0.133

[a] The PID controller is designed in form of $c(s) = K_p(1 + (1/T_i s) + T_d s)$.
[b] The decentralized PID controller are designed by using the method proposed in ref [62].

The simulation results for decentralized control, partial decoupling control and full decoupling control are obtained as shown in figures 7.8 and 7.9. It can be seen from figure 7.8 that full decoupling control provides the best overall control performance among all three control structures. However, the design of full decoupling compensator is a tricky task especially for higher dimensional system [79]. Thus, block diagonal control is a better choice because of its simplicity for design and better overall control performance. Moreover, it is quite clear from figures 7.9 that the block diagonal pairing $\{(\mathbf{y}_1,\ \mathbf{y}_2) - (\mathbf{u}_1,\ \mathbf{u}_2)),\ (\mathbf{y}_3 - \mathbf{u}_3)\}$ provides the best overall control performance among all alternatives, which is consistent with the suggestions from DRGA and SIAI.

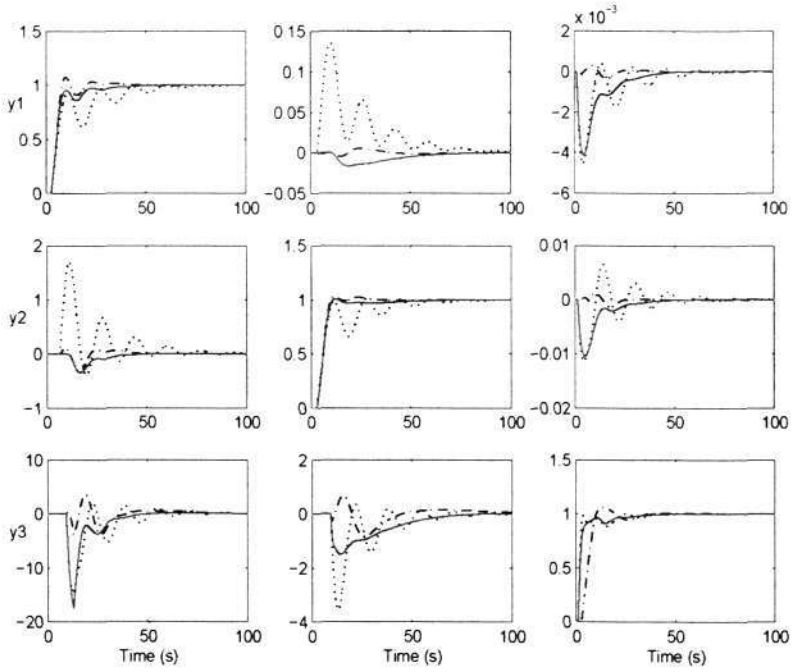

Figure 7.8: The step response of OR system under different control structures: dotted line, decentralized control (He et al.); solid line, partial decoupling control (PD_{12}); dash-dotted line,full decoupling control (FD).

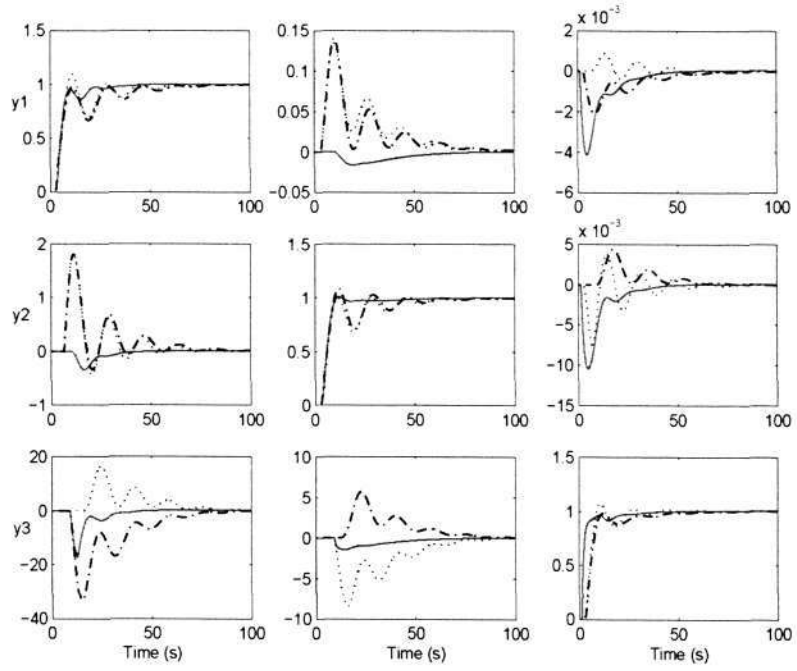

Figure 7.9: The step response of OR system under two blocks control structures: solid line, PD_{12}; dotted line, PD_{13}; dash-dotted line, PD_{23}.

7.4.2 Example 2.

Consider the Alatiqi case 2 (A2) system [39] with the process steady-state gain matrix given by

$$\mathbf{G} = \begin{pmatrix} 4.09 & -6.36 & -0.25 & -0.49 \\ -4.17 & 6.93 & -0.05 & 1.53 \\ -1.73 & 5.11 & 4.61 & -5.48 \\ -11.18 & 14.04 & -0.1 & 4.49 \end{pmatrix}.$$

According to Algorithm 1, both RGA and DRGA are calculated as

$$\mathbf{\Lambda} = \begin{pmatrix} 3.1058 & -0.9007 & -0.4749 & -0.7302 \\ -5.0308 & 4.6742 & -0.0395 & 1.3961 \\ -0.0838 & 0.0543 & 1.5492 & -0.5197 \\ 3.0088 & -2.8278 & -0.0348 & 0.8538 \end{pmatrix},$$

and

$$\mathbf{\Gamma} = \begin{pmatrix} 1.0000 & -0.9549 & -0.0899 & 0.3668 \\ -0.6345 & 1.0000 & 0.0016 & -0.1532 \\ -0.1803 & 0.0048 & 1.0000 & -0.1790 \\ 1.3343 & -0.8384 & -0.3247 & 1.0000 \end{pmatrix}.$$

By selecting SIAI as $\varepsilon_1 = 0$, $\varepsilon_2 = 0.35$, $\varepsilon_3 = 0.96$, and $\varepsilon_4 = 1$, respectively, four $\mathbf{\Gamma}_{\varepsilon_m}$s are obtained.

$$\mathbf{\Gamma}_0 = \mathbf{\Gamma},$$

$$\mathbf{\Gamma}_{0.35} = \begin{pmatrix} 1.0000 & -0.9549 & 0 & 0.3668 \\ -0.6345 & 1.0000 & 0 & 0 \\ 0 & 0 & 1.0000 & 0 \\ 1.3343 & -0.8384 & 0 & 1.0000 \end{pmatrix},$$

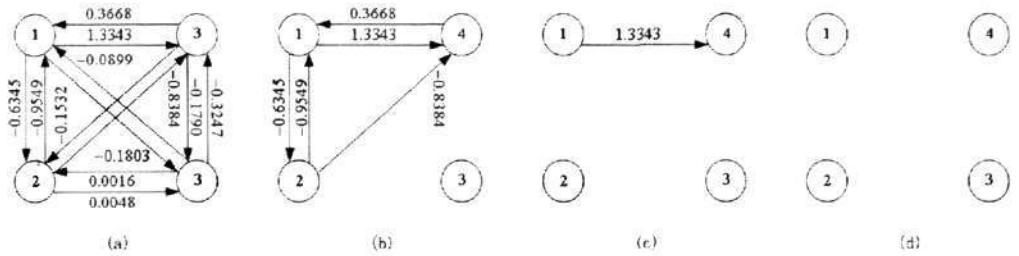

Figure 7.10: The C-H diagram for A2 system: (a) $\varepsilon = 0$, centralized control/full decoupling control; (b) $\varepsilon = 0.35$, two blocks control; (c) $\varepsilon = 0.96$, three blocks control, and (d) $\varepsilon = 1$, full decentralized control.

$$\mathbf{\Gamma}_{0.96} = \begin{pmatrix} 1.0000 & 0 & 0 & 0 \\ 0 & 1.0000 & 0 & 0 \\ 0 & 0 & 1.0000 & 0 \\ 1.3343 & 0 & 0 & 1.0000 \end{pmatrix},$$

and

$$\mathbf{\Gamma}_1 = \mathbf{I}_{4\times 4}.$$

The C-H diagrams for these four cases are shown as in figure 7.10, where apart from one block control (centralized/full decoupling control) and full decentralized control, pairing $\{(y_1,\ y_2,\ y_4) - (u_1,\ u_2,\ u_4), (y_3 - u_3)\}$ is the best alternative to be selected for two blocks control structures, while pairing $\{(y_1,\ y_4) - (u_1,\ u_4), (y_2 - u_2), (y_3 - u_3)\}$ is the best alternative for three blocks control structures. On the basis of above analysis, we suggest full decentralized control rather than three blocks control because of simplicity, and two blocks control rather than centralized control because of less degrading of control performance.

A simple yet effective approach for control structure selection was proposed in this chapter. On the basis of structure decomposition, three portions of the transmitting interaction in the subsystem $\mathbf{G}^{ii}$ were investigated. Using the concept of DRIA, all interaction transmitting channels to individual control loop from all the other closed control loops were decoupled and the DRGA has been constructed to

evaluate the comprehensive transmitted interaction to individual control loop from another one. Consequently, the synthesis of the control structure can be dealt with in a straightforward manner by using SIAI. The C-H diagram was also proposed to facilitate the control structure selection process. Two examples were presented to illustrate the effectiveness of the proposed approach.

As only the subject of static interactions has been deeply studied in the present chapter, the issues in terms of system dynamics and model mismatch should be considered to reinforce the proposed method. These topics are currently under investigation with the concept of effective relative gain array (ERGA) [80] in mind, and the results will be reported later.

Chapter 8

Conclusions and Recommendations

8.1 Conclusions

Selection of control structure and design of decentralized control system have been two of the main areas of interest within the process control community during the last several decades. This thesis has studied these two topics through decomposed relative interaction analysis. In particular, loop-pairing configuration, decentralized closed loop integrity evaluation, decentralized PID controller design, and block diagonal control structure selection have been discussed. The contributions of this thesis are illustrated by figure 8.1 and summarized as following:

- A novel interaction measure and a new criterion for selecting control configuration were proposed. The loop-by-loop interactions between a particularly loop and all other loops in their open and closed status are effectively evaluated by DRIA. The GI based on the concept of interaction energy and DRIA can determine control loops with the minimum interaction. Compared with those existing methods, the present interaction measure as well as loop pair-

ing criterion is more accurate and effective.

- The necessary and sufficient conditions for DCLI and a simple and effective algorithm for evaluating the DCLI of decentralized control structure were developed. The DRIS as well as DRIF provide an important insight into the cause effect results of loop interactions in the face of single- or multiple-loop failure. Compared with those existing methods, the present method is necessary and sufficient, very simple and effective for evaluating the DCLI of an individual loop under both single- and multiple-loop failure.

- An effective decentralized PID controller design procedure was suggested. The dRI was developed to estimate the dynamic interactions to individual control loop when the other loops closed under imperfect control. On the basis of dRI, the behaviors of the interacted control loop can be described at an arbitrary frequency point without complex calculation. An effective decentralized PID controller design procedure was developed. Compared with those existing methods, the dRI is more accurate and the present design procedure is easier to be understood and implemented.

- A simple yet effective algorithm to design decentralized IMC-PID controllers was presented. Empirical rules for establishing equivalent transfer functions of six common used low order process models and parameters of their IMC-PID controllers are developed. 10 classical industrial processes are studied to verify the performance of proposed decentralized IMC-PID controller design method. The simulation results show that the present decentralized IMC-PID controller design method is very simple and effective and easily implemented especially for higher dimensional processes.

- By quantifying the interaction effect to a particular control loop from other individuals was, a systematic approach to treat the block control structure selection problem under a unified framework was developed. The DRGA was proposed to quantify the interaction effect to a particular control loop from

other individuals. The user defined SIAI makes the synthesis of the control structures which range from full decentralized control to centralized control be dealt with in a straightforward manner. The proposed C-H diagram can effectively facilitate control structure selection process. Compared with conventional methods, the proposed approach is simple, effective and easy to be understood and implemented.

8.2 Recommendations for Further Research

The work of this thesis has laid a strong formulation for systematically analysis and design of multivariable control system. In order to make it fully applicable to process control industry, further research topics are illustrated by figure 8.1 and recommended as following:

- It is well known all practical processes are controlled with bandwidth limitation, which means both gain and bandwidth of transfer functions should be considered during selecting loop-pairing configuration [80]. Extension of the proposed various interaction measures, DRIA and GI, and the loop pairing criterion in Chapter 3 to frequency domain is expected.

- A decentralized integral controllable system provides benefits in both better system reliability and easier implementation for field application engineer, since it allows the operator to reduce the controller gains independently to zero without introducing instability to other loops [27]. Even though some necessary and/or sufficient conditions for decentralized integral controllability (DIC) were developed, there is a lack of necessary and sufficient condition for DIC. Extension of the concepts proposed in Chapter 4 to derive the necessary and sufficient condition for DIC and meanwhile develop an effective algorithm for DIC evaluation is expected.

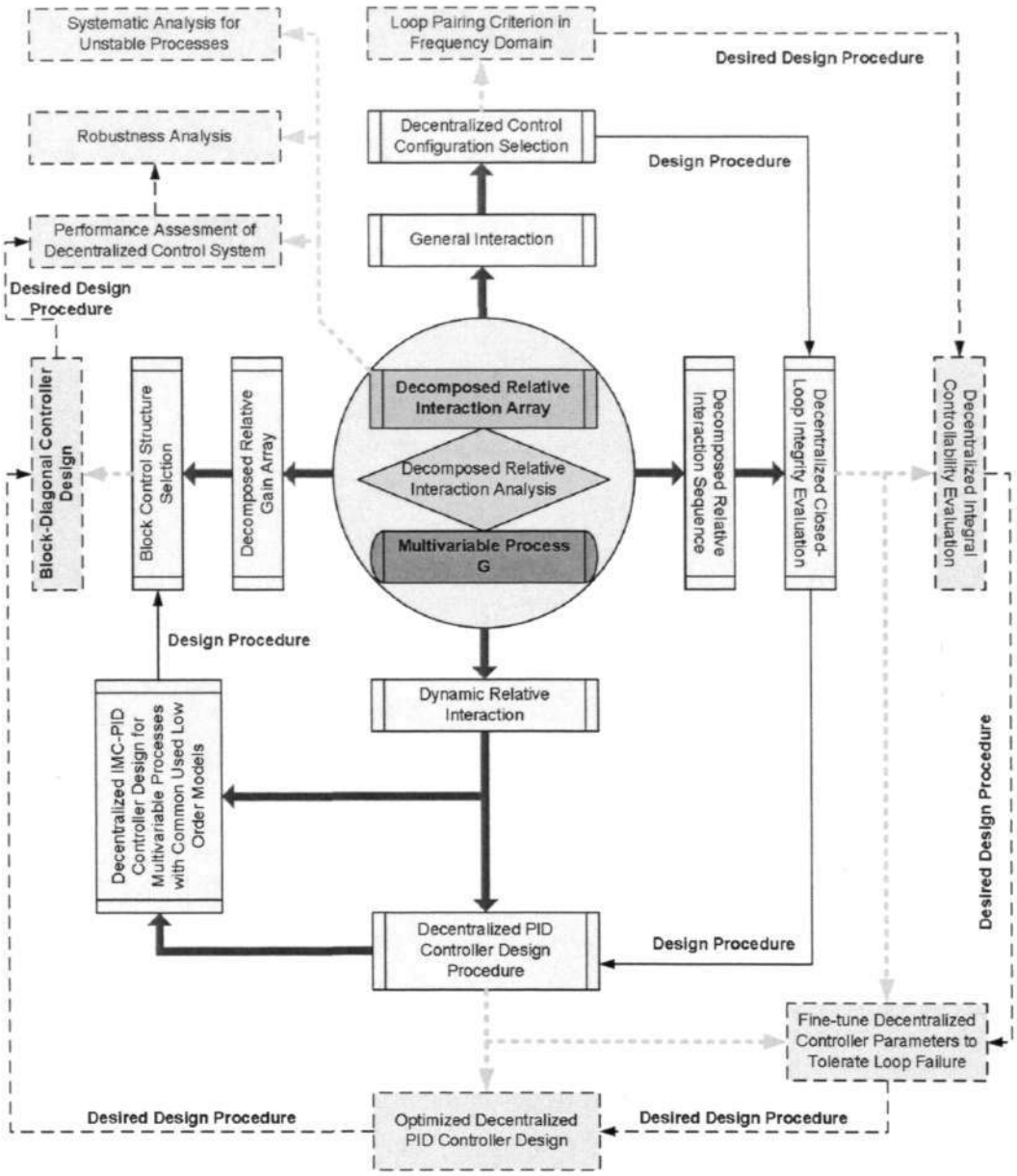

Figure 8.1: Block diagram for Conclusion (— solid lines, boxes, circle and diamond) and Further Research (– – dash lines and boxes)

- Single- or multiple-loop failure is inevitably for the real industrial processes. Even though the DCLI can guarantee the remaining system is structurally stable, the stability of the remaining closed system depends on the values taken of the controller parameters. Developing an effective method to fine-tune the decentralized PID controller parameters so that the whole control

system can tolerate single- or multiple- loop failure is expected.

- The proposed decentralized PID controller design procedure in Chapter 5 is iterative, i.e. design the initial decentralized controller first, secondarily analyze the dynamic interaction between control loops, and then design the decentralized controller. Even though the obtained decentralized controller can provide better control performance, it is not optimal. Developing a simple yet effective algorithm to search the optimal controller parameters by extending the iterative design procedure to more circles is expected.

- Once the block control structure is determined by following the procedure proposed in Chapter 7, how to design the block-decentralized controller would be the next research topic [3]. Developing an effective procedure to design the block decentralized control system in a unified framework is expected.

- In Chapter 6, as many as 10 industrial processes are used to illustrate the effectiveness of the proposed decentralized IMC-PID controller design method. However, it would be more convenience by some performance assessment methods rather than examples for control performance evaluation. Developing a systematic methodology to assess the control performance and combine it with the controller design procedure into a unified framework is expected.

- Modeling uncertainties and neglected and unmodelled dynamics uncertainties are inevitable for control system design. The robustness analysis for the proposed techniques with respect to these kinds of uncertainties is necessary and expected.

- The theories, tools and algorithms proposed in this work are mainly for open loop stable processes. However, some practical processes might be open loop unstable, which makes process control system design tricky. Therefore, extending the presented ideas as well as theories, tools and algorithms to the unstable processes is expected.

Author's Publications

[1] M.-J. He and W.-J. Cai, "New Criterion for Control Loop Configuration of Multi-variable Processes," *Ind. Eng. Chem. Res.*, vol. 43, pp. 7057-7064, 2004. (**Chapter 3**)

[2] M.-J. He, W.-J. Cai, and S.-Y. Li, "Evaluation of Decentralized Closed-Loop Integrity for multivariable control system," *Ind. Eng. Chem. Res.*, vol. 44, pp. 3567-3574, 2005. (**Chapter 4**)

[3] M.-J. He, W.-J. Cai, B.-F. Wu, and M. He, "A simple decentralized PID controller design method based on dynamic relative interaction analysis," *Ind. Eng. Chem. Res.*, vol. 44, pp.8334-8344, 2005. (**Chapter 5**)

[4] M.-J. He, W.-J. Cai, and B.-F. Wu, "Design of Decentralized IMC-PID Controller Based on dRI Analysis," *AIChE J.*, vol. 52, no. 11, pp. 3852-3863, Nov. 2006. (**Chapter 6**)

[5] M.-J. He, W.-J. Cai, and B.-F. Wu, "Control structure selection based on relative interaction decomposition," *International Journal of Control,* vol. 79, no. 10, pp. 1285-1296, Oct. 2006. (**Chapter 7**)

[6] M.-J. He, W.-J. Cai, and B.-F. Wu, "Block control structure selection based on relative interaction decomposition," *The 9th International Conference on Control, Automation, Robotics and Vision*, Singapore, Dec. 2006.

[7] M.-J. He, W.-J. Cai, and S.-Y. Li, "New Criterion for Control Loop Configuration of Multi-variable Processes," *The 8th International Conference on Control, Automation, Robotics and Vision*, Kunming, Dec. 2004.

[8] Q. Xiong, W.-J. Cai, and M.-J. He, "Decentralized Control System Design for Multivariable Processess – A Novel Method Based on Effective Relative Gain Array," *Ind. Eng. Chem. Res.*, vol. 45, pp. 2769-2776, 2006.

[9] Q. Xiong, W.-J. Cai, and M.-J. He, "A practical loop pairing criterion for multivariable processes," *J. Process control*, vol. 15, pp. 741-747, 2005.

[10] Q. Xiong, W.-J. Cai, and M.-J. He, "Equivalent transfer function method for PIPID controller design of MIMO processes," *J. Process control*, Accepted in press.

[11] W.-J. Cai, Q. Xiong, and M.-J. He, "Control System Design for Multivariable Processes with Multiple Time Delays – a Unified Framework Based on Relative Interaction Energy," Submitted to Automatica.

Appendix

Table **A1.** Process open-loop transfer functions of 2 × 2 systems

	TS (Tyreus stabilizer)	WB (Wood and Berry)	VL (Vinante and Luyben)	WW (Wardle and Wood)
g_{11}	$\frac{-0.1153(10s+1)e^{-0.1s}}{(4s+1)^3}$	$\frac{12.8e^{-s}}{16.7s+1}$	$\frac{-2.2e^{-s}}{7s+1}$	$\frac{0.126e^{-6s}}{60s+1}$
g_{12}	$\frac{0.2429e^{-2s}}{(33s+1)^2}$	$\frac{-18.9e^{-3s}}{21s+1}$	$\frac{1.3e^{-0.3s}}{7s+1}$	$\frac{-0.101e^{-12s}}{(48s+1)(45s+1)}$
g_{21}	$\frac{-0.0887e^{-12.6s}}{(43s+1)(22s+1)}$	$\frac{6.6e^{-7s}}{10.9s+1}$	$\frac{-2.8e^{-1.8s}}{9.5s+1}$	$\frac{0.094e^{-8s}}{38s+1}$
g_{22}	$\frac{0.2429e^{-0.17s}}{(44s+1)(20s+1)}$	$\frac{-19.4e^{-3s}}{14.4s+1}$	$\frac{4.3e^{-0.35s}}{9.2s+1}$	$\frac{-0.12e^{-8s}}{35s+1}$

Table **A2.** Process open-loop transfer functions of 3 × 3 systems

	OR (Ogunnaike and Ray)	T1 (Tyreus case 1)	T4 (Tyreus case 4)
g_{11}	$\frac{0.66e^{-2.6s}}{6.7s+1}$	$\frac{-1.986e^{-0.71s}}{66.67s+1}$	$\frac{-1.986e^{-0.71s}}{66.67s+1}$
g_{12}	$\frac{-0.61e^{-3.5s}}{8.64s+1}$	$\frac{5.984e^{-2.24s}}{14.29s+1}$	$\frac{5.24e^{-60s}}{400s+1}$
g_{13}	$\frac{-0.0049e^{-s}}{9.06s+1}$	$\frac{0.422e^{-8.72s}}{(250s+1)^2}$	$\frac{5.984e^{-2.24s}}{14.29s+1}$
g_{21}	$\frac{1.11e^{-6.5s}}{3.25s+1}$	$\frac{0.0204e^{-0.59s}}{(7.14s+1)^2}$	$\frac{0.0204e^{-0.59s}}{(7.14s+1)^2}$
g_{22}	$\frac{-2.36e^{-3s}}{5s+1}$	$\frac{2.38e^{-0.42s}}{(1.43s+1)^2}$	$\frac{-0.33e^{-0.68s}}{(2.38s+1)^2}$
g_{23}	$\frac{-0.01e^{-1.2s}}{7.09s+1}$	$0.513e^{-1s}$	$\frac{2.38e^{-0.42s}}{(1.43s+1)^2}$
g_{31}	$\frac{-34.68e^{-9.2s}}{8.15s+1}$	$\frac{0.374e^{-7.75s}}{22.22s+1}$	$\frac{0.374e^{-7.75s}}{22.22s+1}$
g_{32}	$\frac{46.2e^{-9.4s}}{10.9s+1}$	$\frac{-9.811e^{-1.59s}}{11.36s+1}$	$\frac{-11.3e^{-3.79s}}{(21.74s+1)^2}$
g_{33}	$\frac{0.87(11.61s+1)e^{-s}}{(3.89s+1)(18.8s+1)}$	$\frac{-2.368e^{-27.33s}}{33.3s+1}$	$\frac{-9.811e^{-1.59s}}{11.36s+1}$

Table **A3.** Process open-loop transfer functions of 4×4 systems

	DL (Doukas and Luyben)	A1 (Alatiqi case 1)	A2 (Alatiqi case 2)
g_{11}	$\frac{-9.811e^{-1.59s}}{11.36s+1}$	$\frac{2.22e^{-2.5s}}{(36s+1)(25s+1)}$	$\frac{4.09e^{-1.3s}}{(33s+1)(8.3s+1)}$
g_{12}	$\frac{0.374e^{-7.75s}}{22.22s+1}$	$\frac{-2.94(7.9s+1)e^{-0.05s}}{(23.7s+1)^2}$	$\frac{-6.36e^{-0.2s}}{(31.6s+1)(20s+1)}$
g_{13}	$\frac{-2.368e^{-27.33s}}{33.3s+1}$	$\frac{0.017e^{-0.2s}}{(31.6s+1)(7s+1)}$	$\frac{-0.25e^{-0.4s}}{21s+1}$
g_{14}	$\frac{-11.3e^{-3.79s}}{(21.74s+1)^2}$	$\frac{-0.64e^{-20s}}{(29s+1)^2}$	$\frac{-0.49e^{-5s}}{(22s+1)^2}$
g_{21}	$\frac{5.984e^{-2.24s}}{14.29s+1}$	$\frac{-2.33e^{-5s}}{(35s+1)^2}$	$\frac{-4.17e^{-4s}}{45s+1}$
g_{22}	$\frac{-1.986e^{-0.71s}}{66.67s+1}$	$\frac{3.46e^{-1.01s}}{32s+1}$	$\frac{6.93e^{-1.01s}}{44.6s+1}$
g_{23}	$\frac{0.422e^{-8.72s}}{(250s+1)^2}$	$\frac{-0.51e^{-7.5s}}{(32s+1)^2}$	$\frac{-0.05e^{-5s}}{(34.5s+1)^2}$
g_{24}	$\frac{5.24e^{-60s}}{400s+1}$	$\frac{1.68e^{-2s}}{(28s+1)^2}$	$\frac{1.53e^{-2.8s}}{48s+1}$
g_{31}	$\frac{2.38e^{-0.42s}}{(1.43s+1)^2}$	$\frac{-1.06e^{-22s}}{(17s+1)^2}$	$\frac{-1.73e^{-17s}}{(13s+1)^2}$
g_{32}	$\frac{0.0204e^{-0.59s}}{(7.14s+1)^2}$	$\frac{3.511e^{-13s}}{(12s+1)^2}$	$\frac{5.11e^{-11s}}{(13.3s+1)^2}$
g_{33}	$\frac{0.513e^{-s}}{s+1}$	$\frac{4.41e^{-1.01s}}{16.2s+1}$	$\frac{4.61e^{-1.02s}}{18.5s+1}$
g_{34}	$\frac{-0.33e^{-0.68s}}{(2.38s+1)^2}$	$\frac{-5.38e^{-0.5s}}{17s+1}$	$\frac{-5.48e^{-0.5s}}{15s+1}$
g_{41}	$\frac{-11.3e^{-3.79s}}{(21.74s+1)^2}$	$\frac{-5.73e^{-2.5s}}{(8s+1)(50s+1)}$	$\frac{-11.18e^{-2.6s}}{(43s+1)(6.5s+1)}$
g_{42}	$\frac{-0.176e^{-0.48s}}{(6.9s+1)^2}$	$\frac{4.32(25s+1)e^{-0.01s}}{(50s+1)(5s+1)}$	$\frac{14.04e^{-0.02s}}{(45s+1)(10s+1)}$
g_{43}	$\frac{15.54e^{-s}}{s+1}$	$\frac{-1.25e^{-2.8s}}{(43.6s+1)(9s+1)}$	$\frac{-0.1e^{-0.05s}}{(31.6s+1)(5s+1)}$
g_{44}	$\frac{4.48e^{-0.52s}}{11.11s+1}$	$\frac{4.78e^{-1.15s}}{(48s+1)(5s+1)}$	$\frac{4.49e^{-0.6s}}{(48s+1)(6.3s+1)}$

Bibliography

[1] A. S. Foss, "Critique of chemical process control theory," *American Institute of Chemical Engineers Journal*, vol. 19, pp. 209–214, 1973.

[2] D. E. Seborg, T. F. Edgar, and D. A. Mellichamp, *Process Dynamics and Control*. John Wiley and Sons: New York, 1989.

[3] D. E. Rivera and K. S. Jun, "An integrated identification and control design methodology for multivariable process system applications," *IEEE Control Systems Magazine*, vol. 20, pp. 25–36, 2000.

[4] P. Grosdidier and M. Morari, "A computer aided methodology for the design of decentralized controllers," *Computers and Chemical Engineering*, vol. 11, pp. 423–433, 1987.

[5] V. K. Tzouanas, C. Georgakis, W. L. Luyben, and L. H. Ungar, "Expert multivariable control," *Computers and Chemical Engineering*, vol. 12, pp. 1065–1074, 1988.

[6] E. H. Bristol, "On a new measure of interactions for multivariable process control," *IEEE Transactions on Automatic Control*, vol. 11, pp. 133–134, 1966.

[7] F. G. Shinskey, *Process Control Systems*. McGraw-Hill: New York, 1988.

[8] E. A. Wolff and S. Skogestad, "Operation of integrated three- product (petlyuk) distillation columns," *Industrial & Engineering Chemistry Research*, vol. 34, pp. 2094–2103, 1995.

[9] J. E. Hansen, S. B. Jørgensen, J. Heath, and J. D. Perkins, "Control structure selection for energy integrated distillation column," *Journal of Process Control*, vol. 8, pp. 185–195, 1998.

[10] C. D. Schaper, T. Kailath, and Y. J. Lee, "Decentralized control of water temperature for multizone rapid thermal processing systems," *IEEE Transactions on Semiconductor Manufacturing*, vol. 12, pp. 193–199, 1999.

[11] P. Grosdidier and M. Morari, "Closed-loop properties from steady-state gain information," *Industrial and Engineering Chemistry Fundamentals*, vol. 24, pp. 221–235, 1985.

[12] A. Niederlinski, "A heuristic approach to the design of linear multivariable interacting subsystems," *Automatica*, vol. 7, pp. 691–701, 1971.

[13] T. J. McAvoy, *Interaction Analysis*. ISA: Research Triangle Park, NC, 1983.

[14] S. Skogestad, P. Lundstrom, and E. W. Jacobsen, "Selecting the best distillation control configuration," *American Institute of Chemical Engineers Journal*, vol. 36, pp. 753–764, 1990.

[15] Z.-X. Zhu, "Stability and integrity enforcement by integrating variable pairing and controller design," *Chemical Engineering Science*, vol. 53, pp. 1009–1014, 1998.

[16] M. Hovd and S. Skogestad, "Simple frequency dependent tools for control system analysis, structure selection and design," *Automatica*, vol. 28, pp. 989–996, 1992.

[17] M. Witcher and T. J. McAvoy, "Interacting control systems: Steady state and dynamic measurement of interaction," *ISA Transactions*, vol. 16, pp. 35–41, 1977.

[18] E. H. Bristol, "Recent results on interactions in multivariable process control," in *AIChE Annual Meeting*, Chicago, IL, 1978.

[19] L. Tung and T. Edgar, "Analysis of control-output interactions in dynamic systems," *American Institute of Chemical Engineers Journal*, vol. 27, pp. 690–693, 1981.

[20] P. Grosdidier and M. Morari, "Interaction measures for systems under decentralized control," *Automatica*, vol. 22, pp. 309–319, 1986.

[21] ——, "The μ interaction measures," *Industrial & Engineering Chemistry Research*, vol. 26, pp. 1193–1202, 1987.

[22] K. Asano and M. Morari, "Interaction measure of tension thickness control in tandem cold rolling," *Control Engineering Practice*, vol. 6, pp. 1021–1027, 1998.

[23] S. Skogestad and I. Postlethwaite, *Multivariable Feedback Control.* John Wiley and Sons: New York, 1996.

[24] M. Morari, "Robust stability of systems with integral control," *IEEE Transactions on Automatic Control*, vol. 30, pp. 574–577, 1985.

[25] V. Manousiouthakis, R. Savage, and Y. Arkun, "Synthesis of decentralized process control structures using the concept of block relative gain," *American Institute of Chemical Engineers Journal*, vol. 32, pp. 991–1003, 1986.

[26] C. C. Yu and W. L. Luyben, "Design of multiloop siso controllers in multivariable processes," *Industrial & Engineering Chemistry Research*, vol. 25, pp. 498–503, 1986.

[27] S. Skogestad and M. Morari, "Variable selection for decentralized control," in *AIChE Annual Meeting*, Washington, DC, 1988.

[28] C. C. Yu and M. K. H. Fan, "Decentralized integral controllability and d-stability," *Chemical Engineering Science*, vol. 45, pp. 3299–3309, 1990.

[29] M. S. Chiu and Y. Arkun, "Decentralized control structure selection based on integrity considerations," *Industrial & Engineering Chemistry Research*, vol. 29, pp. 369–373, 1990.

[30] P. J. Campo and M. Morari, "Achievable closed-loop properties of systems under decentralized control: Conditions involving the steady-state gain," *IEEE Transactions on Automatic Control*, vol. 39, pp. 932–943, 1994.

[31] M. Morari and E. Zafiriou, *Robust Process Control*. Prentice-Hall: Englewood Cliffs, NJ, 1989.

[32] K. Yamanaka and N. Kawasaki, "Criterion for conditional stability of mimo integral control," *International Journal of Control*, vol. 50, pp. 1071–1078, 1989.

[33] J. Lee and T. F. Edgar, "Conditions for decentralized integral controllability," *Journal of Process Control*, vol. 12, pp. 797–805, 2002.

[34] ——, "Computational method for decentralized integral controllability of low dimensional processes," *Computers and Chemical Engineering*, vol. 24, pp. 847–852, 2000.

[35] J. G. Ziegler and N. B. Nichols, "Optimum settings for automatic controllers," *Transactions of the ASME*, vol. 64, pp. 759–768, 1942.

[36] D. E. Rivera, M. Morari, and S. Skogestad, "Internal model control. 4. pid controller design," *Industrial and Engineering Chemistry Process Design and Development*, vol. 25, pp. 252–265, 1986.

[37] K. J. Åström and T. H. Hägglund, *PID Controllers: Theory, Design and Tuning (2nd ed.)*. Instrument Society of America: Research Triangle Park, NC, 1995.

[38] S. Skogestad, "Simple analytic rules for model reduction and pid controller tuning," *Journal of Process Control*, vol. 13, pp. 291–309, 2003.

[39] W. L. Luyben, "Simple method for tuning siso controllers in multivariable systems," *Industrial and Engineering Chemistry Process Design and Development*, vol. 25, pp. 654–660, 1986.

[40] T. J. Monica, C. C. Yu, and W. L. Luyben, "Improved multiloop single-input/single-output (siso) controllers for multivariable processes," *Industrial & Engineering Chemistry Research*, vol. 27, pp. 969–973, 1988.

[41] I. L. Chien, H. P. Huang, and J. C. Yang, "A simple multiloop tuning method for pid controllers with no proportional kick," *Industrial & Engineering Chemistry Research*, vol. 38, pp. 1456–1468, 1999.

[42] M. Hovd and S. Skogestad, "Sequencial design of decentralized controllers," *Automatica*, vol. 30, pp. 1601–1607, 1994.

[43] S. J. Shiu and S. H. Hwang, "Sequencial design method for multivariable decoupling and multiloop pid controllers," *Industrial & Engineering Chemistry Research*, vol. 37, pp. 107–119, 1998.

[44] D. Y. Lee, M. Lee, Y. Lee, and S. Park, "Mp criterion based multiloop pid controllers tuning for desired closed loop responses," *Korean Journal of Chemical Engineering*, vol. 20, pp. 8–13, 2003.

[45] M. Lee, K. Lee, C. Kim, and J. Lee, "Analytical design of multiloop pid controllers for desired closed-loop responses," *American Institute of Chemical Engineers Journal*, vol. 50, pp. 1631–1635, 2004.

[46] J. Bao, J. F. Forbes, and P. J. McLellan, "Robust multiloop pid controller design: a successive semidefinite programming approach," *Industrial & Engineering Chemistry Research*, vol. 38, pp. 3407–3419, 1999.

[47] C. Vlachos, D. Williams, and J. B. Gomm, "Genetic approach to decentralised pi controller tuning for multivariable processes," *IEE Proceedings Control Theory & Applications*, vol. 146, pp. 58–64, 1999.

[48] M. Economou and M. Morari, "Internal model control: 6. multiloop design," *Industrial and Engineering Chemistry Process Design and Development*, vol. 25, pp. 411–419, 1986.

[49] M. Hovd and S. Skogestad, "Improved independent design of robust decentralized controllers," *Journal of Process Control*, vol. 3, pp. 43–51, 1993.

[50] D. Chen and D. E. Seborg, "Design of decentralized pi control systems based on nyquist stability analysis," *Journal of Process Control*, vol. 13, pp. 27–39, 2003.

[51] J. Lee, W. Cho, and T. F. Edgar, "Multiloop pi controller tuning for interaction multivariable processes," *Computers and Chemical Engineering*, vol. 22, pp. 1711–1723, 1998.

[52] Q. G. Wang, T. H. Lee, and Y. Zhang, "Multi-loop version of the modified zieglercnichols method for two input two output process," *Industrial & Engineering Chemistry Research*, vol. 37, pp. 4725–4733, 1998.

[53] H. P. Huang, J. C. Jeng, C. H. Chiang, and W. Pan, "A direct method for multi-loop pi/pid contoller design," *Journal of Process Control*, vol. 13, pp. 769–786, 2003.

[54] V. Kariwala, J. F. Forbes, and E. S. Meadows, "Block relative gain: Properties and pairing rules," *Industrial & Engineering Chemistry Research*, vol. 42, pp. 4564–4574, 2003.

[55] Y. Arkun, "Dynamic block relative gain and its connection with the performance and stability of decentralized control structures," *International Journal of Control*, vol. 46, pp. 1187–1193, 1987.

[56] J. C. Doyle, "Analysis of feedback systems with structured uncertainties," *IEE Proceedings Part D: Control Theory and Applications*, vol. 129, pp. 242–250, 1982.

[57] V. Zhang, J. Bao, and P. L. Lee, "Control sturucture selection based on block-decentralized integral controllability," *Industrial & Engineering Chemistry Research*, vol. 42, pp. 5152–5156, 2003.

[58] J. W. Chang and C. C. Yu, "Relative disturbance gain array," *American Institute of Chemical Engineers Journal*, vol. 38, pp. 521–533, 1992.

[59] M. E. Salgado and A. Conley, "Mimo interaction measure and controller structure selection," *International Journal of Control*, vol. 77, pp. 367–383, 2004.

[60] M.-J. He and W.-J. Cai, "New criterion for control loop configuration of multivariable processes," *Industrial & Engineering Chemistry Research*, vol. 43, pp. 7057–7064, 2004.

[61] M.-J. He, W.-J. Cai, and S.-Y. Li, "Evaluation of decentralized closed-loop integrity for multivariable control system," *Industrial & Engineering Chemistry Research*, vol. 44, pp. 3567–3574, 2005.

[62] M.-J. He, W.-J. Cai, B.-F. Wu, and M. He, "A simple decentralized pid controller design method based on dynamic relative interaction analysis," *Industrial & Engineering Chemistry Research*, vol. 44, pp. 8334–8344, 2005.

[63] M.-J. He, W.-J. Cai, and B.-F. Wu, "Design of decentralized imc-pid controller based on dri analysis," *American Institute of Chemical Engineers Journal*, vol. 52, pp. 3852–3863, 2006.

[64] ——, "Control structure selection based on relative interaction decomposition," *International Journal of Control*, vol. 79, pp. 1285–1296, 2006.

[65] G. Stanley, M. Marino-Galarranga, and T. J. McAvoy, "Short operability analysis. 1. the relative disturbance gain," *Industrial and Engineering Chemistry Process Design and Development*, vol. 24, pp. 1181–1188, 1985.

[66] E. H. Bristol, "On a philosophy of interaction in a multiloop world," in *ISA Chemical & Petroleum Division Chempid Symposium*, St. Louis, Missouri, May, 1967.

[67] E. D. Nering, *Linear Algebra and Matrix Theory.* Willey, 1970.

[68] B. A. Ogunnaike and W. H. Ray, *Process Dynamics, Modeling, and Control.* Oxford University Press: New York, 1994.

[69] Z.-X. Zhu, "Structural analysis and stability conditions of decentralized control systems," *Industrial & Engineering Chemistry Research*, vol. 35, pp. 736–745, 1996.

[70] ——, "Variable pairing selection based on individual and overall interaction measures," *Industrial & Engineering Chemistry Research*, vol. 35, pp. 4091–4099, 1996.

[71] ——, "Steady state structural analysis and interaction characterization for multivariable control systems," *Industrial & Engineering Chemistry Research*, vol. 36, pp. 3718–3726, 1997.

[72] Y. Arkun and Y. J. Downs, "A general method to calculate input-output gains and the rga for integrating processes," *Computers and Chemical Engineering*, vol. 14, pp. 1101–1110, 1990.

[73] T. P. Chiang and W. L. Luyben, "Comparison of the dynamic performance of three heat-integrated distillation configurations," *Industrial & Engineering Chemistry Research*, vol. 27, pp. 99–104, 1988.

[74] T. J. McAvoy, Y. Arkun, R. Chen, D. Robinson, and P. D. Schnelle, "A new approach to defining a dynamic relative gain," *Control Engineering Practice*, vol. 11, pp. 907–914, 2003.

[75] J. Lee and T. F. Edgar, "Dynamic interaction measures for decentralized control of multivariable processes," *Industrial & Engineering Chemistry Research*, vol. 43, pp. 283–287, 2004.

[76] H. P. Huang and J. C. Jeng, "Monitoring and assessment of control performance for single loop systems," *Industrial & Engineering Chemistry Research*, vol. 41, pp. 1297–1309, 2002.

[77] A. Ingimundarson and T. Hägglund, "Performance comparison between pid and dead-time compensating controllers," *Journal of Process Control*, vol. 12, pp. 887–895, 2002.

[78] C. E. Garcia and M. Morari, "Internal model control - 1. unifying review and some new results," *Industrial and Engineering Chemistry Process Design and Development*, vol. 21, pp. 308–323, 1982.

[79] Q.-G. Wang, Y. Zhang, and M.-S. Chiu, "Non-interacting control design for multivariable industrial processes," *Journal of Process Control*, vol. 13, pp. 253–265, 2003.

[80] Q. Xiong, W.-J. Cai, and M.-J. He, "A practical loop pairing criterion for multivariable processes," *Journal of Process Control*, vol. 15, pp. 741–747, 2005.